

# **Doctoral Thesis**

**Design and characterization of modified powder metallurgy titanium surfaces obtained by  $\beta$ -stabilizing elements diffusion treatments for biomedical applications**

**Author:**

Julia Ureña Alcázar

**Supervisors:**

Dra. Elena Gordo Odériz

Dra. Antonia Jiménez-Morales

**Tutor:**

Dra. Antonia Jiménez-Morales

**Materials Sciences and Engineering Department at University  
Carlos III of Madrid (UC3M)**

**Group of Powder Metallurgy (GTP)**

**Leganés, January 2018**



# Contents

<b>Abstract</b> .....	5
<b>Resumen</b> .....	6
<b>Preface</b> .....	7
<b>Chapter 1. Introduction</b> .....	11
<b>Chapter 2. Motivations and Objectives</b> .....	31
<b>Chapter 3. Experimental Work</b> .....	36
<b>Chapter 4. Summary of Results and Discussion</b> .....	58
<b>Chapter 5. Concluding Remarks</b> .....	93
<b>Chapter 6. Future Lines</b> .....	97
<b>Paper 1</b> .....	98
<b>Paper 2</b> .....	108
<b>Paper 3</b> .....	120
<b>Paper 4</b> .....	138
<b>Paper 5</b> .....	144
<b>Paper 6</b> .....	151
<b>Paper 7</b> .....	170
<b>Paper 8</b> .....	182



## Abstract

Titanium (Ti) is a metal highly recognized by its employment in the biomedical sector since 1950. Nevertheless, in these last two decades from 1990 till date, a second generation of Ti biomaterials has received high attention. They are known as  $\beta$ -Ti alloys and its strong interest comes from their excellent combination of properties for biomaterials. Currently, due to the great demand to develop new biomaterials, the surface modification is one of the main alternatives for the design of new Ti biomaterials with improved properties for the biomedical sector.

In this PhD Thesis, the design of new Ti surfaces modified by diffusion of niobium (Nb) and molybdenum (Mo) as  $\beta$ -stabilizing elements is presented as alternative to Cp-Ti or fully  $\beta$ -Ti alloys; preserving their lightness of Ti in the core. These diffusion elements share their capacity of decreasing the elastic modulus of titanium as well as their biocompatibility character. Thus, the global idea of this work is the design and study of these modified Ti surfaces produced by powder metallurgy with their evaluation on mechanical performance, tribological properties, corrosion and biocompatibility character to be considered as possible candidates for biomedical applications. Regarding this matter, different modified Ti surfaces were designed with several conditions: i) titanium substrate (green or sintered), ii) diffusion element (Nb or Mo), and iii) diffusion treatments (co-sintering plus diffusion, diffusion or thermo-reactive diffusion). These systems were compared with the behaviour of the commonly employed Ti biomaterial, the commercially pure titanium (Cp-Ti) obtained through powder metallurgy (PM).

The  $\beta$ -stabilizing elements were deposited by means of aqueous suspensions through spraying. The gradients in microstructure and composition were analyzed by spectroscopy and diffraction techniques, and their differences were related to the designing parameters. The final surface conditions were investigated to obtain the most suitable ones in function of the final properties measured: mechanical properties according to hardness and elastic modulus, wear, corrosion and tribocorrosion behaviour and biocompatibility features.

Therefore, this doctoral work covers the whole process from the design of the materials employing preparation and deposition of suspensions, diffusion treatments, surface conditions selection and microstructure investigations to their final characterization of hardness, modulus of elasticity, wear, corrosion and their synergistic effect (tribocorrosion), and bioactivity and cell-material response.

Although some questions were found during different stages that should be further investigated, these new Ti surfaces have demonstrated some suitable characteristics for biomaterials, providing improvements with respect to titanium with a promising character for bone replacements.

## Resumen

El titanio (Ti) es un metal altamente reconocido y empleado en el sector biomédico desde 1950. Sin embargo, una nueva generación de biomateriales de titanio ha recibido gran atención en estas dos últimas décadas. Esta se conoce con el nombre de segunda generación de biomateriales de titanio y su alto interés deriva de la excelente combinación de propiedades que presentan para biomateriales. Actualmente, debido a la gran demanda del desarrollo de nuevos biomateriales, la modificación superficial es una de las principales alternativas para el diseño de nuevos biomateriales de Ti con mejores propiedades para aplicaciones del sector biomédico.

En esta tesis doctoral, se presenta una alternativa al titanio comercialmente puro (Cp-Ti) y a las aleaciones completamente beta ( $\beta$ -Ti) mediante el diseño de nuevas superficies de titanio modificadas con elementos betágenos, niobio (Nb) y molibdeno (Mo), mediante procesos de difusión. Estos elementos de difusión comparten la capacidad de disminuir el módulo elástico del titanio, mientras que son elementos biocompatibles. Por tanto, la idea global de este trabajo se centra en el diseño y estudio de superficies modificadas de titanio pulvimetalúrgico, junto con la evaluación de las propiedades mecánicas y comportamiento a desgaste, corrosión y tribocorrosión. Además, de la evaluación de la biocompatibilidad de estos para considerarlos como posibles candidatos para aplicaciones biomédicas. Para ello se diseñaron diferentes superficies modificadas de Ti basadas en las siguientes condiciones: i) substrato de titanio (prensado o sinterizado), ii) elemento de difusión (Nb o Mo), y iii) tratamiento de difusión (co-sinterización + difusión, difusión o difusión termo-reactiva). Todos los materiales se compararon con el material de titanio obtenido mediante pulvimetalurgia (PM). Los elementos betágenos se depositaron mediante pulverización de suspensiones acuosas. Los gradientes de microestructura y composición se analizaron con técnicas de espectroscopia y difracción. Se estudiaron las condiciones superficiales más idóneas para la caracterización mecánica (dureza y módulo elástico), comportamiento a desgaste, corrosión, tribocorrosión y biocompatibilidad.

Por tanto, esta tesis doctoral abarca todo el proceso desde el diseño de los materiales, preparación y pulverización de las suspensiones, tratamientos de difusión, caracterización microestructural y superficial, hasta la evaluación de dureza, módulo de elasticidad, desgaste, corrosión, tribocorrosión y biocompatibilidad de las superficies modificadas de Ti.

Aunque se necesita la evaluación más profunda de algunos aspectos, estas superficies modificadas de Ti han demostrado que presentan características adecuadas para biomateriales con mejoras con respecto al titanio, por tanto con propiedades prometedoras para reemplazo óseo.

## Preface

This PhD Thesis is a work carried out at the Group of Powder Technology (GTP), Department of Materials Science and Engineering and Chemical Engineering of the University Carlos III of Madrid (UC3M) during the period from September 2014 to March 2018.

The structure of this work consists of: i) an introduction with the requirements of biomaterials and the main surface modification techniques employed in the improvement of titanium properties for biomedical applications, ii) the motivation and partial objectives to accomplish the main goal, iii) the experimental work and techniques employed during this period, iv) a summary of the main results which are reported in the appended papers, v) the main conclusions, and vi) a perspective of future lines.

The results of this doctoral Thesis are presented in detail in the following appended papers:

1. J. Ureña, C. Mendoza, B. Ferrari, Y. Castro, S. Tsipas, A. Jiménez-Morales and E. Gordo, Surface modification of powder metallurgy titanium by colloidal techniques and diffusion processes for biomedical applications, *Adv. Eng. Mater.*, Vol. 19, no. 6, 1600207, 2016
2. J. Ureña, E. Tejado, J.Y. Pastor, F. Velasco, S. Tsipas, A. Jiménez-Morales and E. Gordo, Role of beta-stabilizing elements on the microstructure and mechanical properties evolution of modified powder metallurgy Ti surfaces designed for biomedical applications, *Powder Metall.*, 2018, doi: 10.1080/00325899.2018.1426185
3. J. Ureña, E. Tabares, F. Toptan, A. M. Pinto, S. Tsipas, A. Jiménez-Morales and E. Gordo, Dry sliding wear behaviour of  $\beta$ -type Ti-Nb and Ti-Mo surfaces designed by diffusion treatments for biomedical applications, *J. Mech. Behav. Biomed. Mater.*, 2018 (*Accepted*)
4. J. Ureña, E. Gordo, E. Ruiz-Navas, N. Vilaboa, L. Saldaña and A. Jiménez-Morales, Electrochemical comparative study on corrosion behavior of conventional and powder metallurgy titanium alloys in physiological conditions, *Met. Powder Rep.*, vol. 72, no. 2, pp. 118-123, 2017
5. E. Gordo, J. Ureña, F. Toptan, A. M. Pinto, B. Ferrari, S. Tsipas and A. Jiménez-Morales, Design and evaluation of powder metallurgy titanium surfaces modified by colloidal techniques and diffusion processes for

biomedical applications, Proceedings of World PM16 Conference, Hamburg, Germany, October 2016

6. J. Ureña, F. Toptan, A. M. Pinto, B. Ferrari, S. Tsipas, A. Jiménez-Morales and E. Gordo, Corrosion and tribocorrosion behaviour of  $\beta$ -type Ti-Nb and Ti-Mo surfaces designed by diffusion treatments for biomedical applications *Corrosion Science*, 2018 (*Submitted*)
7. J. Ureña, S. Tsipas, A. Jiménez-Morales, E. Gordo, R. Detsch and A. R. Boccaccini, In-vitro study of the bioactivity and cytotoxicity response of titanium surfaces modified by niobium and molybdenum diffusion treatments, *Surf. Coat. Technol.*, vol. 335, pp. 148-158, 2018
8. J. Ureña, S. Tsipas, A. Jiménez-Morales, E. Gordo, R. Detsch and A. R. Boccaccini, Cellular behaviour of bone marrow stromal cells on modified Ti-Nb surfaces, *Mater. Des.*, vol. 140, pp. 452-459, 2018

With this PhD Thesis has been also contributed to the following scientific production to congress:

### **International conferences**

1

Author: J. Ureña, S.A. Tsipas, B. Ferrari, A. Jiménez-Morales, E. Gordo

Title: Surface modification of titanium produced by powder metallurgy by chemical diffusion of molybdenum for biomedical applications

Participation: Poster (invited)

Congress: TitaniumEurope 2015, Birmingham (UK), 11-13 May 2015

---

2

Author: J. Ureña, E. Gordo, E. Ruiz-Navas, N. Vilaboa, L. Saldaña, A. Jiménez-Morales

Title: Electrochemical comparative study of corrosion behaviour in physiological conditions of conventional and powder metallurgy titanium alloys

Publication: Euro PM2015 Proceedings (CD), ISBN 978-1-899072-47-7

Participation: Poster

Congress: EuroPM 2015, Reims (France), 04-07 October 2015

---



---

3

Author: J. Ureña, C. Mendoza, B. Ferrari, Y. Castro, S.A. Tsipas, A. Jiménez-Morales, E. Gordo

Title: Surface modification of powder metallurgy titanium by colloidal techniques and diffusion processes for biomedical applications

Publication: AMPT 2015 Proceedings (Book), ISBN:

Participation: Oral

Congress: AMPT 2015, Madrid (Spain), 14-17 December 2015

---

4

Author: J. Ureña, F. Toptan, B. Ferrari, S.A. Tsipas, A. Jiménez-Morales, E. Gordo

Title: Design and evaluation of PM Ti and Ti6Al4V alloy surfaces modified by colloidal techniques and diffusion processes for applications in the biomedical sector

Participation: Oral

Congress: JREUROMAT 2016, Lausanne (Switzerland), 10-14 July 2016

---

5

Author: J. Ureña, F. Toptan, B. Ferrari, S.A. Tsipas, A. Jiménez-Morales, E. Gordo

Title: Design and evaluation of PM Ti surfaces modified by colloidal techniques and diffusion processes for biomedical applications

Publication: World PM2016 Proceedings (CD), ISBN

Participation: Oral

Congress: WorldPM 2016, Hamburg (Germany), 09-13 October 2016

---

6

Author: J. Ureña, R. G. das Neves, S. Tsipas, A. C. Alves, A. M. Pinto, F. Toptan, B. Ferrari, A. Jiménez-Morales, E. Gordo

Title: Strategies for improvement the wear and tribocorrosion behaviour of titanium alloys

Publication: Programme & Book of Abstract, ISBN 978-972-99596-2-2

Participation: Oral

Congress: IBERTRIB 2017, Guimarães (Portugal), 12-13 June 2017

---

7

Author: J. Ureña, S. Tsipas, A. Jiménez-Morales, E. Gordo, R. Detsch, A. R. Boccaccini

Title: In-vitro study of the bioactivity and biological response of powder metallurgy modified Ti surfaces

Participation: Oral

Congress: EUROMAT 2017, Thessaloniki (Greece), 17-22 September 2017

---

---

8

Author: J. Ureña, E. Tejado, J.Y. Pastor, F. Velasco, A. Jiménez-Morales, E. Gordo  
Title: Role of beta-stabilizer elements in microstructure and mechanical properties evolution of PM modified Ti surfaces designed for biomedical applications  
Publication: Euro PM2017 Proceedings (CD), ISBN 978-1-899072-49-1  
Participation: Oral (Keynote lecture)  
Congress: EUROPM 2017, Milan (Italy), 01-05 October 2017

---

### **National conferences**

1

Author: J. Ureña, E. Gordo, E. Ruiz-Navas, N. Vilaboa, L. Saldaña, A. Jiménez-Morales  
Title: Estudio electroquímico comparativo del comportamiento a corrosión en condiciones fisiológicas de aleaciones de titanio pulvimetalúrgicas y convencionales  
Publication: VCNP 2015 Proceedings (libro), ISBN: 978-84-606-9427-4  
Participation: Oral  
Congress: VCNP 2015, Girona (Spain), 01-03 July 2015

---

2

Author: J. Ureña, C. Mendoza, B. Ferrari, S.A. Tsipas, A. Jiménez-Morales, E. Gordo  
Title: Modificación superficial de titanio pulvimetalúrgico mediante recubrimientos aplicados por técnicas coloidales y difusión  
Participation: Oral  
Congress: TRATERMAT 2015, Vigo (Spain), 30 Sep - 01 October 2015

---

3

Author: J. Ureña, F. Toptan, B. Ferrari, S.A. Tsipas, A. Jiménez-Morales, E. Gordo  
Title: Diseño y evaluación de superficies de titanio pulvimetalúrgico modificadas por técnicas coloidales y procesos de difusión para aplicaciones biomédicas  
Participation: Oral  
Congress: Congreso Nacional de Materiales 2016, Gijón (Spain), 08-10 June 2016

---

4

Author: J. Ureña, E. Tejado, J. Y. Pastor, F. Velasco, A. Jiménez-Morales, E. Gordo  
Title: Evaluación de propiedades mecánicas y comportamiento a desgaste de superficies de titanio PM diseñadas para aplicaciones biomédicas  
Participation: Oral  
Congress: VI Congreso Nacional de Pulvimetalurgia 2017, Ciudad Real (Spain), 07-09 June 2017

---

# **Introduction**

---

## **1.1 Introduction to the properties of titanium for biomaterials**

1.1.1 Generations of titanium biomaterials

1.1.2 Requirements of a biomaterial

## **1.2 Introduction to surface modification of materials**

## **1.3 Surface treatments for the improvement of titanium properties for biomaterials**

1.3.1 Improvement of the mechanical performance of titanium alloys

1.3.2 Improvement of the corrosion behaviour of titanium alloys

1.3.3 Improvement of the biocompatibility character of titanium alloys

## **1.4 References**

## 1.1 Introduction to the properties of titanium for biomaterials

### 1.1.1 Generations of titanium biomaterials

Titanium (Ti) is a metallic material that has been used as implant biomaterial in different parts of the human body such as heart valves, blood vessel stents or knees, hips, shoulders or spinal replacements since 1950s [1]. Different Ti biomaterials have been developed up to nowadays. Given that Ti presents two different structures: hexagonal closely packed (HCP)  $\alpha$  phase at low temperature or body centered cubic (BCC)  $\beta$  phase at high temperature, two generations of titanium alloys have emerged. The microstructural change is produced at 882 °C known as allotropic transformation temperature, being able to be modified depending on the kind of alloying elements. These alloying elements can be divided in three categories: i)  $\alpha$ -stabilizers (Al, O, C, N, rare earths); ii)  $\beta$ -stabilizers (Mo, Nb, V, Ta) isomorphous, or (Fe, Cr, Co, Si, H, Mn) eutectoid; and iii) neutrals (Zr, Sn). Regarding this, the Ti alloys can be classified as  $\alpha$ , near- $\alpha$ ,  $\alpha+\beta$ , metastable  $\beta$  or  $\beta$  [2].

The first generation of Ti biomaterials developed from 1950 till 1990 consisted of commercially pure CP-Ti ( $\alpha$ -type) and Ti-6Al-4V, Ti-6Al-7Nb or Ti-5Al-2.5Fe ( $\alpha+\beta$ -type) alloys. The second generation corresponds to  $\beta$ -type alloys such as Ti-13Nb-13Zr, Ti-12Mo-6Zr-2Fe (TMZF), Ti-35Nb-7Zr-5Ta (TNZT) or Ti-Mo, being developed from 1990s till date.

The representative properties of the alloys is related to the microstructure, presenting the  $\alpha + \beta$  structures superior strength, ductility and higher low cycle fatigue while  $\beta$  structures exhibit higher fracture toughness and the  $\beta$ -stabilizer content has a direct effect on strength and elastic modulus. Hence, for biomedical applications  $\beta$ -type Ti alloys are still being developed and widely investigated since their microstructure and chemical composition lead to decrease the elastic modulus making it closer to the value of human bone at the same time that these elements are free of toxicity. Modern binary Ti-Mo, Ti-Nb, Ti-Ta; ternary Ti-Mo-Nb, Ti-Nb-Sn or quaternary Ti-Nb-Ta-Zr, Ti-Nb-Mo-Sn alloys are being investigated in order to find biocompatible compositions with the lowest elastic modulus [3]. However, some drawbacks related to the processing of these alloys can be found given the higher melting points of these  $\beta$ -stabilizing elements that worsen melting and solidification behaviour which may lead to chemical segregation [4]. Moreover, these elements present higher density than titanium which increases the titanium alloy final density. Nevertheless, powder metallurgy (PM) processing allows the production of these alloys since the lower temperature needed and the use of protective atmospheres such as vacuum [5].

Table 1.1 shows some biocompatible titanium alloys currently employed in the biomedical sector in many applications together with their main advantages and drawbacks.

**Table 1.1** Titanium based biomaterials used in the human body (adapted from [6]).

Currently used Titanium based biomedical alloys				
<i>Examples</i>	<i>Advantages</i>	<i>Disadvantages</i>	<i>Applications</i>	<i>Implants</i>
CP-Ti	High biocompatibility	Poor tribological properties	Orthopedic	Joints, hip stems, total hip implant, endothelial cells, acetabular cup, hard tissue or bone substitutions, load-bearing implants
Ti-6Al-4V	Excellent corrosion resistance	Toxic effect of Al and V on long term	Dentistry	Dental implants, orthodontic wire leads
Ti-6Al-7Nb	Low Young's modulus		Cardiovascular	Vascular stents, heart valve parts, pacemaker encapsulation
Ti-13Nb-13Zr				
Ti-35Nb-7Zr-5Ta				
Ti-12Mo-6Zr-2Fe				
Ti-15Mo	Low density			

### 1.1.2 Requirements of a biomaterial

Table 1.1 collects some drawbacks showing the weak points of titanium implants usually employed which are related to the main consequences of implant failures as is summarized in Figure 1.1.

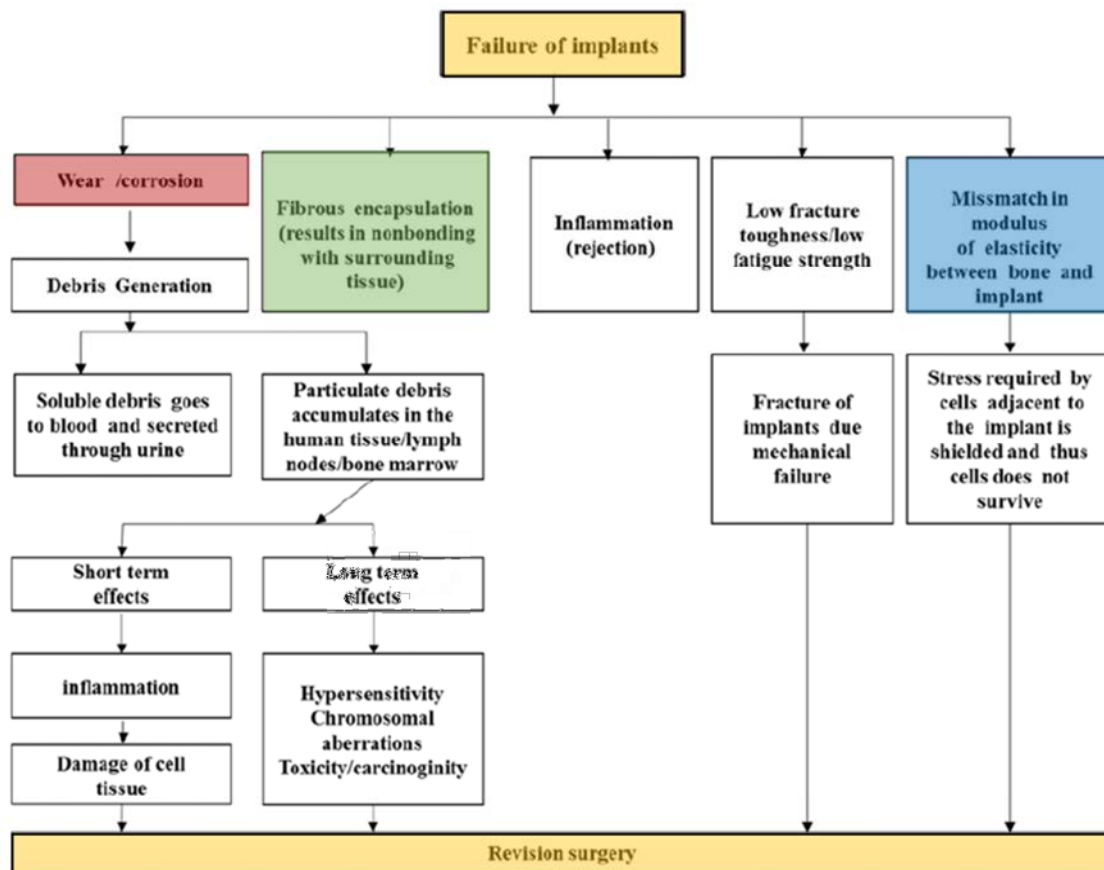


**Figure 1.1** Causes of implant failures [7].

As can be drawn from the figure, most of the causes of failure are related to each other. Thereby, a low wear resistance leads to metallic ions release provoking problems on short and long term with damage of cell tissue and toxicity. To ensure the excellent performance of an implant, a biomaterial should accomplish the following requirements [7], [8]:

### Mechanical properties

Hardness, elastic modulus, tensile and fatigue strength are among the main mechanical properties which determine the specific application of the material. For biomaterials, the combination of low elastic modulus and high strength lead to increase the service period of the implant, preventing the revision surgery [9]. The stress shielding effect is known as the death of bone cells due to higher stiffness of the implant material with respect to that of bone which results in the no stress transfer to the adjacent bone, provoking bone resorption in areas surrounded the implant and thus the implant loosening [10]. This negative effect can be prevented by matching the modulus of elasticity of biomaterials to that of bone, which varies from 4 to 30 GPa. Figure 1.2 collects the elastic modulus of different implant alloys. This gives an idea of how far are the elastic modulus values of some biomaterials such as Co or stainless steel alloys from the value of human bone. The modulus of  $\alpha+\beta$  Ti alloys and CP-Ti is relatively lower with respect to those materials mentioned before but still higher than that of bone. However, the design of Ti alloys with  $\beta$ -stabilizing elements lead to reduce the modulus varying from 90 GPa to 55 GPa, meaning values very close to that of bone. These  $\beta$ -Ti alloys have received great attention since they present biocompatible elements and elastic modulus closer to that of bone. This biomechanical compatibility allows researchers continuing their development.

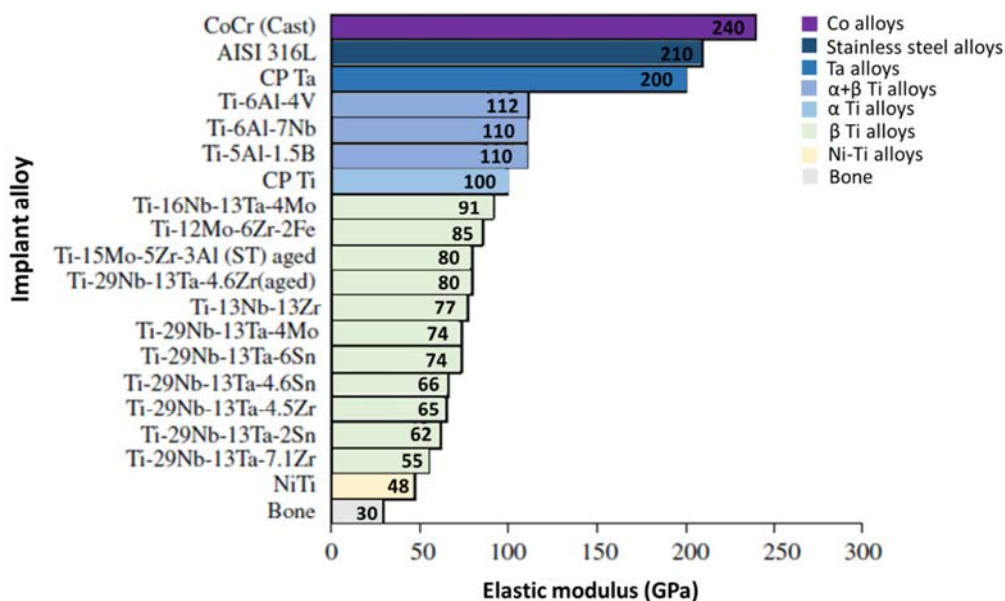
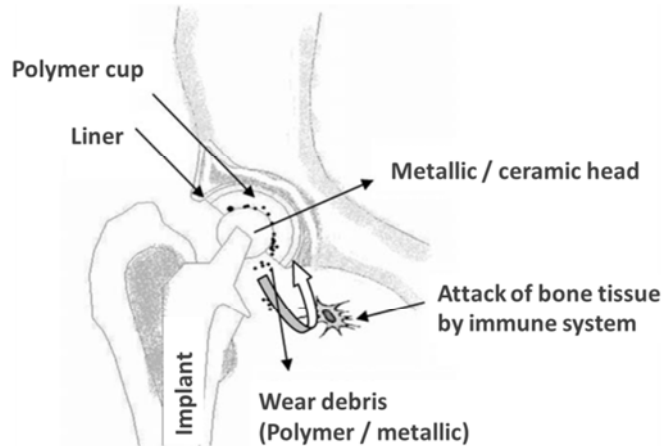


Figure 1.2 Elastic modulus of biomaterials [1].

### **Wear resistance**

High wear resistance together with low friction coefficient against human body tissues are essential requirements to ensure the long service period of an implant. The low wear resistance (Figure 1.3) results in wear debris formation and accumulation in human tissues leading to short or long term effects such as inflammation and damage of cell tissue, or toxicity, respectively [7].



**Figure 1.3** Wear of a hip joint [1].

Three basic wear mechanisms can be identified in biomaterials: adhesive, abrasive and third body wear mechanism. Adhesion is found when atomic forces between the materials surface subjected to load are stronger than their inherent properties. Abrasion is identified when there is a softer and a harder material in the contact pair, due to the friction of the harder one. The third body wear mechanisms occurs when hard particles of an abraded brittle material get embedded in a soft surface [8].

Wear mechanisms and rates vary for congruent joints (hip, shoulder, etc.) and incongruent joints (knee, ankle, etc.). In congruent joints the stress distribution is quite homogenous, whereas in incongruent joints is inhomogeneous due to contacts of hard surfaces. Metal-on-metal and metal-on-ceramic wear is highly lower than at interfaces with polymers. The highest amount of debris results from polymers sliding against metals and ceramics, whereas adhesion usually occurs in metal-on-metal couples [6].

Wear rate is usually higher within a short time period after the implantation and continuously decreases until a stable value. Although the newly developed  $\beta$ -Ti alloys consist of compatible elements and present elastic modulus closer to bone, their wear resistance needs to be enhanced because of their low resistance to plastic shear. Generally, the wear rate for  $\alpha+\beta$  Ti alloys is lower than for  $\beta$  type alloys. However, some  $\beta$ -Ti alloys have shown lower wear rates than  $\alpha+\beta$  structures

depending on their chemical composition (Nb, Ta additions...) or surface modifications [3].

### **Corrosion resistance**

Similar to a low wear resistance, a biomaterial with low corrosion resistance can generate debris soluble into the blood that are composed of non-compatible metal ions such as Fe, Ni, Cr, Co, Al, V which can lead to toxic reactions. Small concentration of these ions may not cause harmful effects but the presence in higher quantity can lead to adverse effects such as: damage of protein, DNA or lipids (with increased Fe amount), alteration of sugar levels in the blood (with increased Cr amount), toxicity reactions after 4-5 years (with increased Ni or Co amount), etc. The corrosion phenomenon of metals takes place through the formation of with electrochemical cells conducting different forms of corrosion reactions: (general/uniform, pitting/localized or electrochemical/mechanical) [11].

General/uniform corrosion takes place when the whole surface metal is exposed to the cathodic reactants during the localized corrosion. This process can be stopped with the protective film passivation. The passive layers must be non-porous with high abrasion resistance and structure that restrict the electrons and ions migration through the oxide boundary-solution boundary. Pitting/localized corrosion refers to pitting attacks in terms of spots or pits on the surface metal. Electrochemical/mechanical processes involve fretting, fatigue, stress corrosion cracking (SCC), corrosion and shielding forces, causing premature degradation.

One of the main reasons of the wide employment of titanium in orthopedic implants is their high corrosion resistance. Furthermore, it has been demonstrated that the addition of  $\beta$ -stabilizing elements enhances the corrosion resistance by means of the stabilization of their surface oxide layers in biological fluids [12].

As can be seen in Figure 1.1, one of the principal reasons of orthopedic implants failure is wear which sequentially starts to hasten corrosion. This leads to the simultaneous effect of wear and corrosion known as “**tribocorrosion**”. This synergy between mechanical and corrosion interactions results in irreversible transformation of materials which usually accelerates the implant degradation with respect to the effect of wear or corrosion, individually. Dental and hip replacements are very susceptible to tribocorrosion related problems often causing swelling, pain or biological reactions [10].

### **Biocompatibility**

An implant material should be compatible with living systems without causing negative effects such as inflammatory or allergic responses when they are emplaced in the biological system. This implies that the material should be non-toxic and thus, neither genotoxic (not altering the genome DNA) nor cytotoxic (not damage



individual cells) [1], [7]. Biocompatibility has been defined as the ability of a material to perform in the presence of an appropriate host for a specific application. Generally, titanium and its alloys have been considered as biocompatible materials since they adsorb different proteins (albumin, collagenase, fibronectin, etc.) from the biological fluid and support cell growth and differentiation [2].

Biomedical metals have been widely used in implantable devices because of their excellent mechanical properties for supporting or fixation functions. Nevertheless, nowadays new functions such as bioactivity, anti-tumor or anti-microbial have been introduced to the biomedical metals [13].

The ability of a material surface to integrate with the adjacent bone or tissue forming new bone and bone healing is known as “**osseointegration**”. This is a desirable property for a biomaterial in order to ensure the proper integration of the implant with the bone and other tissues. The lack of osseointegration is associated to the formation of thin connective fibrous tissue capsules between the bone and implant, leading to the implant rejection and its failure [8]. Although biomaterials are classified in bio-tolerant, bioactive or bio-reabsorbable materials, their biological response will depend on their surface properties and thus can be modified through surface treatments. They play a crucial role in biocompatibility, being surface roughness, topography, and chemistry the critical parameters to be evaluated in osseointegration [14]. Traditionally, titanium has been considered as an inert material, included among the bio-tolerant materials, with formation of thin connective tissue capsules instead of forming bony tissue around the implant. However, it has been demonstrated that with suitable surface properties titanium can act as a bioactive material promoting the formation of hydroxyapatite (main mineral component of bone) (Figure 1.4).

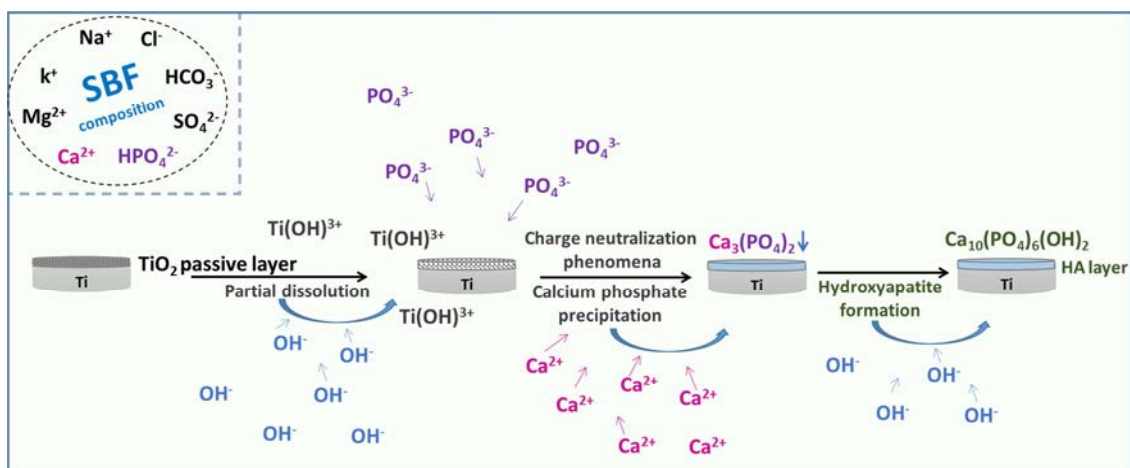


**Figure 1.4** *In vitro* hydroxyapatite formation on titanium surface in a simulated body fluid.

## 1.2 Introduction to surface modification of materials

Nowadays, metallic biomaterials are the first choice for implant devices and are not replaced by ceramics or polymers because of their superior mechanical properties. Excellent mechanical properties, high wear and corrosion resistance and biocompatibility are requirements of extreme importance in the selection of Ti biomaterials for a specific application. However, their bulk properties sometimes can lead to some drawbacks such as toxicity derived from poor wear-corrosion properties or mechanical mismatches due to poor bioactivity [4]. Moreover, different surface properties from those in the bulk are needed in some cases, since material surface plays an extremely important role in the response of the biological environment to the artificial medical devices [2]. Figure 1.5 summarizes the main reasons for the development of new alloys and surface treatments.

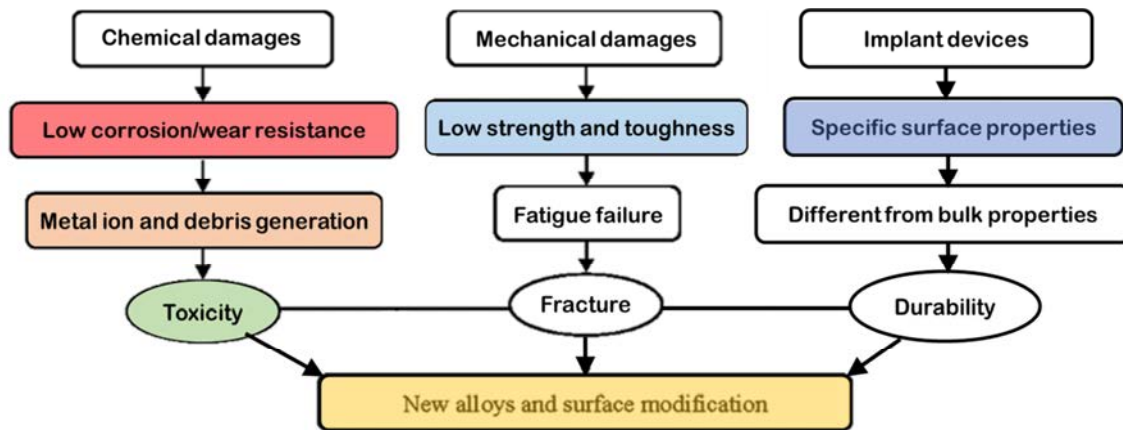


**Figure 1.5** Reasons for the research on surface modification and new alloys (adapted from [4]).

The surface treatments can be grouped attending to many criteria: altering the surface chemistry and microstructure, or applying surface coatings [15]; mechanical, chemical, or physical methods depending on the formation mechanism of the modified layer [2]. Table 1.2 shows examples of currently surface treatments grouped by techniques and categories regarding whether the surface modification is carried out on top or sub-surface, and with or without the addition of elemental species.

**Table 1.2** Categories and examples of surface treatment techniques (adapted from [3]).

<b>Surface treatments techniques</b>		
<i>Category</i>	<i>Technique</i>	<i>Examples</i>
<b>Sub-surface modification</b> (without adding elemental species)	Heating	Furnace treatment [16], flame hardening, convective, and conductive heating
	Electromagnetic irradiation	Laser treatment [17], ultraviolet treatment, gamma sterilization, inductive heating, magnetic stirring & hysteresis
	Ionizing irradiation	Gamma, beta, positron, electron beam, neutron beam, proton beam
	Mechanical modification	Shot peening [18], grit blasting [19], ultrasonic peening, Friction stir processing
<b>Sub-surface modification</b> (by implanting elemental species)	Beam	Ion beam [20], Cluster Ion Beam, Molecular Beam, Accelerated Neutral Atom Beam
	Plasma	Double glow plasma surface alloying [21], Plasma nitriding [22], Plasma sputtering [23], [24] High intensity plasma ion nitriding [25]
	Diffusion	Carburizing, Nitriding [26], Nitrocarburizing [27], Carbonitriding [28], Boriding, Boronizing, Halide-activated pack cementation [29], [30], [31]
	Vacuum	Chemical or physical vapor deposition (CVD or PVD) [32], [33], Ion plating plasma assisted
<b>Top-surface modification</b>	Material removal	Spark erosion, grinding [34]
	Surface patterning, roughening, or chemical activation	Mechanical patterning, ion milling, photolithography, electron beam lithography, chemical etching [35], broad band visible light
<b>Top-surface additions</b> (by depositing or growing layers)	Conversion coating	Anodizing [19], Thermal oxidation [36], Phosphate coatings, Electrophoretic deposition (EPD) [37]
	Spray	High velocity oxygen fuel spray coating, Flame spraying, Plasma spraying [38]
	Chemical	Nanophase patterning [39], nanodot arrays

### 1.3 Surface treatments for the improvement of titanium properties

Table 1.2 illustrates the wide variety of surface treatments techniques. However, depending on the desired property to improve, some of them are more or less suitable. The proper surface treatment will enhance the specific surface properties required by a clinical application, while remaining the excellent bulk aspects of titanium and its alloys (relatively low modulus, good fatigue strength, corrosion resistance, formability or machinability).

#### 1.3.1 Improvement of the mechanical performance of titanium alloys

Regarding mechanical properties, the titanium alloys are characterized by their high specific strength, relatively low elastic modulus (not lower enough compared to bone), and poor tribological properties with low wear resistance due to specially not

high hardness [2]. Hence, numerous researchers are focused on the improvement of these aspects to ensure the durability of biomedical implants.

With the aim of making the elastic modulus closer to that of bone, different treatments are focused on the surface modification of titanium.  $\beta$ -stabilizing elements are employed since they provide low Young's modulus which is favorable for homogeneous stress transfer between implant and bone [9]. Figure 1.6 shows a schematic representation of a diffusion surface process with niobium and titanium as examples. In this case, the diffusion of Nb ( $\beta$ -stabilizing element) in Ti would result in the modification of the surface properties of a titanium implant. This kind of surface modification has been followed by different researchers as alternative to fully  $\beta$ -Ti alloys in order to preserve some advantages of titanium in the core like low density. Different diffusion techniques have been successfully employed in related studies such as ion-beam sputtering to diffuse Nb in a single-phase  $\gamma$ -Ti-54Al-10Nb [20], laser surface alloying to diffuse Nb in Ti obtaining stiffness and hardness gradients [18] or halide-activated pack cementation for molybdenizing titanium and Ti-6Al-4V surfaces [31].

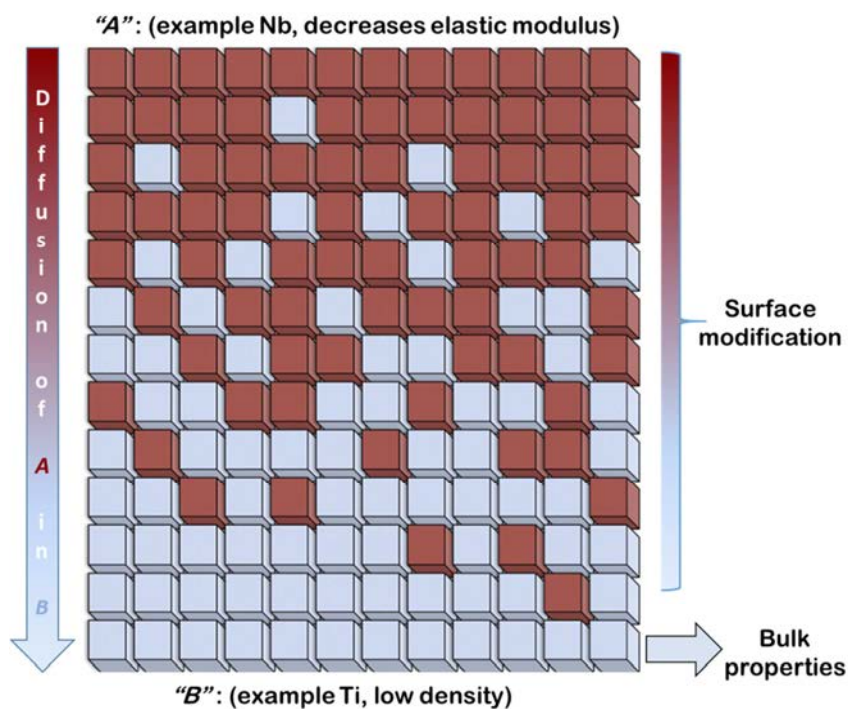


**Figure 1.6** Schematic representation of a diffusion surface process combining A (red) and B (grey), for example: "A" (Nb) providing a decrease of elastic modulus and "B" (Ti) with low density, high corrosion resistance, biocompatibility... without strong interfaces (adapted from [40]).

Numerous differences can be found between these two techniques. In the case of the ion-beam sputtering technique, the device was developed by using a high vacuum chamber, Ar atmosphere, an energy source and a beam current. Whereas in pack cementation, the coating is formed on the substrate by immersion in a powder mixture composed of a metal donor, inert filler and halide salts (activators). This technique has been shown the molybdenum deposition and also the formation of a titanium-nitride layer which is highly interesting due to its high hardness and wear-resistant properties.

Surface hardening is one of the main methods to achieve enhanced wear properties. This can be approached with a wide variety of surface modifications or coatings, for example: nitriding (nitrogen ion implantation or nitrogen diffusion hardening), plasma immersion ion implantation, oxidizing, PVD/CVD coatings, thermal spray or EPD. The deposition of titanium-nitride (TiN) coatings on Ti alloys by means of all of these surface treatments has been reported as one of the most effective techniques to reduce the coefficient of friction between the sliding materials together with the wear volume, resulting in the improvement of wear behaviour [3], [41]. Moreover, non-cytotoxic response have been shown for TiN coatings demonstrating their high biocompatibility [32], [42]. Nevertheless, the development of this type of wear-protective coatings needs to be optimized since defects on them could lead to third body wear due to delamination [43].

On one hand, physical vapor deposition (PVD) techniques are based on vaporizing materials from a source material to be deposited on the substrate. They are classified in vacuum, ion spraying or magnetron sputtering categories, being highly used to coat titanium or Ti alloys. Dense TiN coatings have been obtained through this technique to improve wear resistance, but also hydroxyapatite (HA) coatings, showing excellent adhesion forces and enhanced bioactivity [15].

On the other hand, electrophoretic deposition (EPD) technique has been also successful to coat Ti substrates with TiN layer or even TiN/TiCN multilayer systems by means of the electrophoretic movement of charged particles in a stable suspension and their deposition onto a conducting substrate. This is a suitable method when 3D or complex shapes need to be coated [44].

### 1.3.2 Improvement of the corrosion behaviour of titanium alloys

Surface modification technique has been focused on improving the corrosion resistance of biomedical metals due to the corrosive character of human body surroundings. Since wear, corrosion and tribocorrosion properties are very close related each other, the most employed techniques for corrosion-resistant behaviour are also used for the improvement of wear-corrosion resistance. Deposition of a thin

uniform coating, development of stable passivation oxide layer, ion beam processing and surface texturing are among the main surface treatments for corrosion protection [11].

For coatings deposition, electrophoretic deposition is also used as in the case for the mechanical improvement. Moreover, sol-gel technique allows not only good corrosion behaviour but also coating titanium alloys with bioactive materials. This is based on mixing different organic precursors in aqueous medium to prepare the “sol” and then, the mixture is poly-condensated to form “gel” used to coat [45].

A stable surface oxide layer on the passivated metal surface has an important effect on corrosion resistance, metal ions release and biocompatibility with human tissues. The surface passivity can be enhanced by using different treatments modifying thickness, morphology, or chemical composition of the surface metal [46]. For example, thermal or electrochemical, and passivation in nitric acid are surface treatments used for the surface passivation. A thermal oxidation treatment was performed on a Ti-6Al-4V surface, leading to a rutile layer with good corrosion behaviour and improved biological response [47].

Regarding chemical composition, Nb addition has a stabilizing effect on the Ti surfaces, being also beneficial in the resistance to dissolution and passivation of the surface by decreasing the quantity of anion vacancies. This is because the niobium oxide formed is very stable in physiological environment [1]. This can be achieved through different techniques such as diffusion, ion beam processing or plasma alloying [18]. Improved corrosion resistance has been also reported for the Mo addition to Ti-6Al-4V and Ti surfaces compared to the bare substrates [36], [48], [49], [50].

Furthermore, surface texturing has been introduced as another method for improving corrosion while promoting osseointegration. This category includes surface plasma-spraying, electro-polishing, anodic oxidation, sandblasting, acid etching or bioactive coatings. They are mainly focused on enhancing bone-surface metallic interactions. Thereby, they will be discussed in the following section.

### 1.3.3 Improvement of the biocompatibility character of titanium alloys

Despite good mechanical properties and excellent corrosion resistance, biomedical metals for hard tissue replacement should present good biocompatibility. Ti alloys have been usually considered as bioinert instead of bioactive materials. However, a recent concept known as “**bio-functionalization**” has gained great attention. Bio-functionalization of biomedical metals means to endow biomaterials with bio-functions, make them more suitable for biomedical applications. Bioactivity, bony

tissue inducing, anti-microbial, anti-tumor, anticoagulation, or drug loading functions are the new functions introduced to biomedical metals [51].

There is a large range of surface modification processes to enhance all of these aspects by altering surface morphology and composition. These can be grouped in two main categories: surface treatments, and inorganic/organic coatings. The first category is associated to the application of physical or chemical agents to the surface, including sandblasting, wet etching, anodization, laser radiation, electron beams or plasma etching [19]. The second one makes reference to apply inorganic or organic coatings such as hydroxyapatite (HA), calcium phosphate (CaP), titanium oxide (TiO<sub>2</sub>), strontium (Sr), polymers (i.e. ethylenediamine, polyethylenediamine, ...), proteins [52]. These surface treatments have shown achievements in bioactive modifications for enhancing bone quality, antimicrobial features, reproducing hydroxyapatite composition naturally formed in bone, or nanostructured modifications to determine the optimal surface nano-topography for intrabony applications.

Surface roughness, wettability, morphology, and composition have been demonstrated to be very important when designing a material since they have a great influence in the bioactivity and biological response.

Regarding roughness, hydroxyapatite grows easier on rougher than on smoother titanium surfaces. Relatively rougher surfaces present higher specific area providing more nucleation places which promotes the hydroxyapatite formation [53]. Among the most employed treatments for bioactivation are: roughening by Ti plasma-spraying, grit-blasting, acid-etching [54], [55] alkali-heat treatment [56], [57] anodization [58], porosity [59], at nanoscale level [60], biomimetic calcium phosphate coatings [61], incorporation of biologically active drugs [62].

However, some of them need to be improved since they solve one problem by bringing another one. On one hand, it has been reported that an artificial hip joint made from titanium with HA-coating was bioactive, but the poor adhesive strength between HA layer and the substrate resulted in the implant failure [63]. Bioactivity was shown on Ti-6Al7Nb alloy after a combination of phosphoric acid etching with alkaline surface treatments [64]. On the other hand, the acid alkali treatment or alkali heat treatment gives basicity to the surface being the cell proliferation highly reduced.

Morphology is considered as another important aspect for the biological properties improvement. Among various surface modification techniques, micro-arc oxidation (MAO) is useful to produce porous, adhesive and bioactive coatings for implantation. Moreover, it has been reported that titanium surfaces subjected to MAO technique in combination with thermal treatment, sandblasting or

electrophoretic deposition present better biocompatibility feature with respect to only MAO [65]. Hydroxyapatite was formed after soaking in simulated body fluid (SBF) for 2 weeks on Ti and Ti-6Al-4V surfaces. Higher cell viability was also shown in the surface-modified materials. The anodic oxidation surface treatment of the low elastic modulus Ti-24Nb-4Zr-7.9Sn alloy enhanced osseointegration and biocompatibility with respect to titanium [66].

Furthermore regarding chemical composition, it has been found that the addition of Nb, Zr or Ta decreases the ion release and relatively increases the cell growth and proliferation in some  $\beta$ -Ti alloys with respect to the Ti-6Al-4V alloy [67], [68], [69], [70]. Different techniques have been used in the deposition of Nb or Ta elements: niobium films by magnetron sputtering [71], aqueous co-precipitation process of Nb-doped HA materials [72], Ta nanocrystalline coating by double cathode glow discharge [73]; resulting all of them in good biological response.

Figure 1.7 shows a bioactive titanium alloy (Ti-6Al-2Nb-Ta) used in a hip joint system. This prosthesis is composed of parts made from different material Ti-6Al-2Nb-Ta or Ti, and also with and without surface modification. In this case, parts made from the Ti alloy (screw, socket and stem) were unmodified, whereas the Ti surfaces (proximal and socket surface) were fabricated with macro-porous topography and a surface alkali heat treatment.

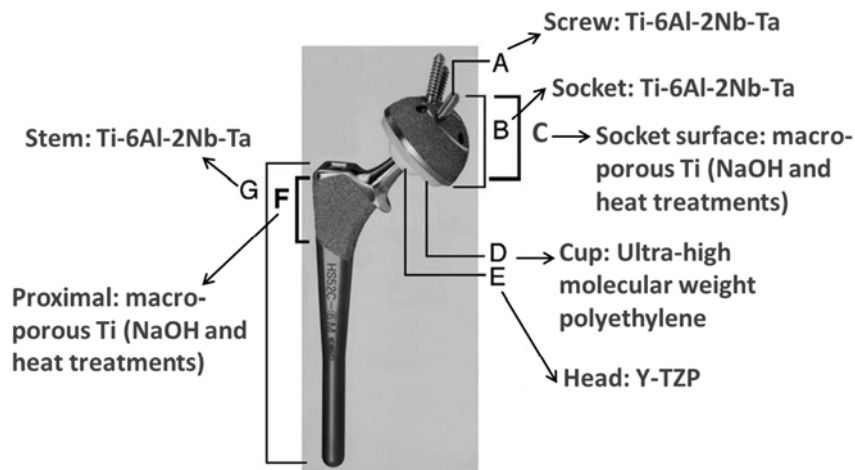


**Figure 1.7** Bioactive titanium metal used in a hip joint system (Kobe steel Ltd., Japan) [13].

## 1.4 References

- [1] M. Geetha, a. K. Singh, R. Asokamani, and a. K. Gogia, "Ti based biomaterials, the ultimate choice for orthopaedic implants - A review," *Prog. Mater. Sci.*, vol. 54, no. 3, pp. 397–425, 2009.



- [2] X. Liu, P. K. Chu, and C. Ding, "Surface modification of titanium, titanium alloys, and related materials for biomedical applications," *Mater. Sci. Eng. R Reports*, vol. 47, no. 3–4, pp. 49–121, 2004.
- [3] L. Kunčická, R. Kocich, and T. C. Lowe, "Advances in Metals and Alloys for Joint Replacement," *Prog. Mater. Sci.*, no. April, 2017.
- [4] Y. Li, C. Yang, H. Zhao, S. Qu, X. Li, and Y. Li, "New Developments of Ti-Based Alloys for Biomedical Applications," *Materials (Basel)*, vol. 7, no. 3, pp. 1709–1800, 2014.
- [5] A. T. Sidambe, "Biocompatibility of Advanced Manufactured Titanium Implants—A Review," *Materials (Basel)*, no. 7, pp. 8168–8188, 2014.
- [6] N. S. Manam *et al.*, "Study of corrosion in biocompatible metals for implants: A review," *J. Alloys Compd.*, vol. 701, pp. 698–715, 2017.
- [7] M. Hussein, A. Mohammed, and N. Al-Aqeeli, "Wear Characteristics of Metallic Biomaterials: A Review," *Materials (Basel)*, vol. 8, no. 5, pp. 2749–2768, 2015.
- [8] Q. Chen and G. A. Thouas, "Metallic implant biomaterials," *Mater. Sci. Eng. R*, vol. 87, pp. 1–57, 2015.
- [9] M. Niinomi, "Mechanical biocompatibilities of titanium alloys for biomedical applications," *J. Mech. Behav. Biomed. Mater.*, vol. 1, no. 1, pp. 30–42, 2008.
- [10] A. Revathi *et al.*, "Current advances in enhancement of wear and corrosion resistance of titanium alloys – a review," *Mater. Technol.*, vol. 7857, no. DOI: 10.1080/10667857.2016.1212780, 2016.
- [11] R. I. M. Asri *et al.*, "Corrosion and surface modification on biocompatible metals: A review," *Mater. Sci. Eng. C*, vol. 77, pp. 1261–1274, 2017.
- [12] M. Talib, Z. A. Khan, and A. Noor, "Surface Modifications of Titanium Materials for developing Corrosion Behavior in Human Body Environment : A Review," *Procedia Mater. Sci.*, vol. 6, no. Icmpe, pp. 1610–1618, 2014.
- [13] T. Kokubo, H. Kim, and M. Kawashita, "Novel bioactive materials with different mechanical properties," vol. 24, pp. 2161–2175, 2003.
- [14] X. Dai, X. Zhang, M. Xu, Y. Huang, and C. Heng, "Synergistic effects of elastic modulus and surface topology of Ti-based implants on early osseointegration," *RSC Adv.*, vol. 6, pp. 43685–43696, 2016.
- [15] M. Z. Ibrahim, A. A. D. Sarhan, F. Yusuf, and M. Hamdi, "Biomedical materials and techniques to improve the tribological, mechanical and biomedical properties of orthopedic implants - A review article," *J. Alloys Compd.*, vol. 714, pp. 636–667, 2017.
- [16] L. Diaz, F. R. García-Galvan, I. Llorente, A. Jiménez-Morales, J. C. Galván, and F. Jr, "Effect of heat treatment of magnesium alloy substrates on corrosion resistance of a hybrid organic–inorganic sol–gel film," *RSC Adv.*, vol. 5, pp. 105735–105746, 2015.

- [17] F. A. Shah, M. L. Johansson, O. Omar, H. Simonsson, A. Palmquist, and P. Thomsen, "Laser-Modified Surface Enhances Osseointegration and Biomechanical Anchorage of Commercially Pure Titanium Implants for Bone-Anchored Hearing Systems," *PLoS One*, vol. 11, no. 6, 2016.
- [18] J. B. Fogagnolo, A. V Rodrigues, E. Sallica-leva, M. S. F. Lima, and R. Caram, "Surface stiffness gradient in Ti parts obtained by laser surface alloying with Cu and Nb," *Surf. Coat. Technol.*, vol. 297, pp. 34–42, 2016.
- [19] P. Mandracci, F. Mussano, P. Rivolo, and S. Carossa, "Surface Treatments and Functional Coatings for Biocompatibility Improvement and Bacterial Adhesion Reduction in Dental Implantology," *Coatings*, vol. 6, no. 7, pp. 1–22, 2016.
- [20] S. Divinski, F. Hisker, C. Klinkenberg, and C. Herzig, "Niobium and titanium diffusion in the high niobium-containing Ti-54Al-10Nb alloy," *Intermetallics*, vol. 14, no. 7, pp. 792–799, 2006.
- [21] W. P. Liang, Z. Xu, Q. Miao, X. P. Liu, and Z. Y. He, "Double glow plasma surface molybdenizing of Ti<sub>2</sub>AlNb," *Surf. Coatings Technol.*, vol. 201, no. 9–11 SPEC. ISS., pp. 5068–5071, 2007.
- [22] F. M. El-hossary, N. Z. Negm, A. M. A. El-rahman, M. Raaif, A. A. Seleem, and A. A. A. El-moula, "Tribo-mechanical and electrochemical properties of plasma nitriding titanium," *Surf. Coat. Technol.*, vol. 276, pp. 658–667, 2015.
- [23] K. Kowalski, a. Bernasik, J. Camra, M. Radecka, and J. Jedliński, "Diffusion of niobium in yttria-stabilized zirconia and in titania-doped yttria-stabilized zirconia polycrystalline materials," *J. Eur. Ceram. Soc.*, vol. 26, no. 15, pp. 3139–3143, 2006.
- [24] S. Sedira, S. Achour, A. Avci, and V. Eskizeybek, "Physical deposition of carbon doped titanium nitride film by DC magnetron sputtering for metallic implant coating use," *Appl. Surf. Sci.*, vol. 295, pp. 81–85, 2014.
- [25] A. M. Kamat, A. E. Segall, S. M. Copley, and J. A. Todd, "Enhancement of CP-titanium wear resistance using a two-step CO<sub>2</sub> laser-sustained plasma nitriding process," *Surf. Coat. Technol.*, vol. 325, pp. 229–238, 2017.
- [26] J. Qian, K. Farokhzadeh, and A. Edrissy, "Ion nitriding of a near- $\beta$  titanium alloy: Microstructure and mechanical properties," *Surf. Coat. Technol.*, vol. 258, pp. 134–141, 2014.
- [27] I. Pohrelyuk, O. Yaskiv, and V. Fedirko, "Forming carbonitride coatings on titanium by thermochemical treatment with C-N-O-containing media," *Jom*, vol. 59, no. 6, pp. 32–37, 2007.
- [28] Y. Qin, D. Xiong, J. Li, and R. Tyagi, "Corrosion and bio-tribological properties of Ti(CN)<sub>x</sub> hard coating on titanium alloy by the pulsed plasma electrolytic carbonitriding process," *Tribology Int.*, vol. 82, pp. 543–550, 2015.
- [29] X. M. Peng, C. Q. Xia, Y. Y. Liu, and J. H. Wang, "Surface molybdenizing on titanium by halide-activated pack cementation," *Surf. Coatings Technol.*, vol. 203, no. 20–21, pp. 3306–3311, 2009.

- [30] X. Peng, C. Xia, Y. Liu, and Z. Zhang, "Comparison of molybdenizing and NiCrAlY coating on Ti and Ti-6Al-4V," *Rare Met.*, vol. 28, no. 1, pp. 49–56, 2009.
- [31] S. A. Tsipas and E. Gordo, "Molybdeno-Aluminizing of Powder Metallurgy and Wrought Ti and Ti-6Al-4V alloys by Pack Cementation process," *Mater. Charact.*, vol. 118, pp. 494–504, 2016.
- [32] A. P. Serro *et al.*, "A comparative study of titanium nitrides, TiN, TiNbN and TiCN, as coatings for biomedical applications," *Surf. Coat. Technol.*, vol. 203, no. 24, pp. 3701–3707, 2009.
- [33] D. Viteri, G. Barandika, R. Bayo, V. Sa, J. E. Moreno, and C. Pe, "Development of Ti–C–N coatings with improved tribological behavior and antibacterial properties," *J. Mech. Behav. Biomed. Mater.*, vol. 55, pp. 75–86, 2016.
- [34] C. Wu, M. Chen, T. Zheng, and X. Yang, "Effect of surface roughness on the initial response of MC3T3-E1 cells cultured on polished titanium alloy," *Biomed. Mater. Eng.*, vol. 26, pp. 155–164, 2015.
- [35] W. F. Ho, C. H. Lai, H. C. Hsu, and S. C. Wu, "Surface modification of a low-modulus Ti-7.5Mo alloy treated with aqueous NaOH," *Surf. Coatings Technol.*, vol. 203, no. 20–21, pp. 3142–3150, 2009.
- [36] N. Somsanith, T. S. N. S. Narayanan, Y. Kim, I. Park, T. Bae, and M. Lee, "Surface medication of Ti–15Mo alloy by thermal oxidation: Evaluation of surface characteristics and corrosion resistance in Ringer's solution," *Appl. Surf. Sci.*, vol. 356, pp. 1117–1126, 2015.
- [37] C. Mendoza, Z. Gonzalez, E. Gordo, B. Ferrari, and Y. Castro, "Protective nature of nano-TiN coatings shaped by EPD on Ti substrates," *J. Eur. Ceram. Soc.*, vol. 38, pp. 495–500, 2018.
- [38] N. H. Faisal, "Development of Plasma-Sprayed Molybdenum Carbide-Based Anode Layers with Various Metal Oxides for SOFC," *J. Therm. Spray Technol.*, vol. 24, no. 8, pp. 1415–1428, 2015.
- [39] K. Xu *et al.*, "Influence of strontium ions incorporated into nanosheet-pore topographical titanium substrates on osteogenic differentiation of mesenchymal stem cells in vitro and on osseointegration in vivo †," *J. Mater. Chem. B*, vol. 4, no. 3, pp. 4549–4564, 2016.
- [40] A. Sola, D. Bellucci, and V. Cannillo, "Functionally graded materials for orthopedic applications – an update on design and manufacturing," *Biotechnol. Adv.*, vol. 34, no. 5, pp. 504–531, 2016.
- [41] S. J. L. Sullivan and L. D. T. Topoleski, "Surface Modifications for Improved Wear Performance in Artificial Joints: A Review," *Miner. Met. Mater. Soc.*, vol. 67, no. 11, pp. 2502–2517, 2015.
- [42] B. Subramanian, C. V. Muraleedharan, R. Ananthakumar, and M. Jayachandran, "A comparative study of titanium nitride (TiN), titanium oxy nitride (TiON) and titanium aluminum nitride (TiAlN), as surface coatings for bio implants," *Surf. Coat. Technol.*, vol. 205, no. 21–22, pp. 5014–5020, 2011.

- [43] R. P. Van Hove, I. N. Siervelt, B. J. Van Royen, and P. A. Nolte, "Titanium-Nitride Coating of Orthopaedic Implants : A Review of the Literature," vol. 2015, 2015.
- [44] L. Besra and M. Liu, "A review on fundamentals and applications of electrophoretic deposition (EPD)," *Prog. Mater. Sci.*, vol. 52, no. 1, pp. 1–61, 2007.
- [45] M. F. Montemor, "Functional and smart coatings for corrosion protection: A review of recent advances," *Surf. Coat. Technol.*, vol. 258, pp. 17–37, 2014.
- [46] T. Hanawa, K. Asami, and K. Asaoka, "Repassivation of titanium and surface oxide film regenerated in simulated bioliquid," *J. Biomed. Mater. Res.*, vol. 40, pp. 530–538, 1998.
- [47] M. C. García-Alonso *et al.*, "In vitro corrosion behaviour and osteoblast response of thermally oxidised Ti6Al4V alloy," *Biomaterials*, vol. 24, pp. 19–26, 2003.
- [48] A. L. Fan, C. G. Zhi, L. H. Tian, L. Qin, and B. Tang, "Corrosion Behaviours of Mo Modified Ti<sub>6</sub>Al<sub>4</sub>V Alloy in Hank's Solution," *Mater. Sci. Forum*, vol. 610–613, pp. 1150–1154, 2009.
- [49] N. T. C. Oliveira and a. C. Guastaldi, "Electrochemical stability and corrosion resistance of Ti-Mo alloys for biomedical applications," *Acta Biomater.*, vol. 5, no. 1, pp. 399–405, 2009.
- [50] X. Yao, B. Tang, A. Fan, L. Tian, and L. Qin, "Structure and corrosion behaviours of Mo modified titanium in saliva," *J. Wuhan Univ. Technol. Sci. Ed.*, vol. 25, no. 4, pp. 570–573, 2010.
- [51] M. Xiao, Y. M. Chen, M. N. Biao, X. D. Zhang, and B. C. Yang, "Bio-functionalization of biomedical metals," *Mater. Sci. Eng. C*, vol. 70, pp. 1057–1070, 2017.
- [52] S. Neubauer, H. Kessler, F. J. Gil, M. Pegueroles, and J. M. Manero, "Tuning Mesenchymal Stem Cell Response onto Titanium–Niobium–Hafnium Alloy by Recombinant Fibronectin Fragments," *ACS Appl. Mater. Interfaces*, vol. 8, pp. 2517–2525, 2016.
- [53] L. Le Guehennec, A. Soueidan, P. Layrolle, and Y. Amouriq, "Surface treatments of titanium dental implants for rapid osseointegration," *Dent. Mater.*, vol. 23, pp. 844–854, 2007.
- [54] P. F. Gostin, A. Helth, A. Voss, R. Sueptitz, M. Calin, and A. Gebert, "Surface treatment, corrosion behavior, and apatite-forming ability of Ti-45Nb implant alloy," *J. Biomed. Mater. Res. B Appl. Biomater.*, vol. 101, no. 2, pp. 269–278, 2013.
- [55] B. C. Von Wilmsky *et al.*, "Osseointegration of Chemically Modified Titanium Surfaces: An in Vivo Study," *Adv. Eng. Mater.*, vol. 10, no. 12, pp. 61–66, 2008.
- [56] S. Nishiguchi *et al.*, "Titanium metals form direct bonding to bone after alkali and heat treatments," *Biomaterials*, vol. 22, pp. 2525–2533, 2001.

- [57] F. Liang, L. Zhou, and K. Wang, "Apatite formation on porous titanium by alkali and heat-treatment," *Surf. Coatings Technol.*, vol. 165, pp. 133–139, 2003.
- [58] A. Kazek-ke *et al.*, "In vitro bioactivity investigations of Ti-15Mo alloy after electrochemical surface modification," *J. Biomed. Mater. Res. B Appl. Biomater.*, vol. 104, no. 5, pp. 903–913, 2016.
- [59] J. Xu *et al.*, "Potential Use of Porous Titanium–Niobium Alloy in Orthopedic Implants: Preparation and Experimental Study of Its Biocompatibility In Vitro," *PLoS One*, vol. 8, no. 11, pp. 1–13, 2013.
- [60] M. Wen, L. Zhou, W. Guan, Y. Li, and J. Zhang, "Formation and bioactivity of porous titania containing nanostructured Ag," *Appl. Surf. Sci.*, vol. 256, pp. 4226–4230, 2010.
- [61] A. Hoppe, J. Will, R. Detsch, A. R. Boccaccini, and P. Greil, "Formation and in vitro biocompatibility of biomimetic hydroxyapatite coatings on chemically treated carbon substrates," *J. Biomed. Mater. Res. A*, vol. 102, no. 1, pp. 193–203, 2014.
- [62] J. P. Cattalini, J. García, A. R. Boccaccini, S. Lucangioli, and V. Mouriño, "A new calcium releasing nano-composite biomaterial for bone tissue engineering scaffolds," *Procedia Eng.*, vol. 59, pp. 78–84, 2013.
- [63] W. A. Camargo *et al.*, "Effect of surface alkali-based treatment of titanium implants on ability to promote in vitro mineralization and in vivo bone formation," *Acta Biomater.*, vol. 57, pp. 511–523, 2017.
- [64] D. P. Oliveira *et al.*, "Surface chemical treatment of ultrafine-grained Ti–6Al–7Nb alloy processed by severe plastic deformation," *J. Alloys Compd.*, vol. 643, pp. S241–S245, 2015.
- [65] Y. Wang, H. Yu, C. Chen, and Z. Zhao, "Review of the biocompatibility of micro-arc oxidation coated titanium alloys," *JMADE*, vol. 85, pp. 640–652, 2015.
- [66] X. Li *et al.*, "Modified surface morphology of a novel Ti–24Nb–4Zr–7.9Sn titanium alloy via anodic oxidation for enhanced interfacial biocompatibility and osseointegration," *Colloids Surfaces B Biointerfaces*, vol. 144, pp. 265–275, 2016.
- [67] M. Niinomi, "Recent Metallic Materials for Biomedical Applications," *Metall. Mater. Trans. A*, vol. 33, no. MARCH, pp. 477–486, 2002.
- [68] D. Perez *et al.*, "Titanium–35niobium alloy as a potential material for biomedical implants: In vitro study," *Mater. Sci. Eng. C*, vol. 56, pp. 538–544, 2015.
- [69] R. Medda *et al.*, "Investigation of early cell–surface interactions of human mesenchymal stem cells on nanopatterned  $\beta$ -type titanium–niobium alloy surfaces," *Interface Focus*, vol. 4, p. doi: 10.1098/rsfs.2013.0046, 2014.
- [70] P. Neacsu, D. Gordin, V. Mitran, T. Gloriant, M. Costache, and A. Cimpean, "In vitro performance assessment of new beta Ti–Mo–Nb alloy compositions," *Mater. Sci. Eng. C*, vol. 47, pp. 105–113, 2015.

- [71] G. Ramírez, S. E. Rodil, H. Arzate, S. Muhl, and J. J. Olaya, “Niobium based coatings for dental implants,” *Appl. Surf. Sci.*, vol. 257, pp. 2555–2559, 2011.
- [72] V. S. Ciminelli and H. S. Mansur, “Niobium-Doped Hydroxyapatite Bioceramics: Synthesis, Characterization and In Vitro Cytocompatibility,” *Materials (Basel)*, vol. 8, pp. 4191–4209, 2015.
- [73] L. Liu, J. Xu, and S. Jiang, “Nanocrystalline  $\beta$ -Ta Coating Enhances the Longevity and Bioactivity of Medical Titanium Alloys,” *Metals (Basel)*, vol. 6, no. 221, pp. 1–27, 2016.

# **Motivations and Objectives**

**2.1 Motivations**

**2.2 Objectives**

**2.3 References**

## 2.1 Motivations

The use of titanium and its alloys in the biomedical sector as bone replacements is really well-known. However, due to the elder population is still growing, there is a great demand on researching biomaterials for knee, hip or shoulder prosthesis with the aim to improve the performance of the most commonly implants employed [1], [2]. Currently, the main advantage of titanium for the biomedical sector is its excellent combination of properties, among the most remarkable ones: low density, high specific strength, high corrosion resistance and good biocompatibility. As it mentioned in the introduction chapter, the importance of titanium in biomedical applications relies on their better response for specific applications in comparison to some stainless steel or Co-Cr alloys employed [3].

However, the employ of titanium and its alloys in the biomedical industry also presents some drawbacks due to the metallic ions release to biological fluid together with the possible cytotoxic effect provoked by the deteriorating of the implant. These harmful effects come from aspects which need to be enhanced such as: problems basically based on the poor wear and tribological properties, the employment of toxic elements (Al, V) in the composition of the titanium alloys, or their Young's modulus values (lower than other metallic alloys but still superior to that of human bone) [2], [4].

Therefore, with the aim to improve these concerning properties of Ti, the surface modification by diffusion of  $\beta$ -stabilizing elements [5] was the strategy selected due to the following reasons:

- The  $\beta$ -stabilizing character of the elements selected (Nb and Mo) will become the Young's modulus closer to that of human bone.
- The creation of functionally gradient Ti surfaces with gradients in their properties while keeping the lightness of Ti in core.
- The use of different thermo-chemical treatments based on diffusion processes as via for the enhancement of wear and tribocorrosion behaviour.
- Nb and Mo are considered as biocompatible elements with an increasing interest in the biomedical sector.

The surface treatments selected in this work consisted of i) deposition and ii) diffusion treatments, require of a proper surface finishing ensuring the good behaviour and reproducibility of their final properties (mechanical, wear, tribocorrosion, corrosion and biocompatibility). However, considering the widely set of techniques to modify the surface of a material [6], [7], it is worth to mention some advantages found in our method of deposition and diffusion, such as: i) the use of water (environmentally-friendly) as solvent for the Mo and Nb suspension, ii) the



use of a low-energy method, iii) the employment of short diffusion times, and thus iv) a cost-effective process [8].

Aside of employing the surface modification, the titanium substrates fabrication was carried out through Powder Metallurgy (PM) route. In this context, this near-net shape technology is able to produce the final pieces with the desiring shape, saving the numerous machining steps and the waste of materials [9]. Therefore, the combination of the powder metallurgy together with the surface modification by diffusion of  $\beta$ -stabilizing elements will allow obtaining modified Ti surfaces with designed properties for biomedical applications.

## 2.2 Objectives

The main objective of this thesis work is the design and development of new modified titanium surfaces by surface modification through niobium and molybdenum diffusion treatments. This work is intended to be accomplished for biomedical applications with the goal of obtaining new Ti surfaces with improvements in some concerning properties, such us biocompatibility, lower Young modulus or wear resistance, while maintaining or improving corrosion behaviour.

This main goal of the investigation is achieved by means of the following partial objectives:

- To design different formulations of surface modification on titanium under different diffusion treatments. The diffusion process is simulated through DICTRA software to select the experimental diffusion conditions and establish a correlation between experimental and theoretical results.
- To investigate reproducible method of deposition guided by aqueous suspensions and diffusion treatments. This set of experiments will give an idea of how the diffusion process is influenced by the state of the titanium substrate, diffusion element or diffusion treatment.
- Once the processing studies are conducted and the surface conditions selected, microstructure and compositional changes are analyzed. Mechanical properties are measured on both surface and cross-section to have a global response on hardness and elastic modulus in order to be compared with those of titanium.

- To investigate wear, corrosion and the synergistic wear-corrosion interactions to evaluate the behaviour of these modified Ti surfaces in order to determine their functional properties. This experimental characterization will allow correlating the influence of the diffusion treatments performed on both dry wear and tribocorrosion behaviour as well as the corrosion resistance of these modified Ti surfaces.
- Finally, to study the biocompatibility features of the designed materials with the best combination of properties. These investigations will allow understanding the influence of the titanium surface modification on the bioactivity, cytotoxicity and osteogenic differentiation response. This will give an idea of their biological character to be proposed as possible candidates for biomaterials.

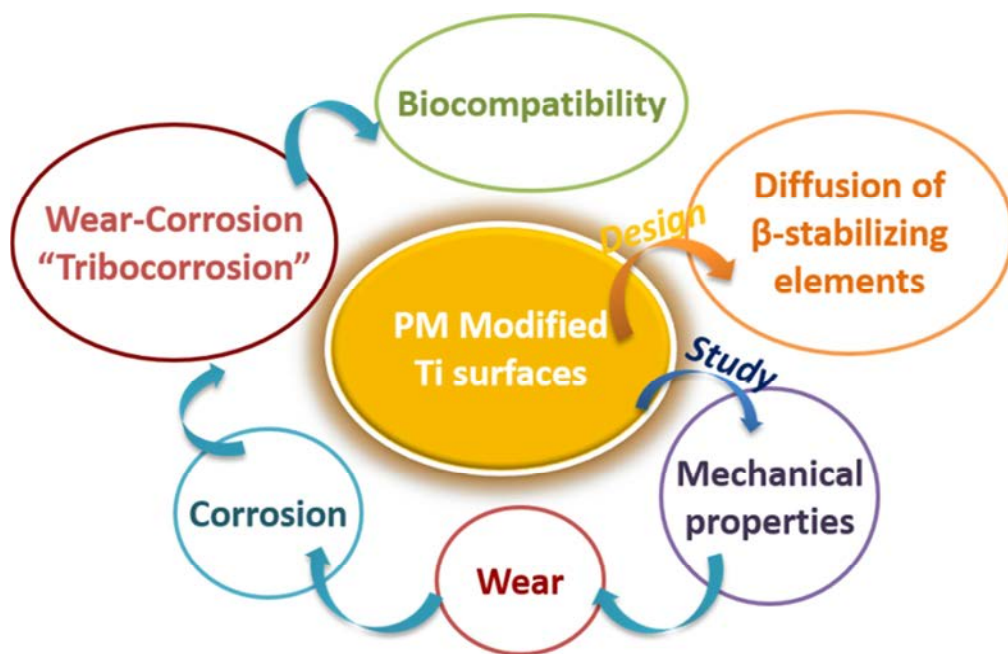


**Figure 2.1** Scheme of the partial goals to accomplish the main objective of this thesis work.

## 2.3 References

- [1] D. Banerjee and J. C. Williams, “Perspectives on Titanium Science and Technology,” *Acta Mater.*, vol. 61, no. 3, pp. 844–879, 2013.
- [2] M. Geetha, a. K. Singh, R. Asokamani, and a. K. Gogia, “Ti based biomaterials, the ultimate choice for orthopaedic implants - A review,” *Prog. Mater. Sci.*, vol. 54, no. 3, pp. 397–425, 2009.
- [3] M. T. Mohammed, Z. A. Khan, and A. N. Siddiquee, “Surface Modifications of Titanium Materials for developing Corrosion Behavior in Human Body

- Environment: A Review,” *Procedia Mater. Sci.*, vol. 6, no. Icmpec, pp. 1610–1618, 2014.
- [4] L. Kunčická, R. Kocich, and T. C. Lowe, “Advances in Metals and Alloys for Joint Replacement,” *Prog. Mater. Sci.*, no. April, 2017.
- [5] Y. Li, C. Yang, H. Zhao, S. Qu, X. Li, and Y. Li, “New Developments of Ti-Based Alloys for Biomedical Applications,” *Materials (Basel)*, vol. 7, no. 3, pp. 1709–1800, 2014.
- [6] X. Liu, P. K. Chu, and C. Ding, “Surface modification of titanium, titanium alloys, and related materials for biomedical applications,” *Mater. Sci. Eng. R Reports*, vol. 47, no. 3–4, pp. 49–121, 2004.
- [7] S. J. L. Sullivan and L. D. T. Topoleski, “Surface Modifications for Improved Wear Performance in Artificial Joints: A Review,” *Miner. Met. Mater. Soc.*, vol. 67, no. 11, pp. 2502–2517, 2015.
- [8] S. A. Tsipas and E. Gordo, “Molybdeno-Aluminizing of Powder Metallurgy and Wrought Ti and Ti-6Al-4V alloys by Pack Cementation process,” *Mater. Charact.*, vol. 118, pp. 494–504, 2016.
- [9] L. Bolzoni, T. Weissgaerber, B. Kieback, E. M. Ruiz-Navas, and E. Gordo, “Mechanical behaviour of pressed and sintered CP Ti and Ti-6Al-7Nb alloy obtained from master alloy addition powder,” *J. Mech. Behav. Biomed. Mater.*, vol. 20, pp. 149–161, 2013.

# **Experimental Work**

---

## **3.1 Scheme of the experimental work**

## **3.2 Materials design**

### 3.2.1 Starting materials

### 3.2.2 Simulation tool: DICTRA software

### 3.2.3 Designed materials

## **3.3 Material characterization**

### 3.3.1 Surface finishing process

### 3.3.2 Density

### 3.3.3 Roughness

### 3.3.4 Wettability

### 3.3.5 X-ray diffraction (XRD)

### 3.3.6 Field emission scanning electron microscopy (FE-SEM)

## **3.4 Mechanical characterization**

### 3.4.1 Microhardness

### 3.4.2 Macrohardness and elastic modulus

### 3.4.3 Nanoindentation and elastic modulus

## **3.5 Wear characterization**

## **3.6 Corrosion characterization**

## **3.7 Tribocorrosion characterization**

## **3.8 Biocompatibility characterization**

## **3.9 References**

### 3.1 Scheme of the experimental work

In this chapter the procedures carried out during the experimental part of the thesis together with a brief summary of the different techniques and methodologies employed for the materials characterization are presented.

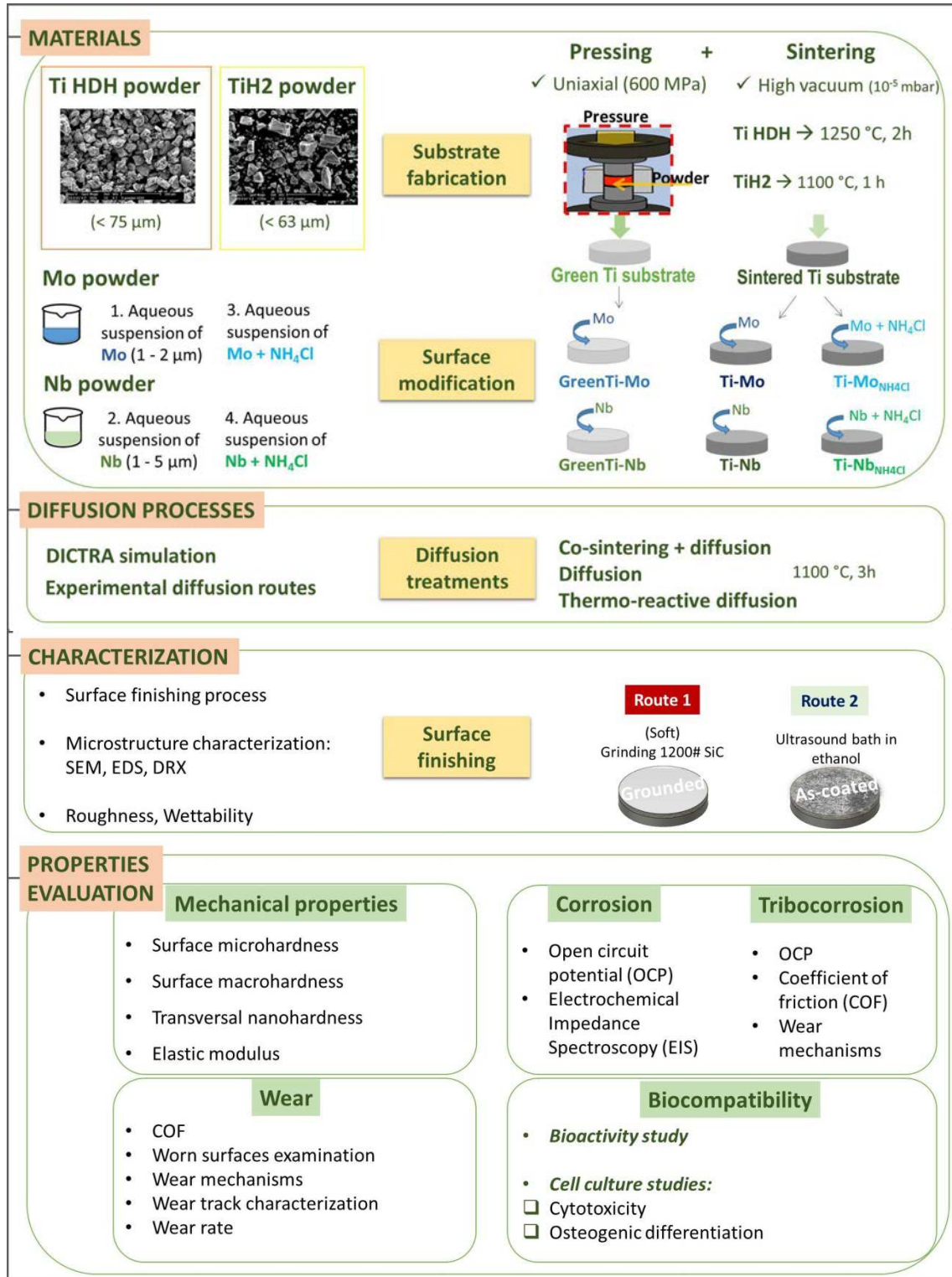


Figure 3.1 Scheme of the experimental work developed during the thesis.

Figure 3.1 shows the scheme of the whole experimental work developed during this thesis, from the design of the materials involving the simulation study of the diffusion process, the preparation of substrates and suspensions of diffusion elements, the experimental diffusion treatments, the microstructural analysis and the surface finishing process to their final characterization in order to determine if the process of surface modification result in an improvement of the Ti properties.

The experimental procedure has been oriented to reach the objectives proposed (see Chapter 2) to face some critical concerns of titanium as biomaterial such as reducing the Young's modulus and the improvement of wear resistance, while enhancing or maintaining the good corrosion behaviour and biological response in order to reach a compromise between these four aspects.

## **3.2 Materials design**

### **3.2.1 Starting materials**

The different powders used during this thesis work to develop the modified Ti materials are collected in Table 3.1. Two types of titanium powders were used to produce the substrates for the surface modification depending on the diffusion route employed. For the co-sintering route green substrates were produced from HDH Ti powders, grade 4, whereas for sintered substrates,  $\text{TiH}_2$  powders were selected, that provide dense Ti substrates after sintering. Mo and Nb powders were selected for diffusion into the titanium substrates due to their  $\beta$ -stabilizing character, while  $\text{NH}_4\text{Cl}$  was the additive employed for the thermo-reactive diffusion route.

**Table 3.1** Materials used for the fabrication of the modified Ti surfaces and their main characteristics according to suppliers.

	<i>Powders</i>				<i>Additive</i>
	<b>Ti HDH (grade 4)</b>	<b>TiH<sub>2</sub></b>	<b>Mo</b>	<b>Nb</b>	<b>NH<sub>4</sub>Cl</b>
<b>Supplier</b>	Advanced Powders and Coatings AP&C Inc	GfE Metals and Materials GmbH	Sigma Aldrich	Alfa Aesar	Alfa Aesar
<b>Particle size [μm]</b>	≈ 45	< 63	1 - 3	1 - 5	----
<b>Purity [%]</b>	----	----	99.9	99.8	99.5
<b>Density [g·cm<sup>-3</sup>]</b>	4.51	3.90	10.28	8.57	1.53
<b>Melting point [°C]</b>	1668		2623	2477	338
<b>Crystalline Structure</b>	Hcc (α)	Hcp	Bcc	Bcc	(CsCl)

### 3.2.2 Simulation tool: DICTRA software

The diffusion conditions were selected from literature [1] and predictions based on the Diffusion Controlled TRANSformations simulation software (DICTRA) [2], which is particularly suitable for problems involving a moving boundary. This software regards a system divided into cells where each cell can contain one or more regions defined in order to solve the diffusion problem. This sophisticated software was able to provide useful guidelines for selecting the optimal diffusion conditions as summarized in Figure 3.2.

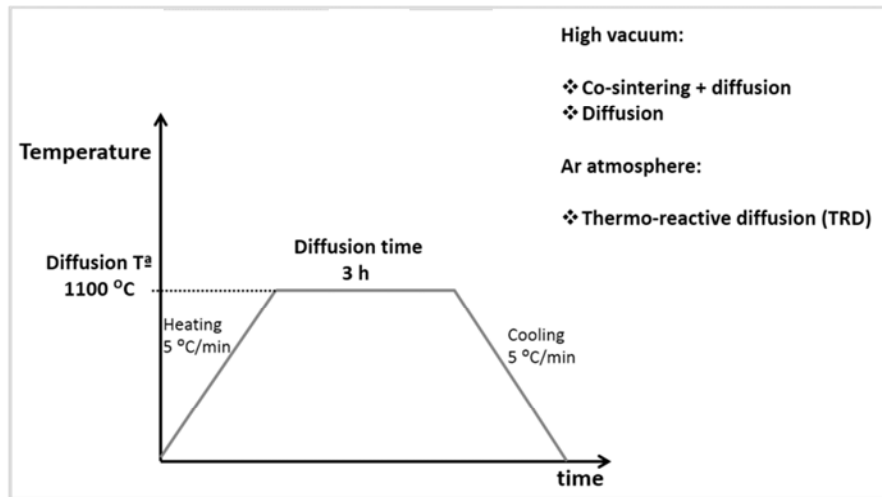


**Figure 3.2** Diffusion time and temperature conditions predicted by DICTRA.

Then, the design of the modified Ti materials is based on thermo-chemical treatments of deposition and diffusion processes. Three different routes were followed:

- **Route 1:** Deposition of an aqueous suspension of Nb or Mo onto green Ti compacts (**co-sintering + diffusion treatment**).
- **Route 2:** Deposition of an aqueous suspension of Nb or Mo onto sintered Ti substrates (**diffusion treatment**).
- **Route 3:** Deposition of an aqueous suspension of (Nb + NH<sub>4</sub>Cl) or (Mo + NH<sub>4</sub>Cl) onto sintered Ti substrates (**thermo-reactive diffusion treatment**).

Table 3.2 collects all the experimental diffusion conditions for the different routes.

**Table 3.2** Experimental diffusion conditions for the three treatments.

Routes	<i>Diffusion conditions</i>				
	Ti substrate	Temperature [°C]	Time [h]	Atmosphere	Activating agent
<b>Co-sintering + diffusion</b>	Green	1100	3	High vacuum	----
<b>Diffusion</b>	Sintered	1100	3	High vacuum	----
<b>Thermo-reactive diffusion</b>	Sintered	1100	3	Ar	NH <sub>4</sub> Cl

### 3.2.3 Designed materials

The conventional powder metallurgy route of pressing & sintering (P&S) was employed for the production of Ti substrates. Based on previous investigations of



the Group of Powder Technologies (GTP) [3], an uniaxial pressing step at 600 MPa using a cylindrical mold of 16 mm in diameter with lubricated walls by zinc stearate was carried out obtaining Ti green compacts of  $16.06 \pm 0.01$  mm in diameter and  $2.6 \pm 0.01$  mm in height. These Ti green compacts were employed for the co-sintering route. For the sintered Ti substrates, same pressing conditions were followed with the TiH<sub>2</sub> powder, obtaining the as-pressed TiH<sub>2</sub> parts which were placed inside a high vacuum furnace in a bed of zirconia balls as a support. Sintered Ti substrates were obtained after a sintering cycle at 1100 °C during 1 h under high vacuum conditions ( $10^{-5}$  mbar). These sintered Ti substrates of  $14.7 \pm 0.01$  mm in diameter and  $2.8 \pm 0.01$  mm in height were employed for the diffusion and thermo-reactive diffusion routes.

An important step for the diffusion treatments is the way to deposit the alloying elements. It is necessary to create a continuous and homogeneous layer of the alloying powder to ensure a correct diffusion in the whole surface. The method selected was the preparation of an aqueous suspension of molybdenum or niobium powder (characteristics shown in Table 3.1) was prepared. A suspension containing 10 % volume of powder particles was adjusted to pH 10 by tetramethylammonium hydroxide (HTMA). After a dilution (0.1 g/L) in KCl  $10^{-2}$  N, the suspension stability was evaluated as a function of its zeta potential at the pH of 2, 4, 6, 8, 10, and 12 (adjusted by HTMA and HNO<sub>3</sub>). Before each zeta potential measure, the different pH suspensions were submitted to an ultrasonic probe (Vibra cell TM, 750 W) at 55 % power for 30 s to homogenize and break unwanted agglomerates. The measure of the zeta potential was performed with the micro-electrophoresis technique by Zeta-Meter 3.0 Equipment. Two characteristic points define the surface state for a particle in a liquid medium: isoelectric point (value of pH which the zeta potential is zero) and point of charge zero (where the positive and negative surface charges are the same). Thus, a suspension can be considered stable if its zeta potential presents an absolute value superior to 20 mV [4]. Finally, 2 h in a ball mill for homogenization was necessary before spraying at room temperature the suspension onto the green and sintered titanium substrates.

The Mo or Nb suspensions were deposited onto the green Ti compacts to follow **route 1 (co-sintering + diffusion)**, where the sintering and diffusion processes take place in a one single step during a thermal treatment at 1100 °C, 3 h in high vacuum. In **route 2 (diffusion)**, the Mo or Nb aqueous suspension were deposited onto sintered Ti substrates. Thereby, the surface modification is reached during the thermal treatment at 1100 °C, 3 h in high vacuum promoting the diffusion.

**In route 3 (thermo-reactive diffusion)**, the activating agent (NH<sub>4</sub>Cl) was added to the Mo or Nb suspensions before spraying them onto the sintered Ti substrates. The addition of the ammonium chloride activator stimulates the diffusion phenomena due to the formation of volatile Mo or Nb chlorides, and titanium nitride is created on the surface, leading to some nitrogen diffusion inwards. 1.5 wt. % of NH<sub>4</sub>Cl was

added to the initial molybdenum or niobium suspensions, obtaining the (Mo + NH<sub>4</sub>Cl) or (Nb + NH<sub>4</sub>Cl) suspensions, respectively.

The deposition of the suspensions was performed through spraying process at room temperature by an advance aerography set composed of an oil free piston compressor (50 Psi) and an airbrush with a nozzle of 0.5 mm in diameter. A schematic view of the experimental procedure of the surface modification processes is shown in Figure 3.4. In each case, the final modified Ti material is composed of a modified layer (Ti-Nb or Ti-Mo) and an unmodified Ti part.

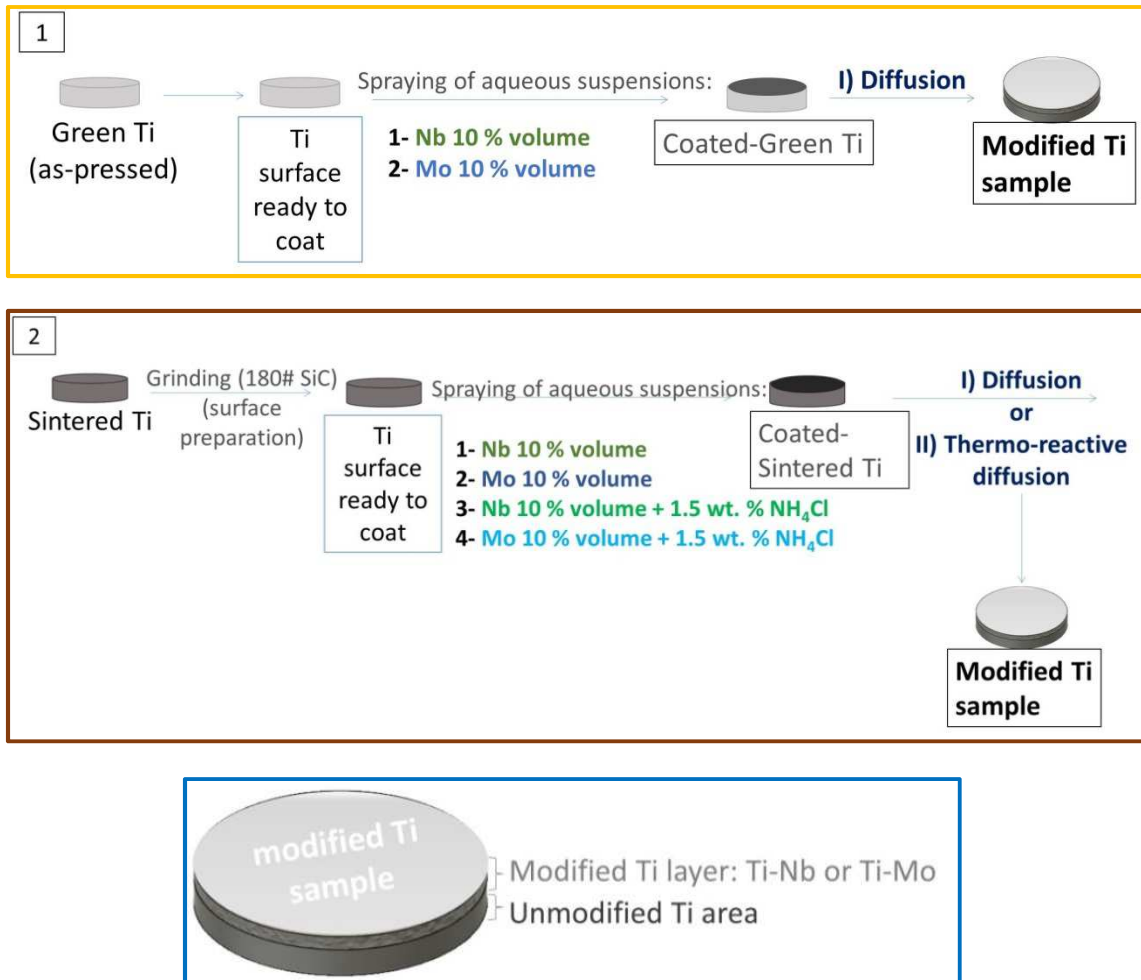


**Figure 3.4** Scheme of the surface modification process on: 1) Green Ti, and 2) Sintered Ti substrates; through the different suspensions designed and diffusion routes. Detailed view of a modified titanium sample.

The final designed materials together with their design parameters are summarized in Table 3.3.

**Table 3.3** Modified Ti surfaces and their design parameters.

Designed materials	Design parameters		
	Ti substrate	Diffusion element	Diffusion route
	<b>Ti</b>	Sintered	----
<b>GreenTi-Mo</b>	Green	Mo	Co-sintering + diffusion
<b>Ti-Mo</b>	Sintered	Mo	Diffusion
<b>Ti-Mo<sub>NH4Cl</sub></b>	Sintered	Mo + NH <sub>4</sub> Cl	Thermo-reactive diffusion
<b>GreenTi-Nb</b>	Green	Nb	Co-sintering + diffusion
<b>Ti-Nb</b>	Sintered	Nb	Diffusion
<b>Ti-Nb<sub>NH4Cl</sub></b>	Sintered	Nb + NH <sub>4</sub> Cl	Thermo-reactive diffusion

### 3.3 Material characterization

#### 3.3.1 Surface finishing process

Surface conditions are one of the main challenging parts of this work due to their influence on the final properties of the materials. The close relationship between chemical composition, roughness and wettability has been found as one of the main factors for a positive corrosion, tribological and biological response. Therefore, after performing the diffusion treatments and obtaining the designed materials, two different routes of surface finishing were followed as presented in Figure 3.5. On one hand (route 1), the surfaces of the modified Ti materials were prepared to remove the possible loose particles and to flatten the surfaces for a correct characterization by a soft grinding step with sandpaper of 1200 grade. This step was carefully performed in order to not remove the modified layers.

On the other hand, another different finishing process (route 2) was followed on the Ti-Nb and Ti-Mo materials in order to evaluate some properties of these coatings. In this route, the surfaces were finished after an ultrasound bath in ethanol for 5 min to remove some possible loose particles. These samples “as-coted” were labelled Ti-Nb<sub>coat</sub> and Ti-Mo<sub>coat</sub> and they were employed in the bioactivity and cytotoxicity tests in order to evaluate the effect of roughness and composition (Nb or Mo coatings) on hydroxyapatite formation and cell behaviour.

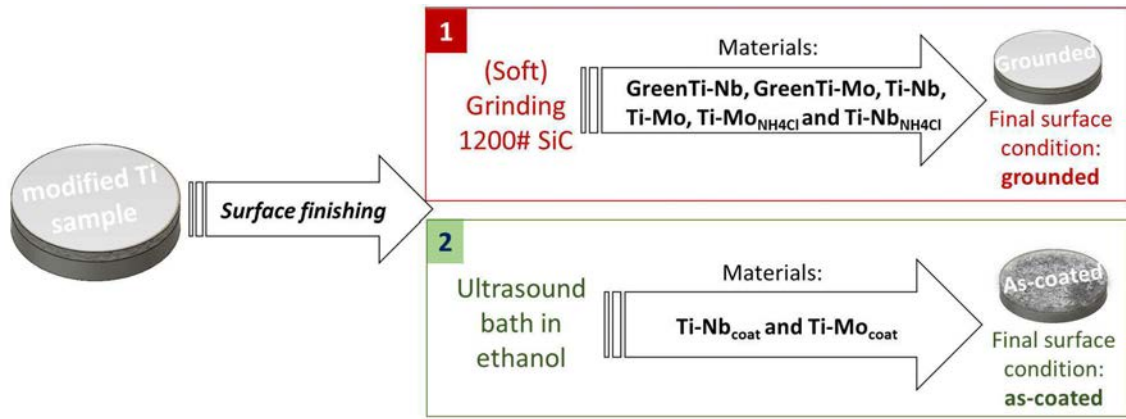


**Figure 3.5** Scheme of the two different routes of surface finishing process of the designed materials. Nomenclature used further on.

### 3.3.2 Density

The density of the green and sintered Ti substrates was geometrically characterized and measured with a Micrometrics Accupyc 1330 helium pycnometer. For these measurements, samples were weighted and placed in the pycnometer. After applying vacuum and fill the equipment with helium, the pressure is measured to calculate the gas volume and determine the sample volume by:

$$V_p = (V_c - V_r) \left[ \left( \frac{P_1}{P_2} \right) - 1 \right] \quad (\text{Eq. 3.1})$$

Where  $V_p$  is the sample volume,  $V_c$  the cell volume,  $V_r$  the reference volume and  $P_1$  and  $P_2$  pressures.

The surface porosity of the activated samples from the thermo-reactive diffusion route was estimated by image analysis with ImageJ software.

### 3.3.3 Roughness

The roughness of a surface is a key factor in the topography of a material, affecting their tribological properties as well as their corrosion and biocompatibility character. In this work, the final surface roughness was determined by a Hommel tester T500 contact profilometer and different roughness parameters ( $R_a$ ,  $R_t$ ,  $R_{max}$ ) were obtained.  $R_a$  is defined as the arithmetic average of the absolute values of all the points of the profile,  $R_t$  the vertical distance between the highest and lowest values of the profile and  $R_{max}$  the largest distance between peak and valley along the profile. In this study, the average roughness parameter ( $R_a$ ) was selected as the main one to be reported.

### 3.3.4 Wettability

Wettability is considered as one of the main factors affecting the biocompatibility character of a material. The measurement of this surface property through the contact angle between a water drop and the surface of a material allows determining their hydrophobicity or hydrophilic behaviour. Contact angle values higher than 90° indicate the more hydrophobic character of the surface while values lower than 90° suggest the hydrophilic behaviour as a sign of more affinity to water by the surface. This feature was evaluated by delivering a 3 µl water drop to the surfaces at room temperature in a DSA 30 Kruss.

### 3.3.5 X-ray diffraction (XRD)

The x-ray diffraction technique was employed in order to complement the microstructure characterization. The surface microstructural change and phase transformation was contrasted and confirmed through this technique by means of a Philips X'Pert x-ray diffractometer.

A fixed wavelength with a monochromatic x-ray beam (Cu K $\alpha$  radiation,  $\lambda=1.5405\text{\AA}$ ) was used. Measurements were performed under conditions of voltage 40 kV and current 40 mA, with a step of 0.02 ° varying the 2  $\theta$  angle from 20 ° to 120 °. The software HighScore allowed the acquisition and treatment of the data. Diffraction peaks obtained were identified and compared with those of patterns PCPDFWIN database.

### 3.3.6 Field emission scanning electron microscopy (FE-SEM)

Microstructural features of all the modified Ti surfaces were evaluated in both surface and cross-sections in order to analyze the phase transformations occurred during heat treatments. For that purpose, a FE-SEM (FEI Teneo) equipment was employed. Samples were previously grinded with sandpapers up to 1200 grade and polished by alumina suspensions depending on the material characteristics. Special care was taken to ensure the same surface finishing for each material.

In the scanning electron microscopy, an accelerated electron beam is bombarded against the sample in vacuum conditions and with different energies from 1 KeV to 50 KeV. Different signals are produced when the electron beam interacts with the material. The main signals are collected by two kinds of detectors, secondary electron (SE) and backscattering electron (BSE). The secondary electrons are low energy electrons emitted by atoms of the sample which are closer to surface during their interaction with the electron beam. This allows obtaining information about the morphology of the sample. On the other hand, the backscattering electrons proceed from the electron beam and they are reflected by atoms of the sample. They are high energy electrons which proceed from deeper zones. Therefore, this detector facilitates information about chemical composition, distinguishing darker and

brighter areas depending on the atomic number, indicating a brighter area a higher atomic number.

In this work, the microstructure characterization has been complemented with EDS profiles and mapping analysis to obtain a detailed information about the element and phase distribution. The chemical composition of all the surfaces was determined through semi-quantitative elements analysis performed by EDAX, energy disperse spectroscopy (EDS) detector. Additionally, the cross-section of all the materials was evaluated in order to obtain the composition profile of all the diffusion layers. These composition profiles and mappings analysis were carried out automatically by an EDAX device equipped in a FE-SEM obtaining detailed information about element distribution.

### **3.4 Mechanical characterization**

#### **3.4.1 Microhardness**

The effect of Nb or Mo diffusion in Ti on surface hardness was studied by Vickers micro-hardness measurements in a Zwick Roell micro-hardness tester. A comparison between the surface hardness of samples obtained by co-sintering + diffusion, diffusion or thermo-reactive diffusion processes were carried out. The measurements were performed with high precision in a microscopic scale. The load selected was 100 g ( $HV_{0.1}$ ) applied during 10 s with a diamond tip. Data was processed by ZH $\mu$  HD software and the results were expressed in HV. Additionally, HV results were converse to GPa multiplying by 0.009807 to be compared to macrohardness and nanohardness results.

#### **3.4.2 Macrohardness and elastic modulus**

To compare the microhardness results with results under macroscopic scale, indentation tests with 5 N load were performed on all the modified Ti surfaces. Three different parameters were evaluated: Vickers hardness, elastic modulus and maximum indentation depths. Measurements were performed by applying a load of 5 N at a speed load application of  $0.5 \text{ mm}\cdot\text{min}^{-1}$  and a speed load removal of  $2 \text{ mm}\cdot\text{min}^{-1}$  in a Zwick Roell Z 2.5 tester.

Vickers hardness was automatically obtained after measuring the footprints and the results were expressed in HV, and conversed to GPa. Elastic modulus values were obtained from the load-unload curves to have the first results about the effect of the  $\beta$ -stabilizing elements introduced in Ti, comparing the  $\beta$ -stabilizing character of Nb and Mo as well as the three diffusion processed employed.

Maximum indentation depth values give an idea of the penetration of the same load into different materials (Figure 3.6). They are related to hardness and they allow observing if the maximum indentation is higher or lower than the diffusion layer.

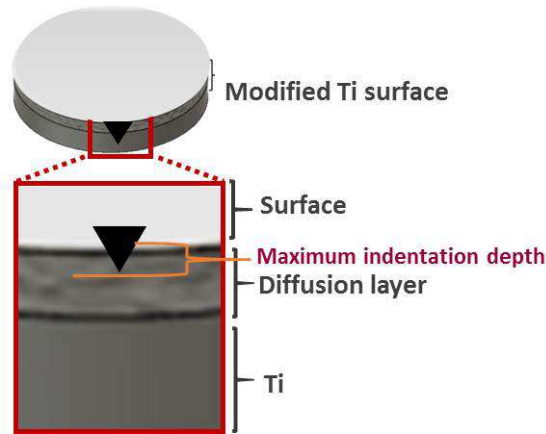


**Figure 3.6** Schematic view of the maximum indentation depth in the materials.

Additionally, these measurements were carried out with a heavier load of 15 N in order to understand the effect of the load applied on these three parameters.

### 3.4.3 Nanoindentation and elastic modulus

For the characterization of the diffusion layers, nanoindentation measurements were carried out assessing the hardness and the elastic modulus variation along deepness. These tests were performed in the cross-section of the samples previously prepared by a metallographic route consisting on cutting the cross-section, embedding in resin and polishing to mirror surface. Measurements were carried out in profiles from the outer area to the inner part.

A maximum load of 10 mN was applied to a depth of 500 to 750 nm. Therefore, the higher precision of this technique allows measuring hardness in determined small areas offering precise information. Elastic modulus values were obtained for the same areas with high precision distinguishing these mechanical properties as function of Nb or Mo contents. A MTS Nanoindenter equipment with a standard Berkovich tip calibrated in fused silica was used.

## 3.5 Wear characterization

Dry sliding tests were performed on a ball-on-plate tribometer (UMT, Bruker) using reciprocating lineal movement. The wear behaviour was characterized under different testing conditions to evaluate the effect of important parameters such as load, counter material and stroke length (Table 3.4). Samples acted as the moving body whereas the static body was the counter material. They were performed in ambient air under unlubricated conditions.

**Table 3.4** Summary of the wear conditions.

<i>Parameters</i>	<i>Setup [1]</i>	<i>Setup [2]</i>	<i>Setup [3]</i>
Load (N)	2	2	5
Counter material (mm)	Stainless steel, 10	Alumina, 6	Alumina, 5
Stroke length (mm)	10	10	5
Frequency (Hz)	1	1	1
Sliding time (s)	1800	1800	1800

The wear evaluation was carried out by means of: a) coefficient of friction (COF) values obtained during the sliding time, b) examination of the worn surfaces for wear details and mechanisms by scanning electron microscopy, c) width, deepness, and volume loss analysis of the wear tracks by optical profilometry, and d) wear rate calculation.

Wear tracks obtained from dry sliding wear tests were measured by optical profilometer (Olympus, complete). 2D profiles were taken from the middle, upper and bottom part of the wear track for each material as is shown in Figure 3.7. Then, wear rate, average depth ( $\bar{D}$ ) and volume loss ( $V$ ) were calculated with the following parameters:  $\bar{A}_w$  (average wear loss area of three 2D profiles in  $\text{mm}^2$ ),  $\bar{W}$  (average width of each track in mm),  $R$  (radius of the alumina ball in mm) and  $l$  (total stroke length in mm),  $W_v$  (wear rate in  $\text{mm}^3/\text{mm}$ ),  $V$  (volume loss in  $\text{mm}^3$ ) and  $S$  (the total sliding distance in mm). For the calculation, the following formulas were used:

$$\bar{D} = \bar{A}_w / \bar{W} \quad (\text{Eq. 3.2})$$

$$V = [1/3 * \pi * \bar{D}^2 * (3R - \bar{D})] + (\bar{A}_w * l) \quad (\text{Eq. 3.3})$$

$$W_v = V/S \quad (\text{Eq. 3.4})$$

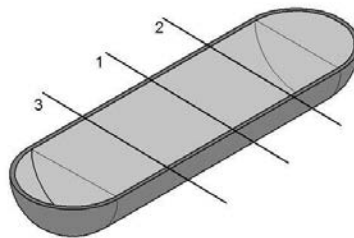


**Figure 3.7** Model used in the wear loss volume calculation where the parallel lines corresponds to the 2 D profiles taken from the middle (1), upper (2) and bottom (3) part of the war track of each material.



Regarding the wear behaviour, apart from studying how wear is affected by load or counter material; the synergistic wear-corrosion interactions (tribocorrosion behaviour) was investigated.

### 3.6 Corrosion characterization

In a first approach to study the corrosion behaviour of titanium alloys, an electrochemical comparative study between conventional and powder metallurgy Ti alloys was conducted in physiological conditions.

One of the most employed titanium alloys in the biomedical sector was selected: Ti-6Al-4V obtained by forge (ELI, extra low interstitial, medical grade, Surgival SL.), and compared to Ti-6Al-4V and Ti-6Al-7Nb alloys obtained by powder metallurgy. The corrosion behaviour was characterized by electrochemical impedance spectroscopy (EIS) technique. Impedance measurements were conducted after being immersed in simulated body fluid: DMEM (Dulbecco's modified Eagle's medium), fetal bovine serum (15%) and antibiotics for different period of times (1, 7, 14, 21 days, 6 and 12 weeks).

The schematic view of the Ti alloys together with the electrochemical cell where the samples are placed and immersed in the physiological solution, and the equipment used for the electrochemical measurements are presented in Figure 3.8.

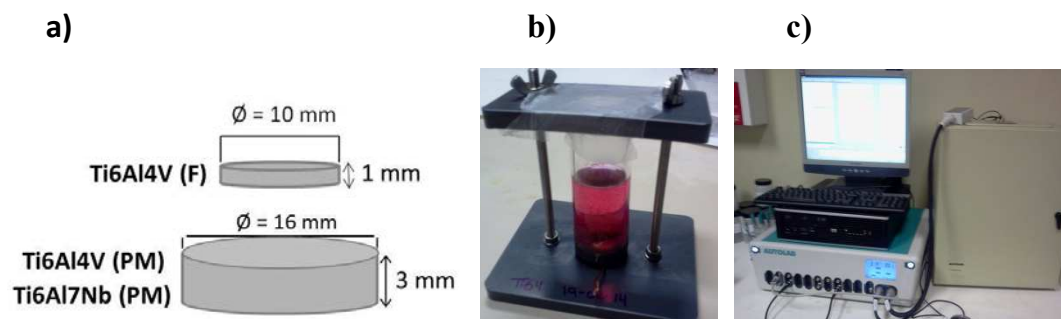


**Figure 3.8** (a) Schematic view of the Ti alloys with their dimension, (b) electrochemical cell with the sample placed in the DMEM medium, and (c) Autolab Potentiostat PGSTAT302N equipment for EIS measurements.

The electrochemical characterization of the modified Ti surfaces designed in this Thesis work was also carried out by measuring the open circuit potential (OCP) and through the non-destructive technique electrochemical impedance spectroscopy (EIS). For both measurements, an electrolyte of 9 g/l NaCl was used due to this represents the major compound of Hank's Balanced Salt Solution and Phosphate Buffered Saline physiological solutions [5]. Figure 3.9 shows an arrangement of the electrochemical cell employed in the EIS tests and the routine used to perform the electrochemical measurements.

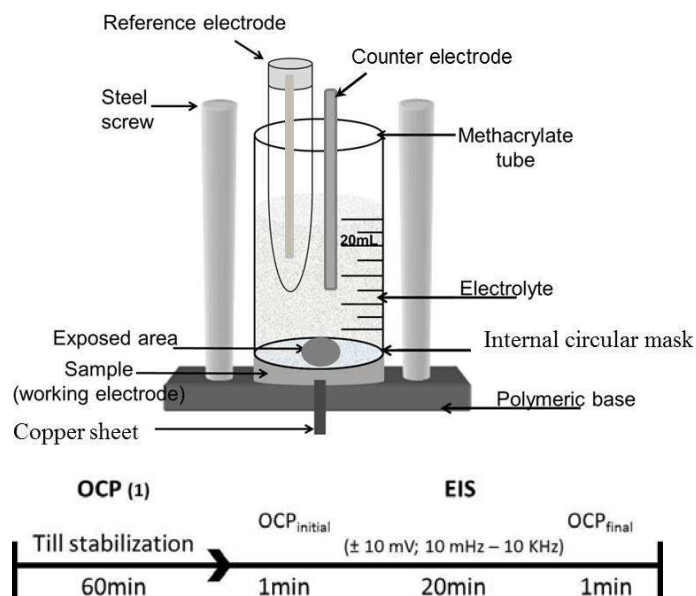


**Figure 3.9** a) Schematic view of the electrochemical cell for the EIS experiments and routine.

Table 3.5 summarizes all the conditions for the EIS measurements. Finally, ZView Version 3.5d software lead the processing of the impedance data obtained and the results were fitted to the most similar equivalent circuit. All tests were repeated three times in order to obtain good reproducibility and validity in the results.

**Table 3.5** Conditions for the electrochemical impedance spectroscopy (EIS) experiments.

<i>EIS conditions</i>							
<i>Reference electrode</i>	<i>Counter electrode</i>	<i>Working electrode</i>	<i>Frequency</i>	<i>Amplitude</i>	<i>Temperature</i>	<i>Electrolyte</i>	<i>Volume</i>
Ag/AgCl (KCl 3M) 205 mV vs. SHE	Platinum	Surface sample	10 mHz - 10 kHz	±10 mV	Room T <sup>a</sup>	9 g/L NaCl	20 mL

### 3.7 Tribocorrosion characterization

The synergistic interactions between wear and corrosion were evaluated through the tribocorrosion behaviour of the materials. These measurements were carried out in an electrochemical cell placed on a ball-on-plate-tribometer (CETR-UMT-2) with reciprocating lineal movement. The working surface of the samples was the moving body facing upwards against the static counter material. Electrochemical

measurements were performed in 9 g/l NaCl solution at room temperature using Voltalab PGZ 100 potentiostat. A two electrode set up consisting on a saturated calomel electrode (SCE) as the reference electrode and the exposed area of 177 mm<sup>2</sup> of the samples as the working electrode. Open circuit potential (OCP) was measured before, during and after sliding, starting the sliding action after OCP stabilization in each test (1 h approximately). A schematic view of the cell and OCP sequences together with the experimental conditions are shown in Figure 3.10.

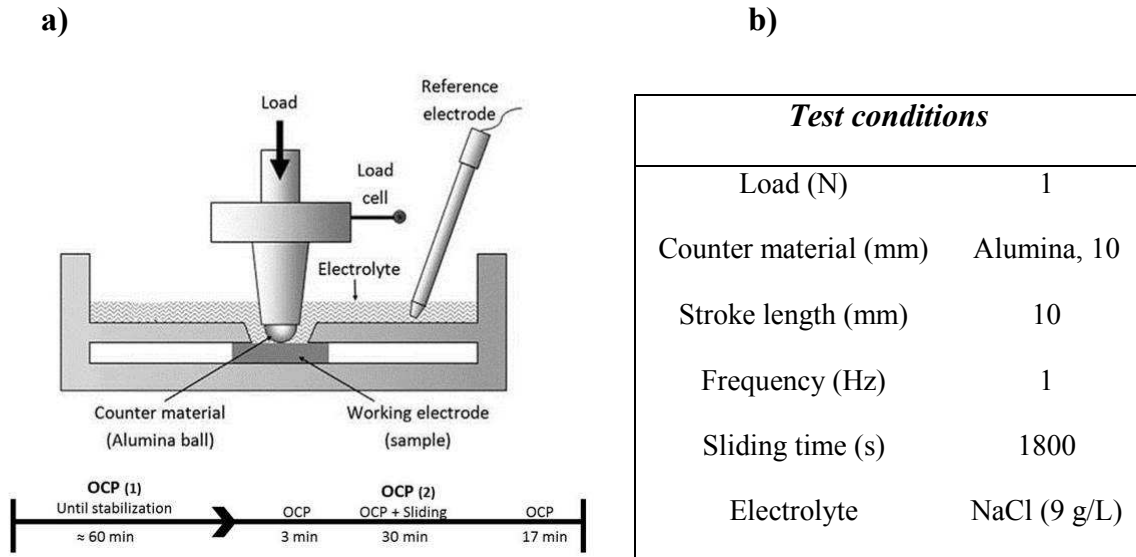


**Figure 3.10** a) Schematic view of the tribocorrosion experimental cell adapted from [6], OCP and sliding sequences. b) Test conditions for tribocorrosion measurements.

The tribocorrosion behaviour was characterized by the coefficient of friction (COF), open circuit potential (OCP) and the worn surfaces examination. COF values were reported by the equipment during all the sliding time as a measure of the contact friction between the counter material and the sample. Two sequences of OCP were established, the first one to ensure the OCP stabilization before the test starting and the second one composed of three stages:

- a) Three minutes of OCP for a constant value.
- b) Thirty minutes of OCP plus sliding for surface damage evaluation.
- c) Seventeen minutes of OCP after sliding for the recovering process evaluation.

Finally, the worn surfaces were analyzed by means of the width track and wear mechanisms.

### 3.8 Biocompatibility characterization

The biocompatibility of the modified Ti surfaces was characterized by three different studies: bioactivity, cytotoxicity and osteogenic differentiation studies.

**The bioactivity study** was carried out on all the materials in order to determine the apatite-forming ability on their surfaces, and thus their bioactive character. A simulated body fluid (SBF) solution was prepared according to Kokubo's method [7] where the samples were placed in for 14 and 21 days. The composition of the prepared SBF is detailed in Table 3.6.

**Table 3.6** Composition of the simulated body fluid (SBF) prepared for 1 L according to Kokubo's procedure.

<i>Reactives order</i>									
1	2	3	4	5	6	7	8	9	10
<i>NaCl</i> (g)	<i>NaHCO<sub>3</sub></i> (g)	<i>KCl</i> (g)	<i>K<sub>2</sub>HPO<sub>4</sub>·3H<sub>2</sub>O</i> (g)	<i>MgCl<sub>2</sub>·6H<sub>2</sub>O</i> (g)	<i>HCl</i> 1M (mL)	<i>CaCl<sub>2</sub>·2H<sub>2</sub>O</i> (g)	<i>Na<sub>2</sub>SO<sub>4</sub></i> (g)	<i>Tris</i> (g)	<i>HCl</i> 1M (mL)
8.0756	0.3532	0.2250	0.2310	0.3033	39	0.3638	0.0716	6.0568	0-5

A schematic view of a sample immersed in SBF and the incubator unity is shown in Figure 3.11. Samples were placed and incubated in the simulated body fluid at 90 rpm, 37 °C for 14 and 21 days.

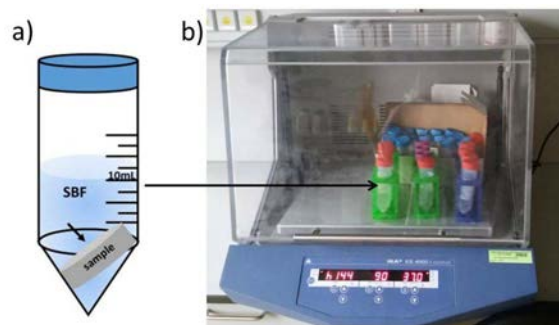


**Figure 3.11** Schematic view of processing the bioactivity test, based on: a) sample placement in the SBF, and b) the incubator equipment.

After the immersion time, the surfaces were examined in order to test the possible hydroxyapatite formation as a sign of bioactive surfaces and thus, the in vitro bone-

bonding ability. Precipitation of Ca and P ions and surface morphology changes were characterized by Fourier transform infrared spectroscopy (FTIR), x-ray diffraction (XRD) and field emission scanning electron microscopy (FE-SEM). Fourier transformed infrared (FTIR) spectra (Impact 420, Nicolet Instr., US) were recorded in the frequency range 400-4000  $\text{cm}^{-1}$ . The spectra were measured using an ATR accessory with torque-limited pressure device (DuraSampIIR™ II, Smiths Detection) for sampling. Hydroxyapatite formation was also characterized by x-ray diffraction (XRD) at an angular range of  $2\theta = 25-100^\circ$  and step scan of 0.02 with a Bruker AXS D8 Advance, and the morphology was analyzed by FE-SEM (2 kV acceleration and 6-8 mm working distance) after 14 and 21 days of immersion in SBF.

**Cell culture studies** were conducted on the modified Ti surfaces by Nb for their biological character assessment. Prior to these studies, the samples were sterilized at 121 °C for 90 min in an autoclave unity as shown in Figure 3.12.

The first study was carried out with Human osteoblast-like (MG-63) cells seeded on the surfaces and cultured during 2 days to evaluate their **cytotoxicity response**. Then, the *cell viability and proliferation*, and aspects such as *cell adhesion and morphology* were evaluated.



**Figure 3.12** Autoclave equipment for sterilization of samples prior to the cell culture studies.

### *Cell viability*

Cellular viability of MG-63 cells on the three modified Ti surfaces plus a Ti control was assessed after 48 hours using a commercial Cell Counting Kit-8 (CCK-8) via WST-8 [2-(2-methoxy-4-nitrophenyl)-3-(4-nitrophenyl)-5-(2,4- disulfophenyl)-2H-tetrazolium, monosodium salt over 48 hours of incubation. CCK-8 allows sensitive colorimetric assays in order to determine the number of viable cells in cell proliferation and cytotoxicity assays. WST-8 acts as a colorimetric indicator which is reduced by dehydrogenases in cells to give a yellow colored product (formazan), which is soluble in the tissue culture medium. The amount of the formazan dye generated by the activity of dehydrogenase in cells is directly proportional to the number of living cells. This test gets higher sensitivity detection than other

tetrazolium salts used as MTT, XTT or MTS. For this test, a mixture preparation of 1 % WST + 99 % DMEM was prepared and an amount of 0.75 mL was added in each sample. After 2 hours, the reaction was completed and prepared for the measurement.

#### *Cell adhesion and morphology*

Samples were also evaluated for cell adhesion, distribution and morphology using laser confocal fluorescent microscope (DM6000 CFS, Leica, Germany). For this purpose, Calcein was the cell-permeable dye chosen due to its ability for determining cell viability in most eukaryotic cells. The medium of the well plates containing the samples and the blanks was removed; and a 4  $\mu\text{L}/\text{mL}$  calcein solution was prepared. A volume of 45  $\mu\text{L}$  Calcein was put in 11.21 mL of PBS and 0.75 mL of the mixture was added in each sample. Finally, the samples need to be removed from the well plates, covered with PBS and stored in the dark. Three images at 20x magnification of each sample (in total 6 images of each material) were acquired and the number of cell was counted by ImageJ software.

SEM analysis of the samples was carried out after 2 days of culture by FE-SEM. For the preparation, they were rinsed with PBS buffer to remove the culture medium and after, two fixing solutions were added with a waiting time of 1 hour each. Before the SEM observation, all the samples were dehydrated by immersion in a set of ethanol solutions of increasing concentration. The finishing process was carried out applying an extra thin gold coating by mean of a sputter coater device.

***An osteogenic differentiation*** study was conducted in order to assess bone mineralization. In this case, Bone marrow stromal (ST-2) cells were seeded and cultured for 21 days, and *cell viability* and *proliferation*, *alkaline phosphatase-(ALP) activity*, *lactate dehydrogenase-(LDH) activity*, *cell differentiation* and *bone mineralization* were evaluated.

After sterilization, samples were placed into an untreated 48-well polystyrene plate (Greiner, Germany; internal well diameter 15 mm). They were seeded with mice bone marrow stromal cells (ST-2) and suspended in a stimulating osteogenic differentiation medium: Dulbecco's modified Eagle's Medium (DMEM) containing 10 % fetal bovine serum, 1 vol % penicillin/streptomycin and doped with 50  $\mu\text{l}/\text{ml}$  of ascorbic acid, 10 mmol of  $\beta$ -glycerolphosphate and 10 nM of dexamethasone. Cells were cultured for 21 days in physiological conditions at 37  $^{\circ}\text{C}$  in a 5 %  $\text{CO}_2$  humidified air atmosphere. The medium was changed on the first and fourth day of each week. Five samples of each material were used for cell viability, three for cytotoxicity and cell differentiation, and two for bone mineralization and cell morphology studies.

#### *Cell viability and proliferation*

Cell viability was measured through Cell Counting Kit-8 (CCK-8) using WST-8 (2-(2-methoxy-4-nitrophenyl)-3-(4-nitrophenyl)-5-(2,4-disulfophenyl)-2H-tetrazolium, monosodium salt), which produces a water-soluble formazan dye upon bio-reduction in the presence of an electron carrier, 1-Methoxy PMS. CCK-8 solution is added directly to the cells and no pre-mixing of components is required. WST-8 is bio-reduced by cellular dehydrogenases to an orange formazan product soluble in tissue culture medium. The number of living cells is directly proportional to the amount of formazan produced. The measurement is based on a sensitive colorimetric assay to determine the number of viable cells in the proliferation and cytotoxicity assays. This test permits higher sensitivity detection than other tetrazolium salts such as MTT, XTT or MTS. After the cells were washed with PBS, 210  $\mu$ L of solution containing 1 % WST-8 was added in each well and the plates were incubated for 1.5 h. Subsequently, the supernatant of all samples was transferred to 1 mL cuvettes and the absorbance was determined at 450 nm in a UV-VIS spectrometer.

*Lactate dehydrogenase (LDH-) activity* was assessed as an indirect measurement of the amount of attached cells on the samples. A commercially available LDH-activity quantification kit (TOX7, Sigma-Aldrich) was used to quantify cell number by the LDH enzyme activity in cell lysate. ST-2 cells cultured were washed with PBS and lysed with lysis buffer (1 mL/sample) for 30 min. 140  $\mu$ L of each sample was added to each cuvette plus 60  $\mu$ L of master-mix containing equal amounts of substrate solution, dye solution, and cofactor solution for LDH assay. The plates were left for 30 min in the dark and the reaction was stopped with HCl. A spectrophotometer (Specord 40) was used to measure the dye concentration at 490 nm.

#### *In vitro cell differentiation and bone mineralization*

Cell differentiation was assessed by determining the alkaline phosphatase (ALP) enzyme activity of the ST-2 cells after incubation during 21 days.

The cells were lysed with a cell lysis buffer containing 20 mM TRIS buffered solution (Merck) with 0.1 wt % Triton X-100 (Sigma, Germany), 1 mM  $MgCl_2$  (Merck) and 0.1 mM  $ZnCl_2$  (Merck). The cell lysate was incubated with a reacting solution containing 0.1 M Tris solution, 2 mM  $MgCl_2$  and 9 mM p-Nitrophenylphosphate. 100  $\mu$ L of ALP buffer solution was then added to 250  $\mu$ L of the lysates obtained from each sample. After 87 min of incubation at 37  $^{\circ}C$ , the color change to yellow was noticed and the reaction was stopped with 1 M NaOH solution. Then, absorption was measured at 405 nm using a spectrometer (Specord 40). The specific activity was calculated respect to the protein concentration of the cell lysates determined by a commercial kit based on Bradford assay (Sigma). It consisted of the release of p-nitrophenol from p-nitrophenolphosphate considering the amount of total protein. This reaction was incubated for 5 min and the change of color to dark blue appeared. Hence, the ALP activity (expressed as  $\mu$ mol of

converted p-nitrophenol per min) was normalized by the amount of total protein, and finally expressed as nmol p-nitrophenol per min per mg protein.

OsteoImage™ Mineralization test (Lonza, Germany) was used for assessing the *in vitro* bone cell mineralization. The fluorescent assay can be used for the differentiation of osteogenic stem cells, based on specific binding of the fluorescent OsteoImage™ staining reagent to the hydroxyapatite portion of bone-like nodules deposited by cells. The *in vitro* mineralization was rapidly assessed qualitatively through laser confocal fluorescent microscope (DM6000 Leica CFS, Germany). The quantitative analysis was determined acquiring four images at 10x magnification of each sample (in total 8 images of each material) and analyzing the area of the bone-like nodules using ImageJ software.

The nuclei of fixed cells were revealed by the fluorescence dye 4', 6-Diamidino-2-phenylindol (DAPI Roti<sup>R</sup>-Mount FluorCare). Firstly, the staining of the samples was carried out by immersion in DAPI-solution (1  $\mu$ L DAPI solution in 1 mL DAPI buffer) for 5 min in the dark. Finally, in order to eliminate the background, the samples were washed three times in PBS. The images were taken by fluorescence microscopy at 360 nm excitation and 460 nm emission; where the cell nuclei appeared as blue fluorescent spots. Four images at 10x magnification of each sample (in total 8 images of each material) were acquired and the number of cell nuclei was counted using ImageJ software.

#### *Cell morphology and adhesion*

The morphology of the ST-2 cells seeded on Ti, Ti-Nb and Ti-Nb<sub>NH<sub>4</sub>Cl</sub> was examined by FE-SEM after culture for 21 days. Before observation, samples were prepared by rinsing with PBS buffer, adding fixing solutions, dehydrating with isopropanol solutions of increasing concentration, air drying and applying an extra thin gold coating using a sputter-coater.

A statistical analysis of the results was carried out with the unmodified Ti samples (Ti) as the reference group. The results were evaluated by one-way analysis of variance (ANOVA, Tukey test) to determine statistical significant differences between the means of the different groups. The level of the statistical significance is given by *p*-values (*p* < 0.05 no significant, *p* > 0.05 significant) calculated by Origin software (version 8.5, OriginPro).

### **3.9 References**

- [1] S. A. Tsipas and E. Gordo, "Molybdeno-Aluminizing of Powder Metallurgy and Wrought Ti and Ti-6Al-4V alloys by Pack Cementation process," *Mater. Charact.*, vol. 118, pp. 494–504, 2016.



- [2] “DICTRA User Guide Version 27, Thermo-Calc Software, Stockholm,” 2013.
- [3] L. Bolzoni, T. Weissgaerber, B. Kieback, E. M. Ruiz-Navas, and E. Gordo, “Mechanical behaviour of pressed and sintered CP Ti and Ti-6Al-7Nb alloy obtained from master alloy addition powder,” *J. Mech. Behav. Biomed. Mater.*, vol. 20, pp. 149–161, 2013.
- [4] R. Moreno, “Reología de suspensiones cerámicas,” *Madrid*, pp. 178–235, 2005.
- [5] Z. Doni, A. C. Alves, F. Toptan, J. R. Gomes, A. Ramalho, M. Buciumeanu, L. Palaghian, and F. S. Silva, “Dry sliding and tribocorrosion behaviour of hot pressed CoCrMo biomedical alloy as compared with the cast CoCrMo and Ti6Al4V alloys,” *Mater. Des.*, vol. 52, pp. 47–57, 2013.
- [6] F. Toptan, a. C. Alves, I. Kerti, E. Ariza, and L. a. Rocha, “Corrosion and tribocorrosion behaviour of Al-Si-Cu-Mg alloy and its composites reinforced with B4C particles in 0.05M NaCl solution,” *Wear*, vol. 306, no. 1–2, pp. 27–35, 2013.
- [7] T. Kokubo and H. Takadama, “How useful is SBF in predicting in vivo bone bioactivity?,” *Biomaterials*, vol. 27, pp. 2907–2915, 2006.

## **Summary of Results and Discussion**

**4.1 Introduction to the experimental results**

**4.2 Design and surface modification of titanium surfaces**

**4.3 Mechanical properties of the modified Ti surfaces: hardness and elastic modulus**

**4.4 Wear, corrosion and tribocorrosion behaviour of the modified Ti surfaces**

**4.5 Biocompatibility features of the modified Ti surfaces: bioactivity, cytotoxicity and osteogenic differentiation response**

## 4.1 Introduction to the experimental results

In this chapter the experimental results obtained during the development of the thesis are summarized. The results are reported in detail in the appended papers. The following four sections compile the full study of the modified Ti surfaces, from designing to the final properties evaluation:

1. Initial study of the diffusion conditions by DICTRA simulation, design of the thermo-chemical treatments and the surface modification process. Microstructure and compositional features of the modified Ti materials.

**Paper 1 and 2**

2. The mechanical performance of the modified Ti surfaces attending to hardness and elastic modulus.

**Paper 1 and Paper 2**

3. The wear, corrosion and the synergistic wear-corrosion behaviour of the final modified Ti surfaces to determine their functional properties.

**Paper 3 to Paper 6**

4. The biocompatibility feature of the modified Ti surfaces establishing suitable surface conditions.

**Paper 7 to Paper 8**

## 4.2 Design and surface modification of titanium surfaces

The aim of this work is to obtain modified Ti surfaces designed by  $\beta$ -stabilizers through diffusion treatments to better understand their functional properties. The  $\beta$ -stabilizing elements selected for the surface modification of titanium were Mo and Nb since both of them are considered as biocompatible elements and present high solubility in Ti. Figures 4.1 and 4.2 show Ti-Mo and Ti-Nb phase diagrams, respectively. It can be seen that by increasing Mo or Nb weight percent, the  $\beta$ -transus temperature decreases and  $\alpha+\beta$ -phase region is created.

In order to define the conditions for the diffusion experiments simulation, studies of the diffusion process with Diffusion Controlled Transformations simulation software (DICTRA) were conducted. For this purpose is necessary to know the phases presented in our systems to define the initial conditions such as temperature. In this case 1100 °C was selected as diffusion temperature since this is above the  $\beta$ -transus temperature and the diffusivity will be higher.

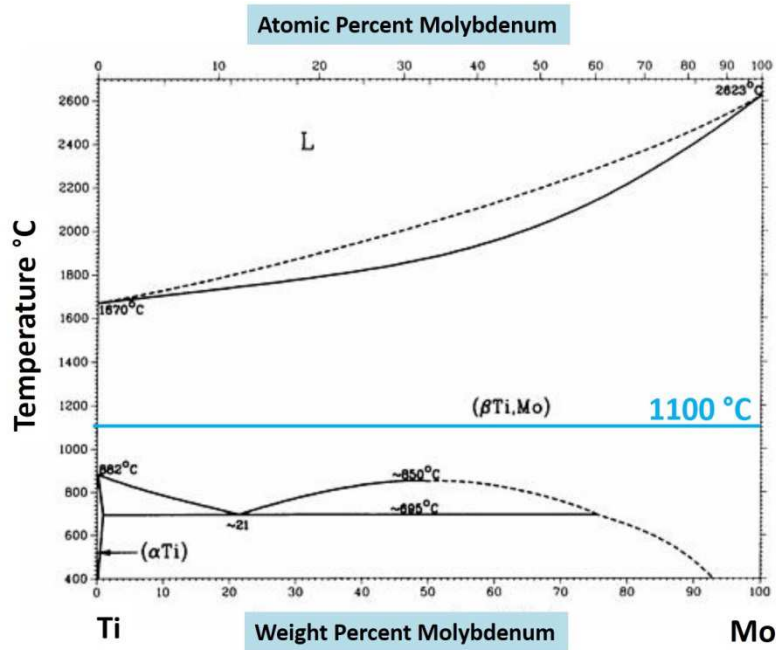


Figure 4.1 Phase diagram of the Ti-Mo system [1].

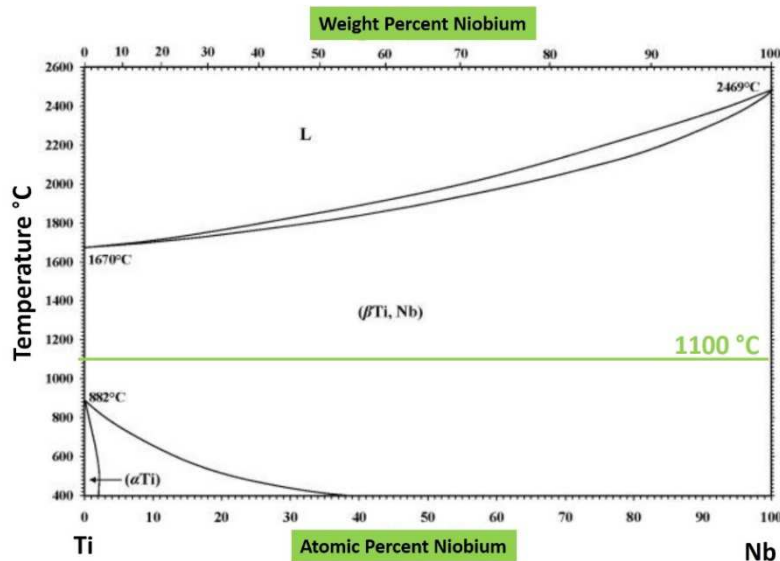
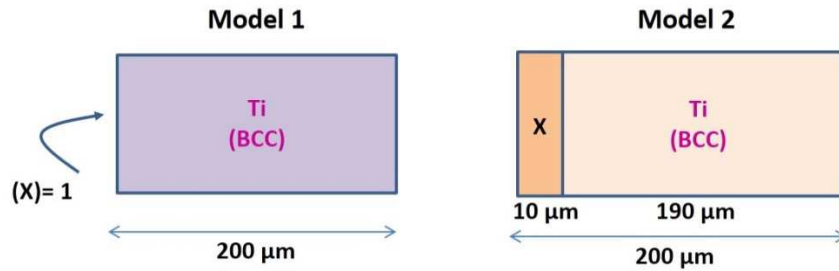


Figure 4.2 Phase diagram of the Ti-Nb system [1].

For the simulation of the Mo or Nb diffusion in Ti, two different cell models were defined (Figure 4.3). In *model 1*, for the diffusion of  $X$  ( $X = Mo, Nb$ ) in Ti,  $X$  is defined at the left with a concentration of 100 % whereas Ti is at the right defined with (bcc)-structure (because of Ti at 1100 °C presents body-center cubic crystal structure). In *model 2*, the diffusion of  $X$  ( $X = Mo, Nb$ ) in Ti is drawn by a 10  $\mu\text{m}$  wide region composed of  $X$ , being Ti (bcc) the rest of the sample [2].

### Ti-X system (X = Mo, Nb)



**Figure 4.3** Schematic diagram of the cell models used in DICTRA for the X diffusion in Ti (X = Mo, Nb) at 1100 °C.

DICTRA simulation results of Mo diffusion in Ti at 1100 °C for *model 1 and 2* are shown in Figure 4.4. Both models *1 and 2* predict the Mo diffusion in Ti in terms of diffusion profiles where Mo decreases from surface to inner areas. In both cases, the deepest Mo diffusion is predicted for 10800 s, suggesting that longer diffusion times result in higher Mo diffusion. However comparing models, *model 1* predicts a significant higher Mo content at the same distance (150 μm from surface) than *model 2* (80 μm). *Model 1* also predict increased diffusion depth probably because Mo is defined as 100 % during the whole experiment.

However, *model 2* predicts a Mo content around 30 % on surface which decreases until around 5 % at a depth of 110 μm. Thereby, experimental work was carried out in order to evaluate which model fits better the experimental results.

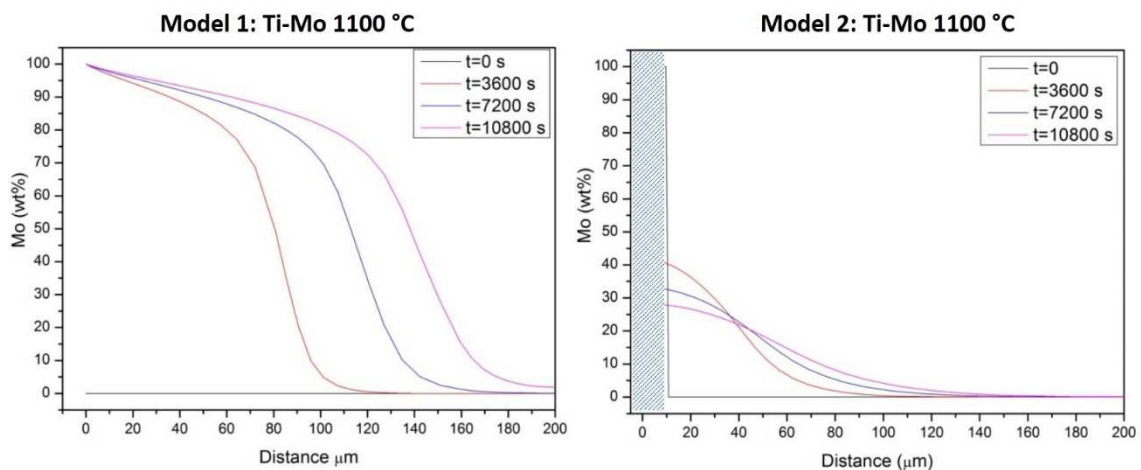


**Figure 4.4** DICTRA simulation of the Mo diffusion in Ti at 1100 °C for 1h, 2h and 3h.

The experimental results of the Mo diffusion in Ti at 1100 °C for 3h are presented in Figure 4.5 (a-b), showing the cross-sectional microstructure with a (EDS) composition profile. The Mo diffusion led to a microstructural gradient where the  $\alpha$ -single phase titanium was transformed into a gradient of  $\beta \rightarrow \alpha + \beta \rightarrow \alpha$  phases from

the surface inwards. The outer brighter zones correspond to rests of non-diffused Mo particles which remained adhered to titanium. Closer to the external surface, the  $\alpha+\beta$  colonies appear closer becoming a single  $\beta$ -region rich in Mo, while getting deeper  $\beta$ -lamellas appear more separated giving the  $\alpha+\beta$ -phase microstructure. Figure 4.5 (a) shows the diffusion layer together with the composition profile. The Mo content changes from 60 to 10 wt. % within a 40  $\mu\text{m}$  wide region, being the whole diffusion layer around 120  $\mu\text{m}$ . The peaks and valleys are related to the separated  $\beta$  lamellas, becoming almost zero at 100  $\mu\text{m}$ . Figure 4.5 (b) presents a detailed view of the area closer to the surface corresponding to the  $\beta$ -phase (Mo-rich region). Regarding DICTRA simulations, *model 2* predicts Mo diffusion profiles more similar to the experimental one, since *model 1* predicted an overestimated diffusion. When comparing the simulated and experimental 3h Mo diffusion profile, they showed relatively good agreement to the Mo diffusion profile and the deepness of the diffusion layer around 110-120  $\mu\text{m}$ .

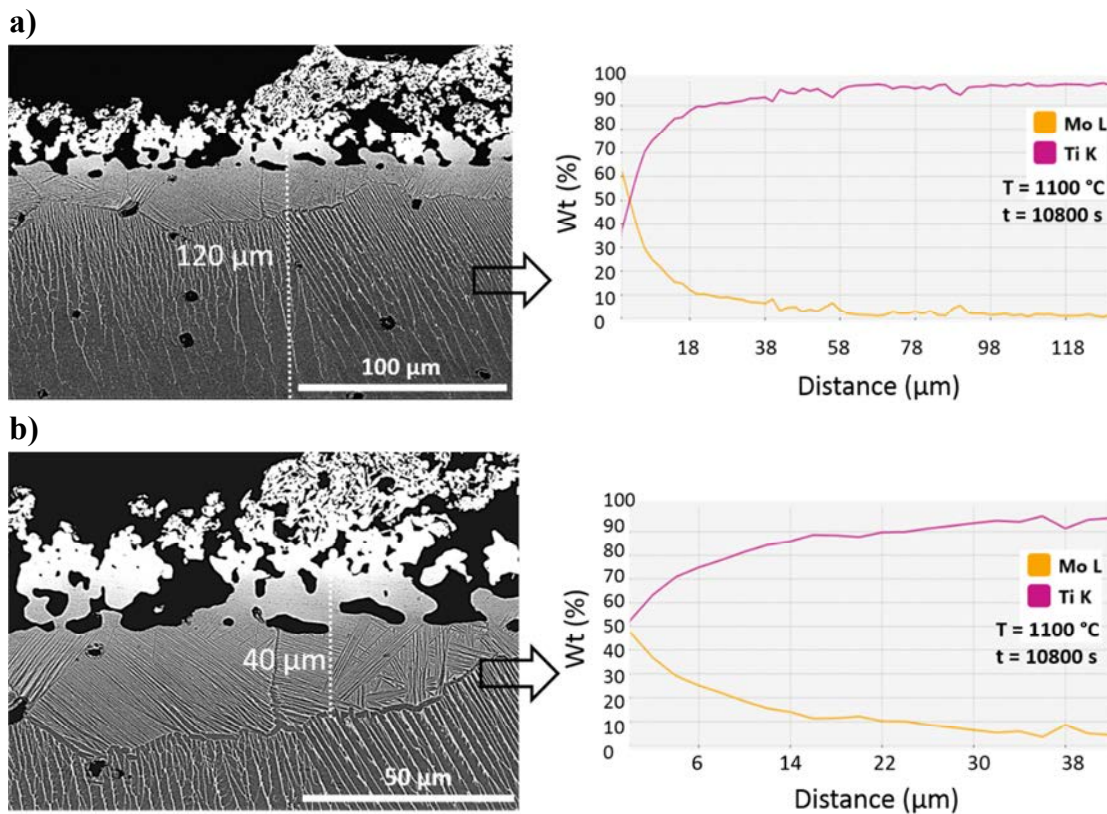


**Figure 4.5** SEM micrograph and EDS profile obtained from the experimental diffusion of Mo in Ti at 1100 °C for 3h. a) ( $\beta \rightarrow \alpha+\beta$ ) diffusion layer, and b) detailed view of the  $\beta$ -region.

DICTRA simulation results of the Nb diffusion in Ti at 1100 °C for *model 1 and 2* are shown in Figure 4.6. Similarly to the Ti-Mo simulations, *model 1* predicts diffusion profiles which Nb decreases along distance from surface inwards.

However, *model 2* suggests that after the 10 first microns defined as Nb region, the Nb content remained constant along the 200 microns of the sample.

In this case *model 1* seems to be more realistic by predicting that Nb decreases from 100 % until 5 % from surface to a depth of 120  $\mu\text{m}$ .

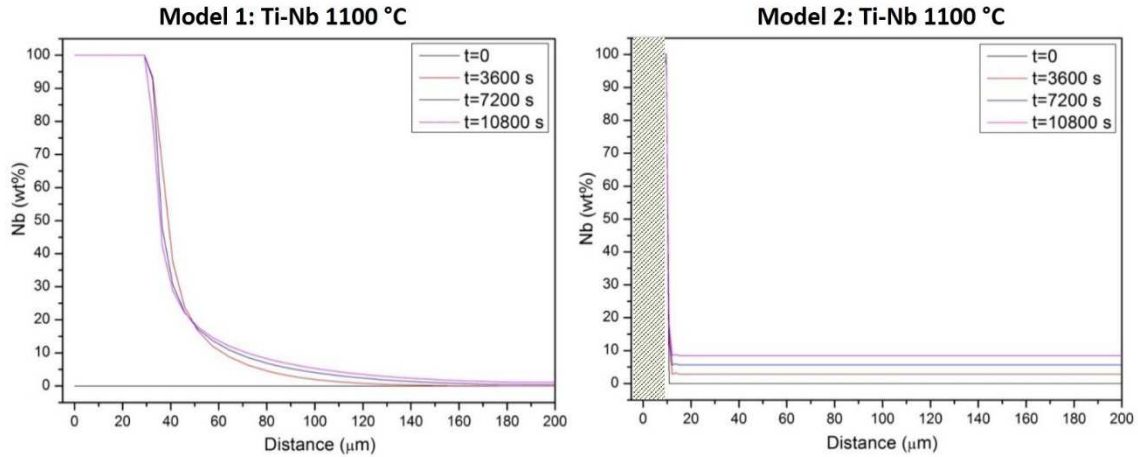


**Figure 4.6** DICTRA simulation of the Nb diffusion in Ti at 1100 °C for 1h, 2h and 3h.

The cross-section and EDS profile of the experimental Nb diffusion in Ti at 1100 °C for 3h is shown in Figure 4.7 (a, b). Similar to the analysis and discussion of the Ti-Mo, the Nb introduction resulted in the phase transformation of the  $\alpha$ -structure of titanium into a microstructural gradient of  $\beta \rightarrow \alpha+\beta \rightarrow \alpha$  phases. The no-diffused Nb particles remained adhered to titanium surface followed by a Nb-rich region of single  $\beta$ -phase, while as moving inward  $\alpha+\beta$ -phase microstructure was found.

Figure 4.7 (a) shows the diffusion layer (120-140  $\mu\text{m}$ ) with the composition profile where Nb decreases from 100 to 10 wt. % within a 30  $\mu\text{m}$  wide region, appearing the beta-lamellas very separated from the  $\alpha+\beta$  region to the end of the diffusion layer. Figure 4.7 (b) shows the Nb-rich region with the gradient in composition. When comparing to the Mo diffusion, the  $\beta$ -lamellas were formed more separated. In the case of the Ti-Nb system, DICTRA simulations fit better to *model 1* than *model 2*. However, results from *model 1* were not strictly in good agreement to the experimental ones, since the predicted Nb-rich region (100 %) is wider (40  $\mu\text{m}$ ) than the experimental one where Nb decreases from 100 % to 15 % within 20  $\mu\text{m}$  wide region. However, the diffusion distance agrees with that experimentally obtained of around 130-140  $\mu\text{m}$ .

Therefore, it could be stated that the diffusion of similar  $\beta$ -stabilizing elements (Mo and Nb) in titanium needs to be simulated with specific models, since the simulation of a diffusion process is influenced by the diffusion behaviour and parameters.

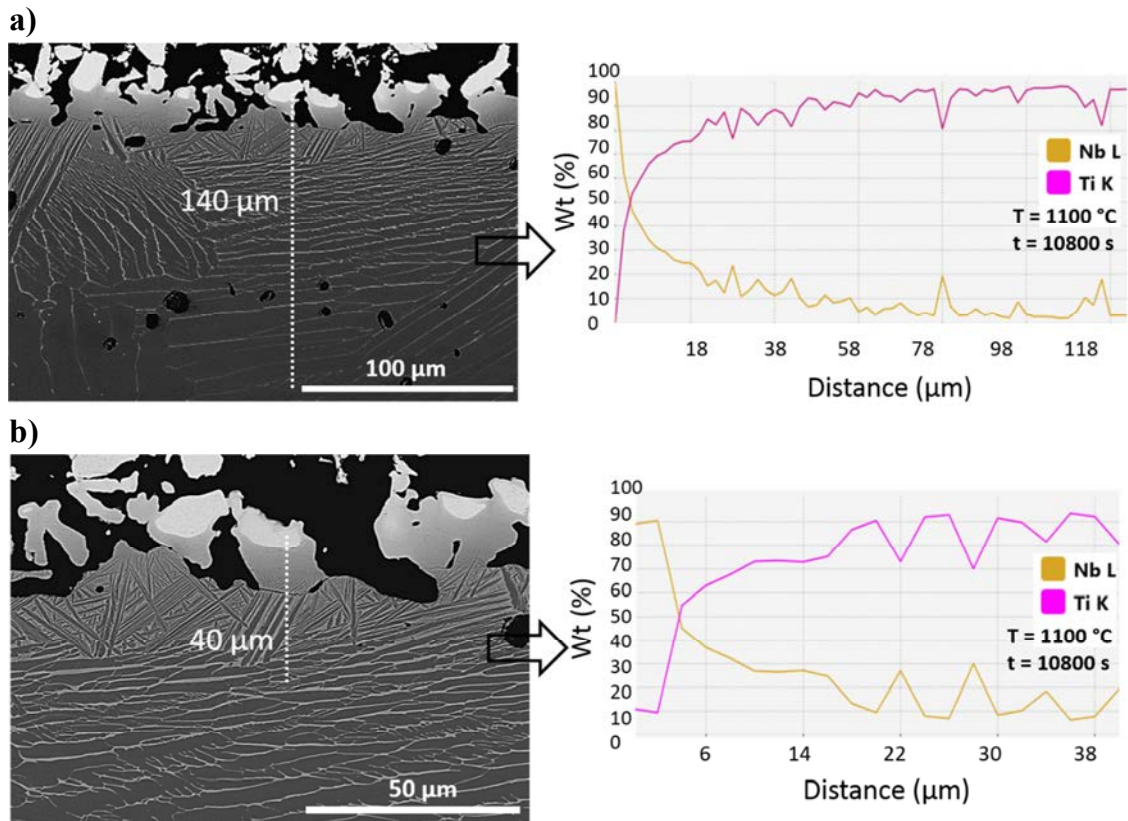


**Figure 4.7** SEM micrograph and EDS profile obtained from the experimental diffusion of Nb in Ti at 1100 °C for 3h. a) ( $\beta \rightarrow \alpha+\beta$ ) diffusion layer, and b) detailed view of the  $\beta$ -region.

Moreover, it was thought that would be interesting to simulate same experiments at higher temperature (1300 °C) in order to see its influence on diffusion. Same conditions were defined in both models due to the new temperature is also above the  $\beta$ -transus. Figure 4.8 shows DICTRA results of Mo and Nb diffusion in Ti at 1300 °C for 1, 2 and 3h, Figure 4.8 a and b, respectively. Both systems Ti-Mo and Ti-Nb showed similar behaviour with respect to that obtained at 1100 °C with both models. Therefore, it could be predicted that the experimental Mo diffusion in Ti would fit to model 2, suggesting a diffusion distance of 200  $\mu\text{m}$  whereas Nb would present better agreement to model 1 with a diffusion area of 200-220  $\mu\text{m}$ . However, the  $\beta$ -region rich in Mo or Nb seems to be reduced with respect to those obtained at 1100 °C. Therefore, based on these simulations together with literature found [1], [3], 1100 °C-3h were the selected diffusion conditions for the diffusion treatments.



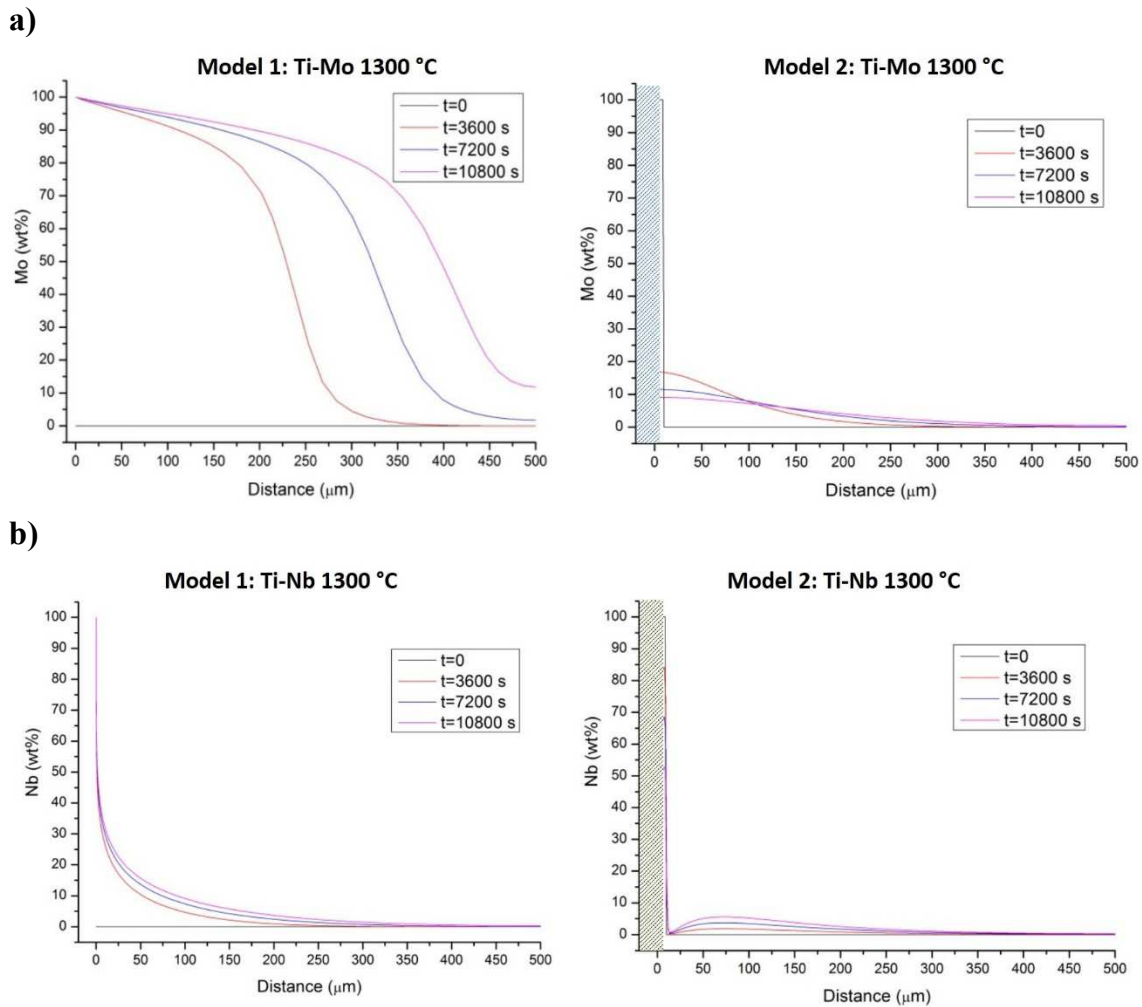


**Figure 4.8** DICTRA simulation of the diffusion of: a) Mo and b) Nb in Ti at 1300 °C for 1h, 2h and 3h.

Once the diffusion process was simulated and the experimental diffusion conditions were established, this section continues with the results presented in **Paper 1** [4] about the process of the surface modification.

For the titanium surface modification, the  $\beta$ -stabilizing elements need to be homogeneously deposited on the surface of the titanium substrates. For this purpose, aqueous suspensions of Mo or Nb micro-sized powders were prepared in order to not introduce organic solvents which could affect the biocompatibility of these materials. A study on the variation of the zeta potential with the pH was conducted. A suspension can be considered stable if its zeta potential presents an absolute value superior to 20 mV. Through these studies, stable aqueous suspensions were achieved and sprayed on the surfaces of the Green Ti compacts and sintered Ti substrates. Details about the experimental procedure of the suspensions are reported in **Paper 1**. Moreover, the suspensions for the thermo-reactive diffusion route (Mo +  $\text{NH}_4\text{Cl}$ )

and (Nb + NH<sub>4</sub>Cl) are also reported in **Paper 2**. Finally, the materials obtained were: GreenTi-Nb, Ti-Nb, Ti-Nb<sub>NH<sub>4</sub>Cl</sub>, GreenTi-Mo, Ti-Mo and Ti-Mo<sub>NH<sub>4</sub>Cl</sub>.

In **Paper 1** is also reported some preliminaries studies about the design of TiN and Ti-Mo-TiN surfaces through the deposition of a colloidal TiN suspension by electrophoretic deposition on a Ti or Ti-Mo surface, respectively. These materials showed an improvement on hardness, and the Ti-Mo-TiN also exhibited Mo and N diffusion creating a diffusion layer composed of a gradient in phases ( $\beta$  /  $\alpha+\beta$  /  $\alpha$ ) and composition (Ti-Mo-N). This indicated the success of these different methods for the surface modification of Ti, and the positive effect of Mo and Ti-N deposition on hardness.

Regarding the modified Ti surfaces designed by co-sintering + diffusion and diffusion treatments in this work, Table 4.1 shows their microstructure. These results together with the DRX results reported in **Paper 1 and 8** [4], [5] allowed observing the phase transformation occurred by Mo or Nb diffusion due to their  $\beta$ -stabilizing character. These results showed the  $\alpha$ -phase transformation into  $\beta$  or  $\alpha+\beta$  with both routes of diffusion: **Route 1**, co-sintering + diffusion treatment in only one step, and **Route 2**, diffusion in sintered titanium. The diffusion layers are composed of a gradient of phases ( $\beta \rightarrow \alpha+\beta \rightarrow \alpha$ ) with deepness between 120-140  $\mu\text{m}$ . The Mo or Nb-rich regions were obtained closer to surface while the content of the  $\beta$ -stabilizing element was decreasing along deepness, appearing the  $\beta$ -lamellas more separated from surface inwards. The EDS profile analysis shown in Figure 4.5 and 4.7 and detailed in **Paper 2** [6] allowed observing the element distribution along the diffusion layers.

**Table 4.1** Summary of microstructure results on the  $\beta$ -Ti surfaces (Ti-Mo and Ti-Nb) after the diffusion treatments of route 1 or 2.

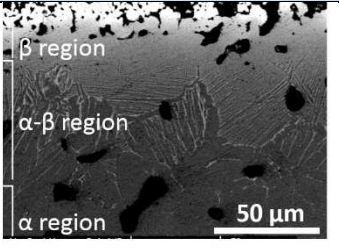
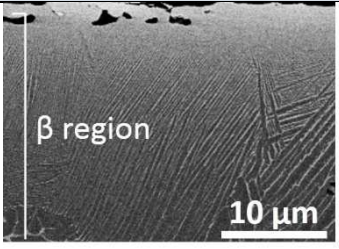
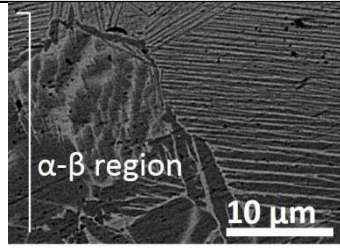
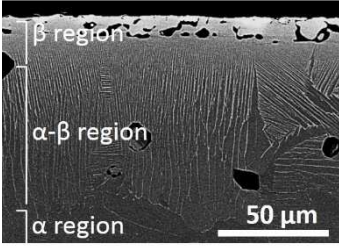
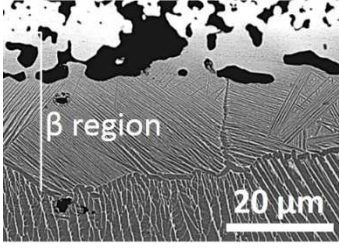
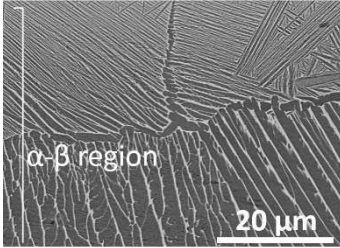
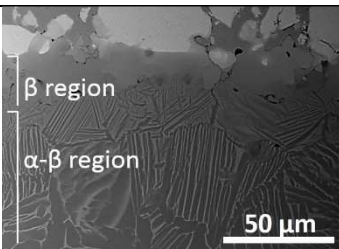
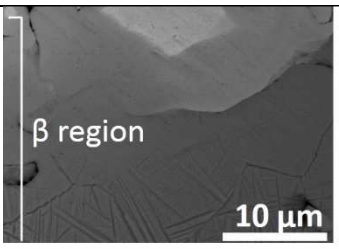
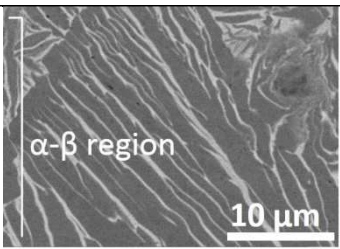
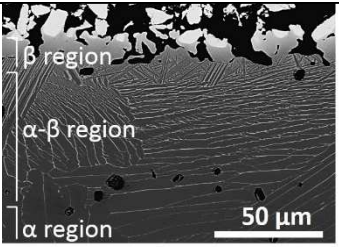
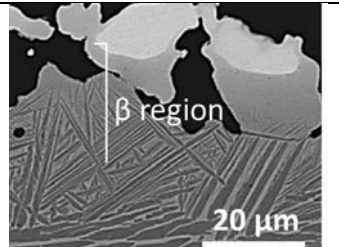
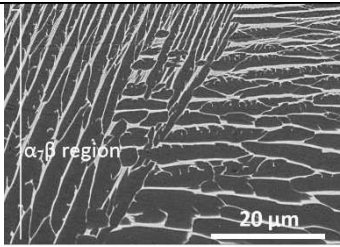
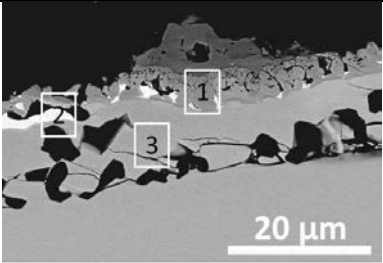
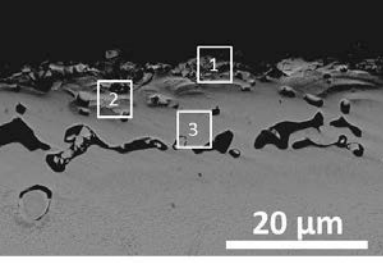
	<i>Diffusion layer</i>	<i><math>\beta</math>-region</i>	<i><math>\alpha+\beta</math>-region</i>
<b>GreenTi-Mo</b>			
<b>Ti-Mo</b>			
<b>GreenTi-Nb</b>			
<b>Ti-Nb</b>			

Table 4.2 shows the microstructure of the modified Ti surfaces obtained through route 3 of thermo-reactive diffusion. Different structures were found for these surfaces with respect to those of Table 4.1 due to the action of the activating agent which controls the diffusion phenomena with the formation of volatile Mo or Nb chlorides. Some porosity typical from this treatment is observed in the upper part of the materials. The addition of the ammonium chloride activator results in a titanium nitride layer on the surface, leading to some nitrogen diffusion inwards which improves the material surface hardness. The  $\alpha+\beta$  regions were not identified in that case, and the Mo or Nb was remained on the surface in very low percentage.

**Table 4.2** Summary of microstructure results and chemical composition on the modified Ti surfaces (Ti-Mo and Ti-Nb) after the diffusion treatments of route 3.

	<i>Diffusion layer</i>	<i>Chemical composition</i>				
<b>Ti-Mo</b> <sub>NH4Cl</sub>		<b>Marked areas</b>	<i>Wt. [%]</i>			
			<i>Ti</i>	<i>Mo</i>	<i>N</i>	<i>O</i>
		<b>1</b>	83.4	2.5	8.6	5.5
		<b>2</b>	69.4	25.5	5.1	--
		<b>3</b>	89.5	--	10.5	--
<b>Ti-Nb</b> <sub>NH4Cl</sub>		<b>Marked areas</b>	<i>Wt. [%]</i>			
			<i>Ti</i>	<i>Nb</i>	<i>N</i>	<i>O</i>
		<b>1</b>	85.2	2.2	10.1	2.5
		<b>2</b>	89.0	--	9.2	1.8
		<b>3</b>	90.4	--	7.5	2.1

The complete results and detailed discussion is published in: [Papers 1 and 2]

### 4.3 Mechanical properties of the modified Ti surfaces: hardness and elastic modulus

This section summarizes the results on the mechanical properties of the modified Ti surfaces designed. **Paper 1 and 2** present the hardness and elastic modulus results. Among the mechanical requirements of biomaterials for implants, hardness improvement and low Young's modulus are the most important [7]. This could result in an improvement of the wear resistance and the reduction of the stress shielding effect provoked by the different Young's modulus value between the materials and the bone.

Therefore, hardness and elastic modulus of all the modified surfaces were measured on surface and in the cross-section by three different techniques:

- Vickers micro-hardness ( $HV_{0.1}$ ) in surface.
- Macro-indentation ( $HV_5$  and  $HV_{15}$ ) in surface.
- Nanoindentation (10 mN) transversally.

Table 4.3 summarizes the hardness results obtained from micro to macro scale measured on the surfaces of the modified Ti samples. In all the cases, the designed materials showed an increase on hardness with respect to Ti. Specially, a pronounced increase was noticed for the activated surfaces Ti-Mo<sub>NH<sub>4</sub>Cl</sub> and Ti-Nb<sub>NH<sub>4</sub>Cl</sub> with values around  $1025 \pm 25$  HV and  $873 \pm 20$  HV, respectively, meaning values three times higher than Ti. This is ascribed to the high hardness of the titanium nitride (TiN) layer on the activated materials.

Indentation measurements with bigger loads (5 N and 15 N) showed similar results without experimenting very notorious changes between  $HV_5$  and  $HV_{15}$ . However, a significant difference was observed in the activated materials due to their surface porosity, since hardness is influenced by porosity. Comparing micro-hardness ( $HV_{0.1}$ ) and macro-hardness ( $HV_{15}$ ) tests, smaller values with bigger load were obtained, known as indentation size effect (ISE) which means higher hardness for low loads [8].

Maximum indentation depth values were also obtained from the load-unload curves at 5 N and 15N. All the modified Ti materials exhibited maximum indentation depth below to that of Ti. Moreover, the indentation remained in the diffusion layers, reaching values close to 20  $\mu$ m for the samples with lower stiffness. Although the surface porosity on the activated samples could suggest deeper indentation marks, their higher hardness resulted in less deep indentations. Therefore, it could be stated that hardness has stronger influence on the maximum depth indentation than

porosity. The hardness improvement lead to smaller indentation depth with respect to Ti.

**Table 4.3** Summary of hardness results on the modified Ti surfaces from micro to macro scale.

	<i>Hardness [HV]</i>						
	Ti	GreenTi-Mo	Ti-Mo	Ti-Mo <sub>NH4Cl</sub>	GreenTi-Nb	Ti-Nb	Ti-Nb <sub>NH4Cl</sub>
<b>HV<sub>0.1</sub></b>	279 ± 10	370 ± 17	430 ± 21	1025 ± 25	295 ± 16	315 ± 14	873 ± 20
<b>HV<sub>5</sub></b>	227 ± 2	----	233 ± 8.7	957 ± 34	238 ± 6	256 ± 13	636 ± 45
<b>HV<sub>15</sub></b>	248 ± 9	----	244 ± 14.5	835 ± 22	210 ± 8	269 ± 13	573 ± 28

The assessment of hardness and elastic modulus on the cross-section of the materials in order to evaluate the effect of the gradient in microstructure on these properties was among the main aims of the **Paper 2**. Nanoindentation allowed characterizing these properties in the cross-section of the materials, and confirms a hardness improvement on all the modified Ti surfaces with values around 4 GPa, twice the hardness of pure Ti, and about 5.3 GPa for the Ti-Mo<sub>NH4Cl</sub> material.

Table 4.4 presents the Young's modulus results on the designed materials. A dependence of elastic modulus with microstructure and thus, with the Nb or Mo content, was obtained. This indicates that a gradient in microstructure and composition results in a gradient of mechanical properties. The lowest elastic modulus values were achieved for the  $\beta$ -regions (Nb-rich or Mo-rich regions). A decrease up to 40-50 % with respect to the elastic modulus of two of most used Ti alloys for biomedical applications: Cp-Ti (102-105 GPa) and Ti6Al4V (110-114 GPa) was achieved. These elastic modulus values are in the order of other reported in similar  $\beta$ -Ti alloys [9], [10].

**Table 4.4** Summary of Young's modulus results on the modified Ti surfaces and their variation along the microstructural gradient (from surface to inward). Value of the  $\alpha$ -CP Ti: 105±3 GPa.

Region	<i>Young's modulus [GPa]</i>			
	GreenTi-Mo	Ti-Mo	GreenTi-Nb	Ti-Nb
<b><math>\beta</math></b>	65±9	63±8	54±5	64±5
<b><math>\alpha+\beta</math></b>	89±9	87±7	79±7	88±1

**The complete results and detailed discussion is published in: [Paper 1 and 2]**

## 4.4 Wear, corrosion and tribocorrosion behaviour of the modified Ti surfaces

### Dry sliding wear behaviour of the modified Ti surfaces

This section summarizes the results of the dry sliding wear behaviour of the designed materials and the effect of load, counter material and stroke length on wear resistance. Wear results are presented extensively in **Paper 3** [11] including coefficient of friction (COF), wear mechanisms, wear track profiles and wear rate results.

Since wear behaviour is highly dependent on parameters such as load, counter material or stroke length, three setups were designed in order to evaluate the dry sliding wear behaviour on metal-on-metal and ceramic-on-metal:

- **Setup 1:** 2 N, 1 Hz, and 10 mm against metal (stainless steel ball).
- **Setup 2:** 2 N, 1 Hz, and 10 mm against ceramic (alumina ball).
- **Setup 3:** 5 N, 1 Hz, and 5 mm against ceramic (alumina ball).

As mentioned in the introduction chapter, in synovial joints such as hip and knee there is a great effort to change the cup material from polymer to metal or ceramic due to the long-term problems derived from the ultra-high-molecular weight polyethylene (UHMWPE) wear debris [12]. Therefore, the selected testing conditions will be useful to understand the wear of the designed modified Ti surfaces against metal or ceramic.

Table 4.5 collects the main wear results on the modified Ti materials at the different conditions. Regarding coefficient of friction, different behaviour was observed on the designed Ti surfaces between metal-on-metal and ceramic-on-metal. Slightly higher COF values were obtained when the surfaces were tested against stainless steel compared to against alumina ball. This was also observed in the wear track profiles; the metal ball produced to higher wear than ceramic ball leading to deeper wear tracks and higher wear rate values. This could be attributed to the higher adhesion tendency between metals which leads to increase friction. However, all the modified samples exhibited better wear resistance against metal with respect to unmodified Ti.

When comparing ceramic-on-metal wear, the effect of load (2 or 5 N) was evidenced. As it was expected, a bigger load was found to produce more wear and COF values increased earlier during sliding time than by applying 2 N. This resulted in wider and deeper wear tracks for 5 N with higher wear rate values. Nevertheless, comparing to Ti an improved dry sliding wear resistance against ceramic was also reached on all the modified Ti surfaces as in the case of metal-on-metal. A

significant wear rate reduction with respect to wear of titanium was achieved on all the modified surfaces, raising up to 96 % and 79 % on the Ti-Mo<sub>NH<sub>4</sub>Cl</sub> material when it was rubbed against alumina under 2 N and 5 N, respectively.

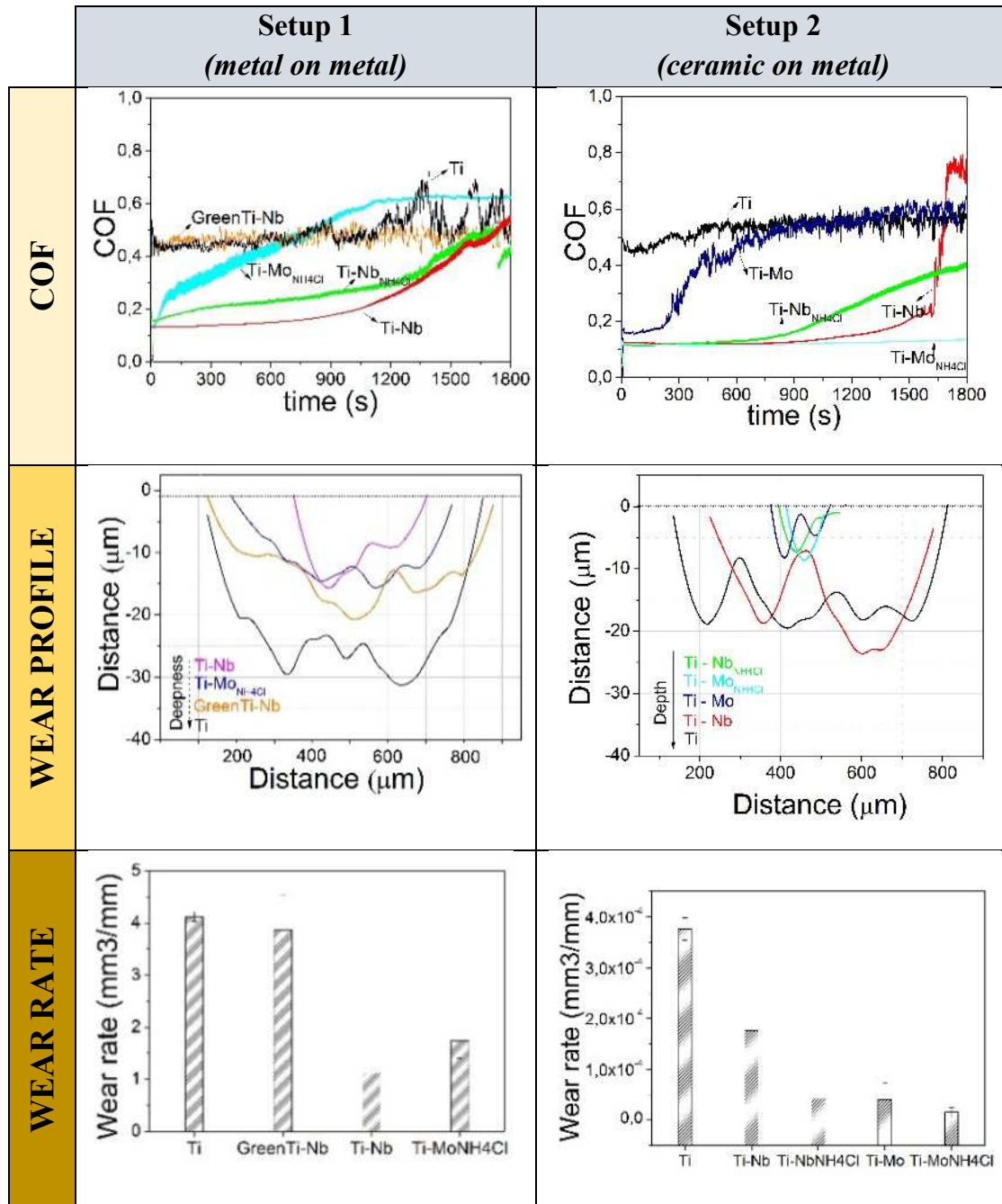
The evolution of COF under the three testing conditions showed same tendency suggesting that the  $\beta$ -surfaces protect the material from the wear action lowering the friction value, but becoming gradually worn reaching the  $\alpha+\beta$  region of the samples. Therefore, the evolution of COF could be associated to the change in microstructure, with lowest COF values corresponding to the rubbing action against the surface composed of  $\beta$ -phase and higher COF values may be indicating the second layer of the diffusion layer composed of  $\alpha+\beta$  phases.

Under the three testing conditions, the wear tracks remained in the diffusion layers of the modified Ti samples. Specifically, in the microstructural ( $\beta / \alpha+\beta / \alpha$ ) gradient, the maximum depth of the wear tracks reached the  $\alpha+\beta$  region of the diffusion layers but not the  $\alpha$ -area of the Ti substrate. This explained the COF evolution from lower to higher values, suggesting the partial removal of the  $\beta$ -area of the surfaces. This was more noticeable depending on the severity of the wear conditions: 2 N-ceramic was found to wear the least, 5 N-ceramic the most and 2 N-metal in-between both of them. Wear was less pronounced in the case of the hardest surfaces (Ti-Nb<sub>NH<sub>4</sub>Cl</sub> and Ti-Mo<sub>NH<sub>4</sub>Cl</sub>) indicating superior wear resistance and an improvement of the load-bearing capacity.

From the wear track analysis on the samples, the amount of wear volume was obtained following the model detailed in the chapter 3. All of the surfaces exhibited reduced wear volume compared to Ti which resulted in low wear rate values. Wear volume is an important issue in biomaterials since high wear volume is related to metallic ions release and adverse reactions in the body [12], [13].



**Table 4.5** Summary of dry sliding wear (COF, wear profile and wear rate) results on the modified Ti surfaces for metal on metal and ceramic on metal under 2 N load.



Regarding metal-on-metal wear mechanisms, abrasion with some oxide formation and adhesion marks was evidenced. Abrasive wear was clearly observed by means of grooves parallel to the sliding direction while chemical analysis revealed the existence of oxides and adhesion marks from the stainless steel ball to the surface. Abrasion was not evidenced on the activated material  $\text{Ti-Mo}_{\text{NH}_4\text{Cl}}$  which exhibited a surface structure practically not damaged with only reduced signs of oxides and adhesion as a consequence of its harder TiN layer on surface.

Wear mechanisms related to the ceramic-on-metal sliding resulted in a combination of different grades of abrasion, oxidation and adhesive mechanisms. Adhesion was mainly evidenced on Ti since some rest of alumina was found through chemical analysis. However, Ti-Nb surfaces seemed to be affected by abrasion and oxidation. However, comparing metal-on-metal and ceramic-on-metal under the influence of same load, alumina on Ti surfaces seems to reduce adhesive wear, being the oxidative wear the main mechanism.

Figure 4.9 shows 3D and SEM images at lower and higher magnifications of the wear tracks on Ti, Ti-Nb and Ti-Mo<sub>NH4Cl</sub> as examples of ceramic-on-metal wear. From the 3D and lower magnification images, reduced wear tracks were observed on the modified Ti surfaces with respect to that of Ti, having the Ti-Mo<sub>NH4Cl</sub> the narrowest and less deep wear track. As it can be seen, grooves are observed with the secondary electron whereas oxides or adhesion marks with the back scattering electron. Abrasive grooves were deeper on Ti followed by the Ti-Nb surface, as well as higher amount of dark areas corresponding to oxides were found on Ti. This shows the reduced abrasion on the modified samples, and practically only oxidation wear on Ti-Mo<sub>NH4Cl</sub>, demonstrating the thermo-reactive diffusion as an effective method to improve wear resistance of Ti.

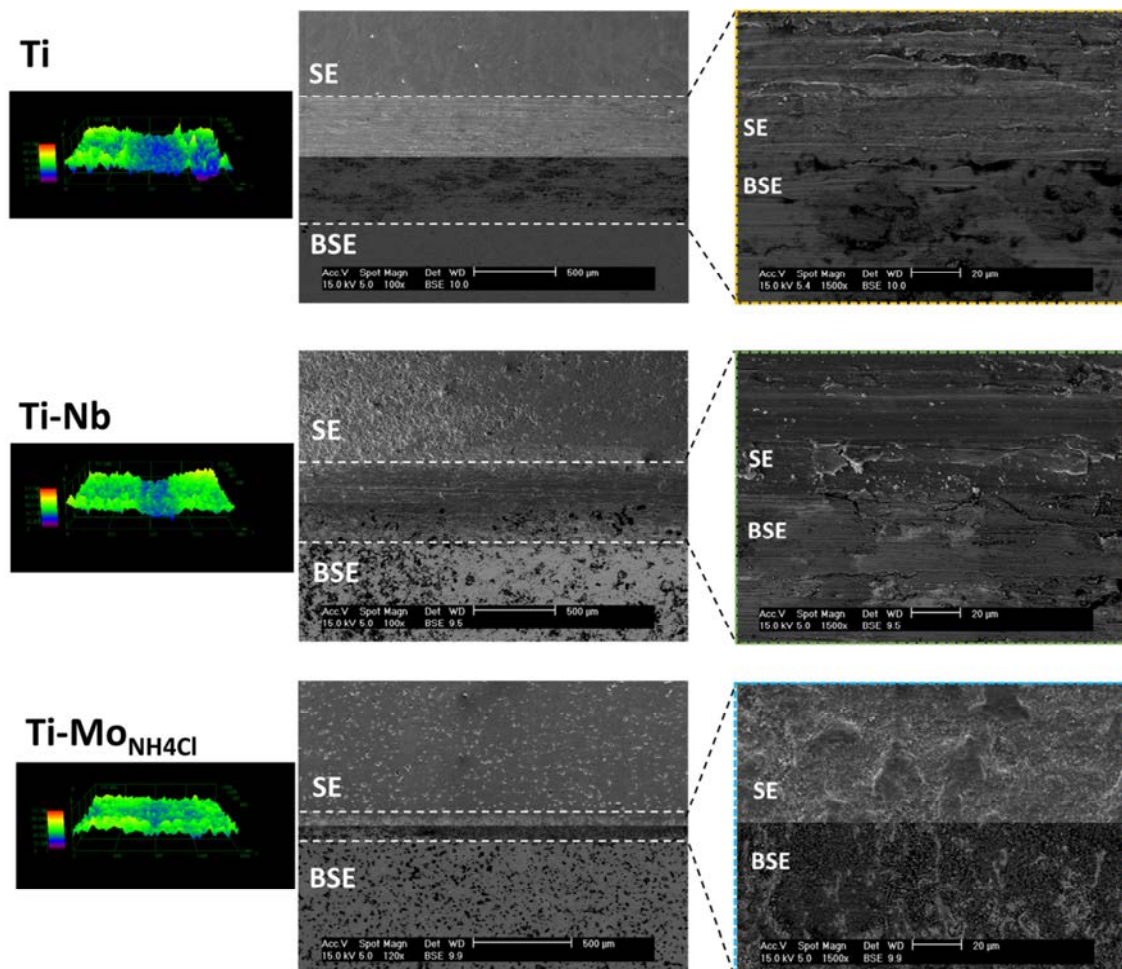


**Figure 4.9** 3D profilometer and SE-BSE images of the wear tracks on Ti, Ti-Nb and Ti-MoNH<sub>4</sub>Cl after dry sliding wear test at 2 N against alumina (setup 2).

The fact of increasing load on the ceramic-on-metal sliding behaviour led to a more severe wear. Reduced wear tracks were reached compared to Ti, but the width reduction under 5 N load was less pronounced than those obtained at 2 N load. Signs of severe abrasion were noticed in Ti, Ti-Nb and Ti-Nb<sub>NH<sub>4</sub>Cl</sub> with some ridges may be produced by wear debris accumulation and material transfer that increased with respect to wear at 2 N suggesting also adhesive wear. Similar wear mechanisms were found on ceramic-on-metal under different load. However, mild adhesion appeared with the bigger load (5 N), which may indicate a transition to higher wear at bigger loads (> 5 N).

**The complete results and detailed discussion is published in: [Paper 3]**

## **Corrosion behaviour of the modified Ti surfaces**

This section studies the corrosion behaviour of: i) one of the most employed titanium alloy in the biomedical sector, Ti-6Al-4V obtained by forged (ELI, extra low interstitial, medical grade, Surgival SL.) together with the Ti-6Al-4V and Ti-6Al-7Nb alloys obtained by powder metallurgy (**Paper 4**); and ii) the modified Ti surfaces designed in this thesis work (**Paper 5 and 6**).

First, **Paper 4** [14] presents the electrochemical comparative results on corrosion behaviour of conventional and powder metallurgy titanium alloys in physiological conditions. The influence of the processing method of alloys (PM or conventional) and their composition (Ti-6Al-4V or Ti-6Al-7Nb) on the corrosion resistance were evaluated in a simulated body fluid (SBF) from one day to twelve weeks of immersion by electrochemical impedance spectroscopy (EIS). These Ti biomaterials were selected because of depending on the type of prosthesis or implants, the  $\alpha+\beta$ -Ti-6Al-4V alloy or  $\alpha$ -CP Ti pure titanium are nowadays the most extensively used Ti biomaterials for bone substitution and dental, heart and cardiovascular devices [12]. However, the  $\alpha+\beta$ -Ti-6Al-7Nb alloy has been also developed for the biomedical sector with the aim of replace the Ti-6Al-4V alloy by offering a free vanadium alloy with better wear resistance and superior behavior in the casting processing. Although this alloy is not such employed as the Ti-6Al-4V, this was designed for hip and femur prosthesis, spine components, staples and wireless, owing its high resistance, good ductility and toughness, and excellent biocompatibility due to the passive stable and dense oxide layer (Nb<sub>2</sub>O<sub>5</sub>) [15].

On other side, it was thought that could be interesting to compare the corrosion resistance between conventional and powder metallurgy (PM) alloys due to the many advantages of the PM processing. Moreover, the corrosion behavior of conventional titanium alloys are widely studied, but the work on PM alloys are more limited and almost always performed on pure Ti or Ti-6Al-4V alloy [16].

From this study, good reproducibility on the conventional and PM Ti6Al4V alloy as well as on the PM Ti-6Al-7Nb alloy was obtained from the Nyquist and Bode diagrams. The three studied alloys displayed high impedance modulus value approximately on the order of  $10^6 \Omega$  from short to long immersion times. This behavior indicates a high corrosion protection performance. These high impedance values from middle to low frequencies in all samples could be ascribed to the spontaneous growth of fresh oxide layers that are covering the entire metal substrate when the metal surfaces are placed in contact with the simulated body fluid. The impedance spectra were fitted with an equivalent circuit describing the behaviour of porous passive layers where the metal-electrolyte interactions take place into the layer pores situated on the metal surfaces.

Although no significant differences in the evolution of the corrosion behavior for different immersion times were found; slight differences can be noticed from the detailed views. The forged Ti-6Al-4V alloy exhibited the maximum impedance value at 14 days while decreasing for longer immersion times. Ti-6Al-4V alloy processed through powder metallurgy reached the maximum value at one day and six weeks while decreased for the longest time of 12 weeks. However, the powder metallurgy Ti-6Al-7Nb alloy delivers a steady growth of corrosion resistance from day one until twelve weeks immersion. Therefore, this composition showed the best performance between the two studied compositions, and the powder metallurgy processing allowed obtaining materials with similar or superior corrosion resistance in physiological conditions than alloys obtained conventionally.

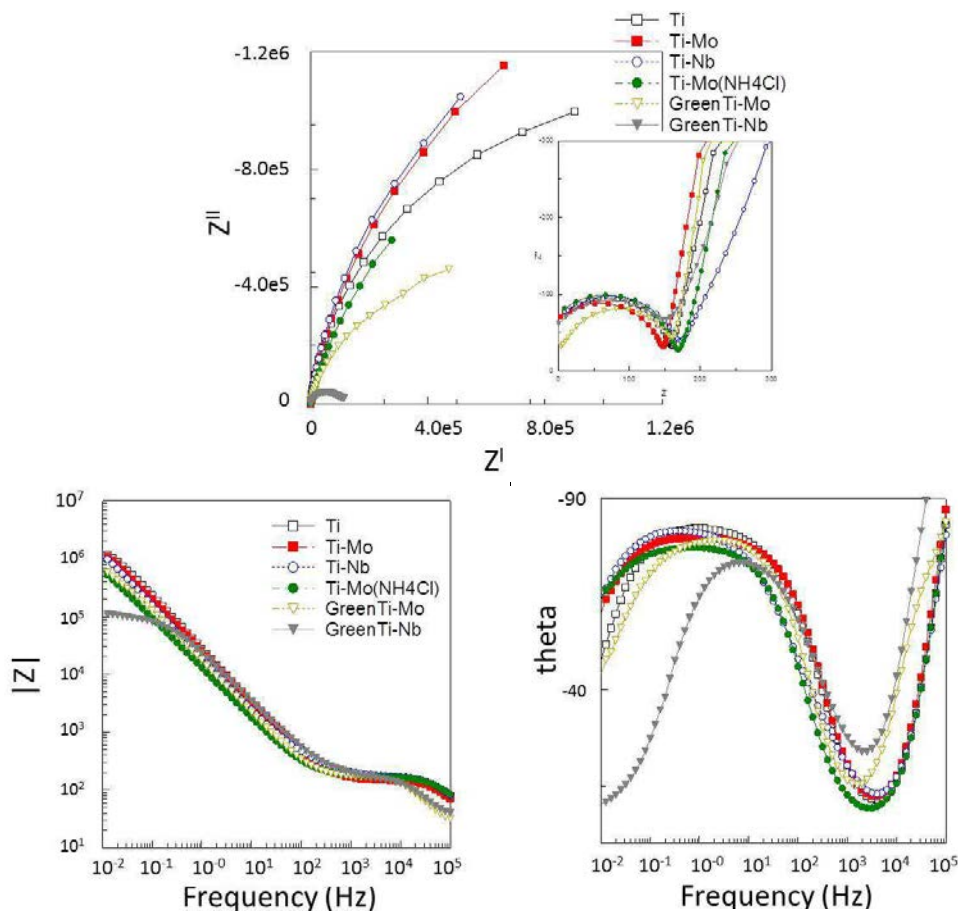
**The complete results and detailed discussion is published in: [Paper 4]**

After the previous electrochemical results on the corrosion behaviour of conventional and powder metallurgy titanium alloys, it was confirmed that the powder metallurgy processing allows obtaining Ti alloys with high corrosion resistance. Therefore, this second part joins the corrosion behaviour of powder metallurgy surfaces designed with  $\beta$ -stabilizing elements. As it was mentioned in the introduction chapter, currently the  $\beta$ -Ti type alloys are the most promising for biomaterials due to their lower Young's modulus and also better corrosion behaviour with respect to the  $\alpha$  or  $\alpha+\beta$  Ti alloys. In this context, it was planned to carry out the surface modification on the powder metallurgy  $\alpha$  CP-Ti employing Mo or Nb elements by diffusion treatments with the aim of improving wear and

mechanical performance while maintaining or increasing the good corrosion resistance.

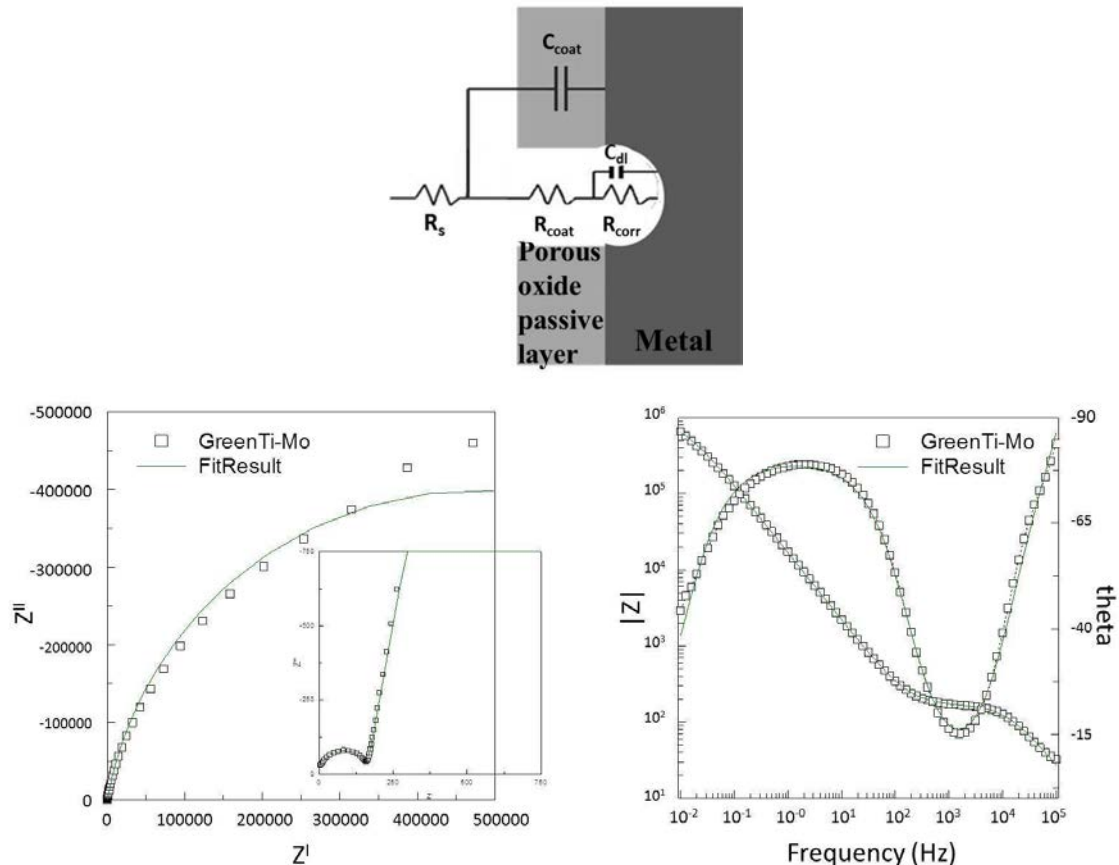
**Paper 5** [17] and **6** [18] present the corrosion behaviour results on the designed modified Ti-Nb and Ti-Mo surfaces and CP-Ti in a 9 g/l NaCl solution, since it represents the major compound of the physiological fluid.

Figure 4.10 showed the Bode plots with a typical shape influenced by the performance of two well-differentiated time constants. This behaviour is typically observed on passivating metals and mainly ascribed to a porous passive layer with metal-electrolyte interactions due to the presence of pores on surface [19]. Similarly to the previous Ti-6Al-4V and Ti-6Al-7Nb alloys, high impedance modulus values around  $10^6 \Omega \text{ cm}^2$  were obtained for all the modified Ti surfaces, suggesting high corrosion resistance in the saline solution. Although, in the case of the co-sintered sample GreenTi-Nb the value was almost one order smaller maybe attributed to the fact that the Nb deposition was deposited on a green Ti substrate in a single step. On the other hand, it seems that the TiN layer of the Ti-Mo<sub>NH4Cl</sub> sample processed by thermo-reactive diffusion acts as a protective passive layer with similar behaviour to Ti.



**Figure 4.10** Nyquist and Bode diagrams obtained for the modified Ti surfaces after 1 h immersion in 9 g/l NaCl solution.

Since all the materials showed similar behaviour, Figure 4.11 presents the Nyquist and Bode plots showing the experimental and fitted data for GreenTi-Mo sample after 1 h of immersion in 9 g/l NaCl solution. The fitted data was obtained after simulation using the electric equivalent circuit shown. The good agreement between fitted and measured data together with the low errors and the small chi-squared confirmed that our systems fitted to a porous oxide passive layer.



**Figure 4.11** Electric equivalent circuit used in the impedance spectra analysis based on a porous oxide passive layer model. Nyquist and Bode plots with fitting for the GreenTi-Mo sample after 1 h of immersion in 9 g/l NaCl solution.

The good corrosion behaviour of our Ti-Mo and Ti-Nb systems led to perform this kind of surface modification on powder metallurgy Ti-6Al-4V substrates. Some preliminary studies of Mo and Nb diffusion in Ti-6Al-4V alloy have been conducted with the aim of testing the corrosion behaviour of those modified surfaces.

Although, less deep diffusion gradients were obtained in the modified-Ti6Al4V surfaces with respect to the modified Ti materials, further studies of their corrosion behaviour would be interesting.

**The complete results and detailed discussion is published in: [Paper 5 to 6]**

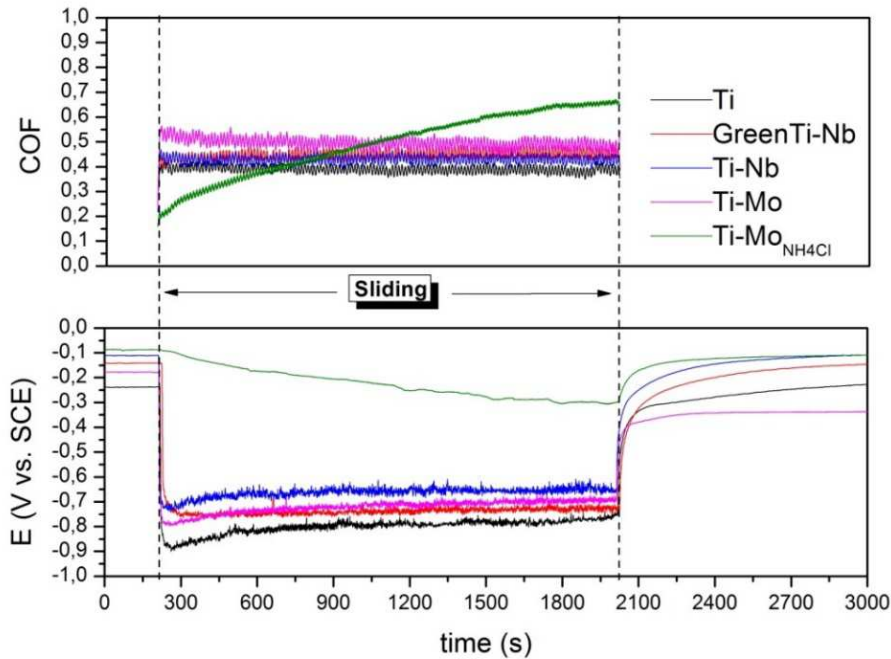
## Tribocorrosion behaviour of the modified Ti surfaces

This section presents a first approach to the tribocorrosion behaviour of the modified Ti materials. As it was introduced in chapter 1, wear-related problems derived from synergistic wear-corrosion interactions lead to drawbacks related to the stability of the implant material caused by tribocorrosion failures. **Paper 5 and 6** presents the results on tribocorrosion behaviour. With the aim of comparing the dry-sliding wear to the tribocorrosion behaviour, similar conditions to those of setup 2 in dry sliding were selected:

- 1 N, 1 Hz, and 10 mm against alumina ball.

Figure 4.12 shows the evolution of the coefficient of friction (COF) during sliding together with the OCP before, during and after sliding. COF values showed similar tendency between GreenTi-Nb, Ti-Nb and CP-Ti with a stable value around 0.45. This may be attributed to the good lubricant properties of the Nb<sub>2</sub>O<sub>5</sub> passive layer and the quickly repassivation of Nb [12]. Ti-Mo also exhibited a stable COF value of 0.5, while COF of Ti-Mo<sub>NH<sub>4</sub>Cl</sub> was increasing during sliding time from 0.2 to 0.65. In the case of Ti-Mo<sub>NH<sub>4</sub>Cl</sub>, the TiN layer on surface created by the activating agent (NH<sub>4</sub>Cl) during the thermo-reactive diffusion seems to lower the COF (0.2) initially. However, the increased COF values during sliding could be related to the increased roughness of the wear track through testing time. The highest hardness ( $\approx$  1025 HV) of the Ti-Mo<sub>NH<sub>4</sub>Cl</sub> surface with respect to rest of the modified surfaces (300-440 HV) lead to the formation of harder wear debris together with their accumulation and packing to the surface increasing roughness and COF values.

Regarding OCP evolution, potentials were stable at similar values for all materials before sliding (-0.1 to -0.25 V). Then when sliding started, all samples showed an abrupt fall of the OCP related to the total or partial destruction of the different passive layers as a consequence of the mechanical action [20]. Under sliding, all modified Ti surfaces exhibited more positive potential values than CP-Ti, indicating lower tendency to corrosion on the modified surfaces. When the wear action was completed and the mechanical contact stopped, the repassivation phenomenon of the worn areas took place in all samples forming new barriers against corrosion [21]. Finally, potential reached higher values (-0.1 to -0.35 V) similar to those before sliding, indicating a great recovery capacity of the passive layers. Generally,  $\beta$ -Ti alloys present a great recovery capacity of their oxide layers due to their good stability.



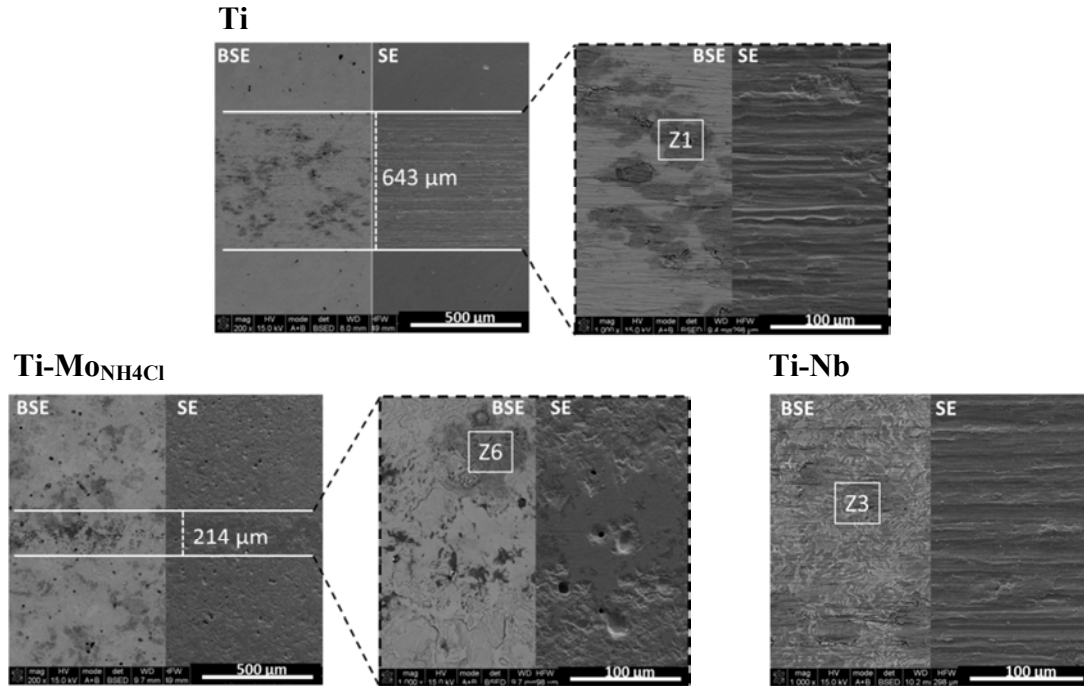
**Figure 4.12** Evolution of COF and OCP during tribocorrosion test in 9 g/l NaCl solution.

Figure 4.13 shows the Ti, Ti-Mo<sub>NH4Cl</sub> and Ti-Nb worn surfaces after the tribocorrosion measurements. These surfaces were selected as examples among all the materials tested, the rest of worn surfaces are presented in Paper 6. Grooves paralleled to the sliding direction as signs of abrasive wear mechanism were found. Nevertheless, grooves observed on the Ti-Mo<sub>NH4Cl</sub> surface were much shallower with respect to the other surfaces due to its higher hardness and increased Young's modulus characteristic from the TiN layer on surface. On the other hand, this surface showed less plastic deformation compared to the other samples, having a narrow, smooth and shallow wear track up to three times smaller ( $\approx 214 \mu\text{m}$ ) with respect to Ti ( $\approx 643 \mu\text{m}$ ). This is mainly attributed to the higher hardness leading to the reduction of plasticity. Thus, the noticeable increased hardness of the Ti-Mo<sub>NH4Cl</sub> led to improve the tribocorrosion behaviour. This agrees with the low COF value (0.2) observed for the Ti-Mo<sub>NH4Cl</sub> material, suggesting that the COF increase at 800 s mainly is attributed to the accumulation of harder wear debris.

The presence of dark areas was highly noticed on the bare Ti surface than on the modified Ti surfaces. EDS analysis showed the composition of these areas, which mainly contains Ti and O elements, corresponding to titanium oxides. The repetitive transfer of Ti between the sliding surfaces and its oxidation leads to the formation of oxidised wear debris and eventually their compacting to the surface under the influence of the applied load. Hence, the wear mechanisms under synergistic interactions between wear and corrosion for all the surfaces were shown as a combination of abrasion by the presence of grooves, with some adhesive oxide areas due to oxides accumulation [22]. The surfaces showed similar wear abrasion



mechanism, although GreenTi-Nb exhibited more abrasive grooves compared to CP-Ti, whereas Ti-Nb and Ti-Mo presented less abrasion areas with respect to Ti, and the Ti-Mo<sub>NH4Cl</sub> surface practically was not damaged. The adhesive oxide areas were mainly observed on CP-Ti.



**Figure 4.13** SE-BSE images of the worn surfaces after tribocorrosion test.

The average wear volume of the modified Ti materials remained around  $8.51 \times 10^{-2} \text{ mm}^3$ ,  $6.54 \times 10^{-2} \text{ mm}^3$ ,  $7.28 \times 10^{-2} \text{ mm}^3$  and  $1.29 \times 10^{-3} \text{ mm}^3$  for GreenTi-Nb, Ti-Nb, Ti-Mo and Ti-Mo<sub>NH4Cl</sub>, respectively; with respect to  $6.04 \times 10^{-2} \text{ mm}^3$  of CP-Ti. Whereas Ti and Ti-Nb exhibited similar results, GreenTi-Nb presented slightly higher wear volume probably associated to the deeper grooves of abrasion. Nonetheless, very low wear volume was noticed for Ti-Mo<sub>NH4Cl</sub> surface which can be ascribed to its high hardness. This can be suggesting that when the surface modification is carried out in GreenTi (as-pressed) during co-sintering and diffusion route, wear resistance seems to be smaller than when Nb diffusion is performed in a sintered Ti substrate. This wear dependence on diffusion treatments could be ascribed to hardness, since high hardness is related to the reduction of plasticity. However regarding the tendency to corrosion under synergistic wear-corrosion interactions, both Ti-Nb materials showed OCP values stabilized above CP-Ti.

The  $\beta$ -Ti surfaces (GreenTi-Nb, Ti-Nb and Ti-Mo) exhibited lower wear resistance in tribocorrosion compared to their dry sliding wear behaviour. This could be explained due to the aggressive effect of the saline solution on the materials surface during wear. However, Ti-Mo<sub>NH4Cl</sub> surface showed similar wear tendency in both

cases, presenting interesting tribocorrosion properties with high corrosion and wear resistance.

The corrosion tendency under wear-corrosion synergism was lower for all the treated-surfaces compared to CP-Ti, including GreenTi-Mo and GreenTi-Nb materials. This means that all the treated-surfaces show a more protective behaviour toward corrosion when a mechanical action starts to take place on their surfaces.

**The complete results and detailed discussion is published in: [Paper 5 to 6]**

## 4.7 Biocompatibility features of the modified Ti surfaces: bioactivity, cytotoxicity and osteogenic differentiation response

This section summarizes the biocompatibility character of the final materials. Prior to the bioactivity and biological tests, the surface conditions were selected in order to ensure a reliable biological response since the surface physico-chemical properties are considered as important factors on cell behaviour. Therefore, chemical composition, roughness and wettability were assessed and discussed.

**Paper 7** [23] presents the results on the surface properties together with the bioactivity and cytotoxicity study. The selection of the materials for the bioactivity analysis was Ti-Nb, Ti-Mo, Ti-Nb<sub>NH4Cl</sub> and Mo<sub>NH4Cl</sub>. Since the surface properties are key parameters in these studies, for comparison purposes two different surface finishing routes were followed on Ti-Nb and Ti-Mo:

- **Route 1:** soft grinding step with 1200# SiC paper → finally labelled as Ti-Nb and Ti-Mo.
- **Route 2:** as coated (without post-treatment) → finally labelled as Ti-Nb<sub>coat</sub> and Ti-Mo<sub>coat</sub>.

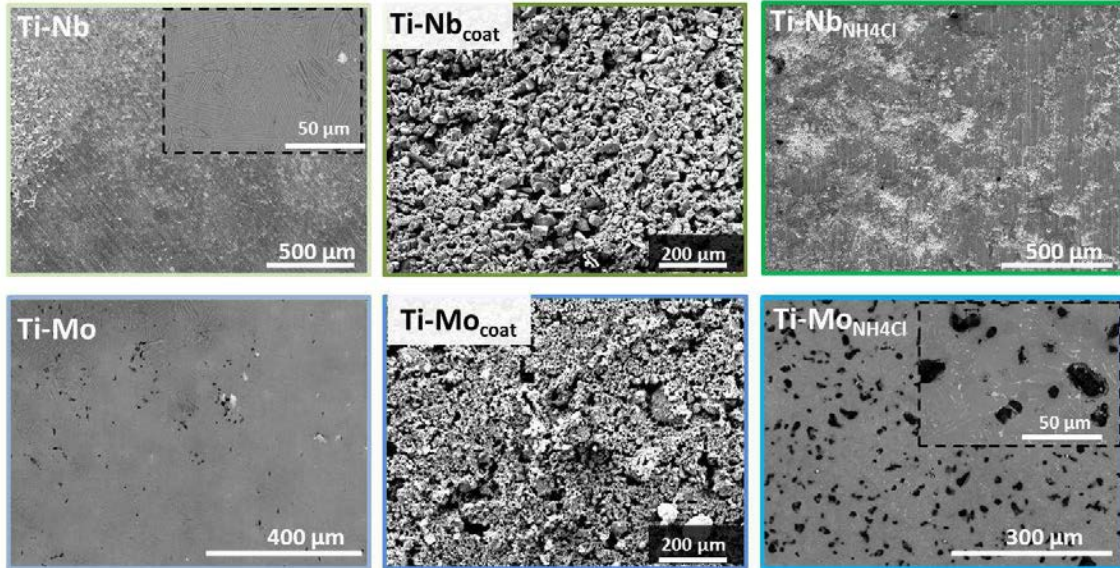
Table 4.6 collects the designed materials employed in the bioactivity analysis together with their final surface properties of chemical composition, roughness and wettability. From these results, it seems that Nb lead to surfaces slightly rougher and more hydrophobic compared to Ti-Mo surfaces.

**Table 4.6** Surface physico-chemical properties of the designed materials.

Designed materials	Chemical composition [wt.%]					Surface condition	
	Ti	Nb	Mo	O	N	Roughness [ $\mu\text{m}$ ]	Wettability [ $^\circ$ ]
<b>Ti</b>	100	----	----	----	----	$0.7 \pm 0.3$	$83.9 \pm 0.8$
<b>Ti-Nb</b>	65	35	----	----	----	$1.4 \pm 0.3$	$83.1 \pm 1.6$
<b>Ti-Nb<sub>coat</sub></b>	1	99	----	----	----	$2.2 \pm 0.2$	$104.0 \pm 2.3$
<b>Ti-Nb<sub>NH4Cl</sub></b>	82	1	----	8	9	$1.8 \pm 0.3$	$91.3 \pm 1.6$
<b>Ti-Mo</b>	65	----	18	----	----	$0.7 \pm 0.3$	$73.4 \pm 2.9$
<b>Ti-Mo<sub>coat</sub></b>	1	99	----	----	----	$0.8 \pm 0.3$	$85.9 \pm 10.9$
<b>Ti-Mo<sub>NH4Cl</sub></b>	86	----	1	7	6	$1.4 \pm 0.2$	$91.3 \pm 1.5$

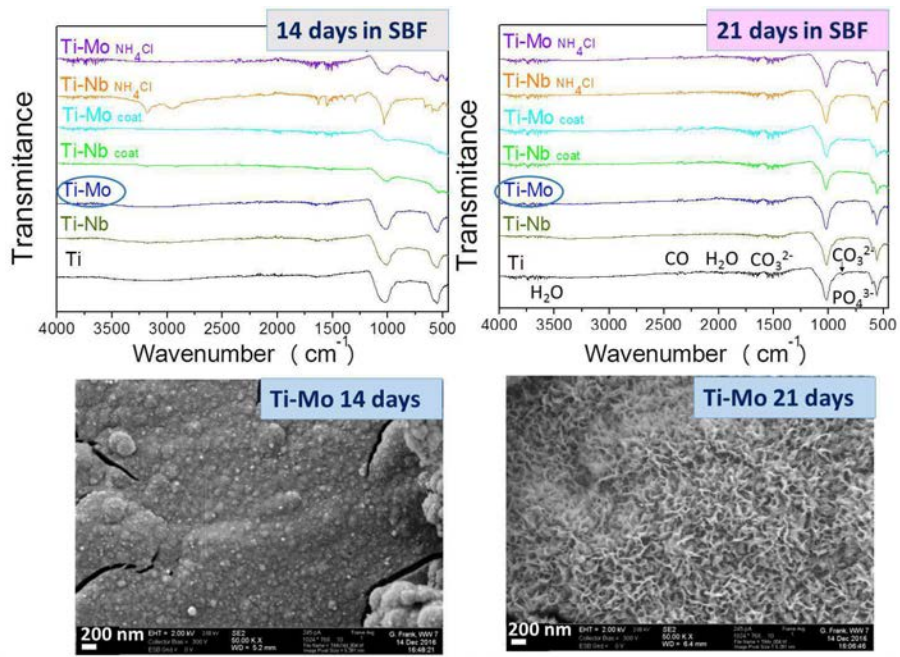
Figure 4.14 shows the scanning electron micrographs of all the modified Ti surfaces. The surface modification by Nb or Mo diffusion treatments led to similar microstructure, but depending on the surface finishing on one hand, a homogeneous

microstructure composed of very close and compact  $\beta$  lamellas was found in Ti-Nb and Ti-Mo, and on the other hand a surface composed of Nb or Mo powder micro-particles in the as-coated samples. The thermo-reactive diffusion treatment led to Ti-Nb<sub>NH4Cl</sub> and Ti-Mo<sub>NH4Cl</sub> materials with porous microstructures and few  $\beta$  lamellas.



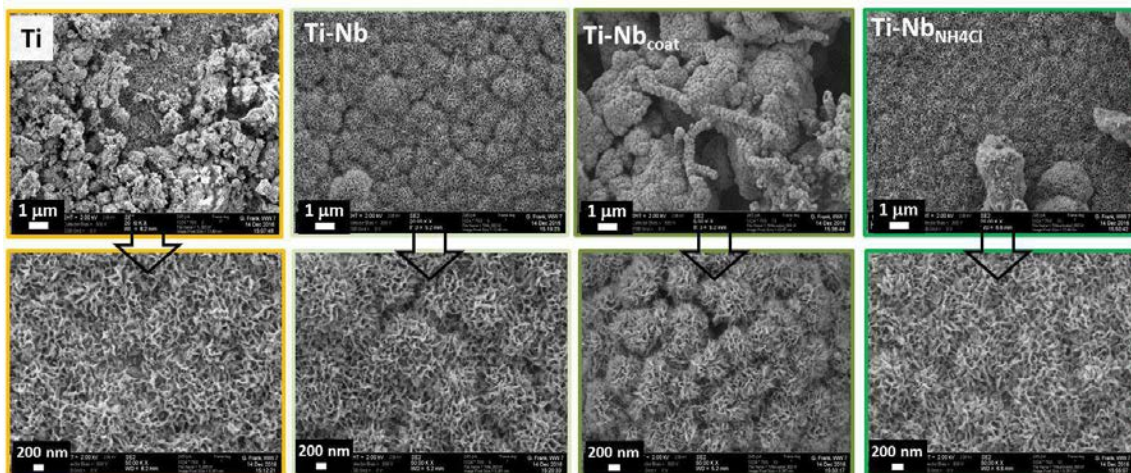
**Figure 4.14** Surface SEM micrographs obtained from the designed materials.

**Paper 7** summarizes the *bioactivity response* of the materials after immersion in simulated body fluid (SBF) during 14 or 21 days, giving an idea of the apatite-forming ability. Figure 4.15 shows the FTIR spectra of all the modified materials after soaking in SBF for 14 or 21 days together with a SEM image of the Ti-Mo surface as an example. Both FTIR spectra exhibited similar peaks although those formed for the longer immersion time of 21 days appeared better defined than those corresponding to 14 days. The strongest bands, at  $563$  and  $1061\text{ cm}^{-1}$  were attributed to the  $\text{PO}_4^{3-}$  group, as well as the less intensive one at  $605\text{ cm}^{-1}$ ; confirming the formation of hydroxyapatite. The carbonate group characteristic bands were also observed at  $873$  and  $1423\text{ cm}^{-1}$ ; and the band at  $2300\text{ cm}^{-1}$  was assigned to a CO group. The SEM examination confirmed the presence of hydroxyapatite in terms of cauliflower structure after 21 days of immersion in SBF but only some ions precipitation after 14 days. Thus, this pointed out the bioactive character of the surfaces for 21 days.



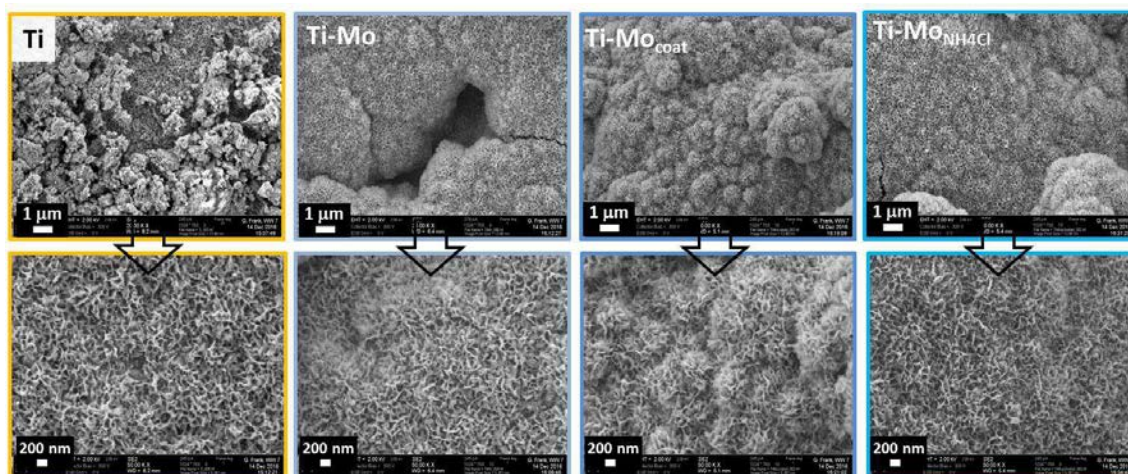
**Figure 4.15** FTIR spectra results on the modified Ti surfaces after immersion in SBF for 14 and 21 days. Surface SEM micrograph obtained for the Ti-Mo material as an example of the different surface morphology depending on the immersion time 14 or 21 days.

Figure 4.16 shows at lower and higher magnification the evidences of the hydroxyapatite precipitates on all the surfaces after 21 days of immersion in SBF. They appeared homogenously distributed over the surface; forming a hydroxyapatite layer. The layer was formed similarly in all the surfaces showing a dense and well-defined cauliflower structure. However at lower magnification, the hydroxyapatite is better observed on the three Ti-Nb surfaces than on Ti, showing the bioactive character of the modified surfaces and the apatite-inducing ability after 21 days immersion in SBF.



**Figure 4.16** FE-SEM micrographs obtained from the Ti-Nb surfaces after 21 days of immersion in SBF showing the hydroxyapatite with cauliflower structure.

Similar morphological features were obtained on the Ti-Mo surfaces after 21 days immersion in SBF as is shown in Figure 4.17. A hydroxyapatite layer was well-formed on all the modified surfaces giving the characteristic cauliflower structure. The hydroxyapatite was much denser in the case of Ti-Mo surfaces which points out the positive effect of the surface modification on the bioactive character.



**Figure 4.17** FE-SEM micrographs obtained from the Ti-Mo surfaces after 21 days of immersion in SBF showing the hydroxyapatite with cauliflower structure.

**Paper 7** also shows the cell culture study of human osteoblast-like cells (MG-63) on the modified Ti samples by niobium diffusion: Ti-Nb, Ti-Nb<sub>coat</sub> and Ti-Nb<sub>NH4Cl</sub> to test their *cytotoxicity response* after two days of cell culturing. Results about cell viability, cell proliferation, and cell adhesion and morphology are shown, discussed and compared to the control Ti sample.

Figure 4.18 shows the Calcein staining of MG-63 osteoblast-like cells in direct contact with the different material surfaces after 48 h of incubation. Living cells are identified by a green fluorescence staining; confirming good cell-material interaction represented by the great concentration of cells on all the surfaces. The cells were well adhered and spread in contact with all the surfaces. Cells on the Ti surface presented an elongated shape while on the modified Ti surfaces they adopted a stellate polygonal morphology with multidirectional spreading and higher connections between each other. Images show the good cell-material interaction of all the surfaces, but especially Ti-Nb<sub>coat</sub> was the most colonized with cells covering most of the surface.

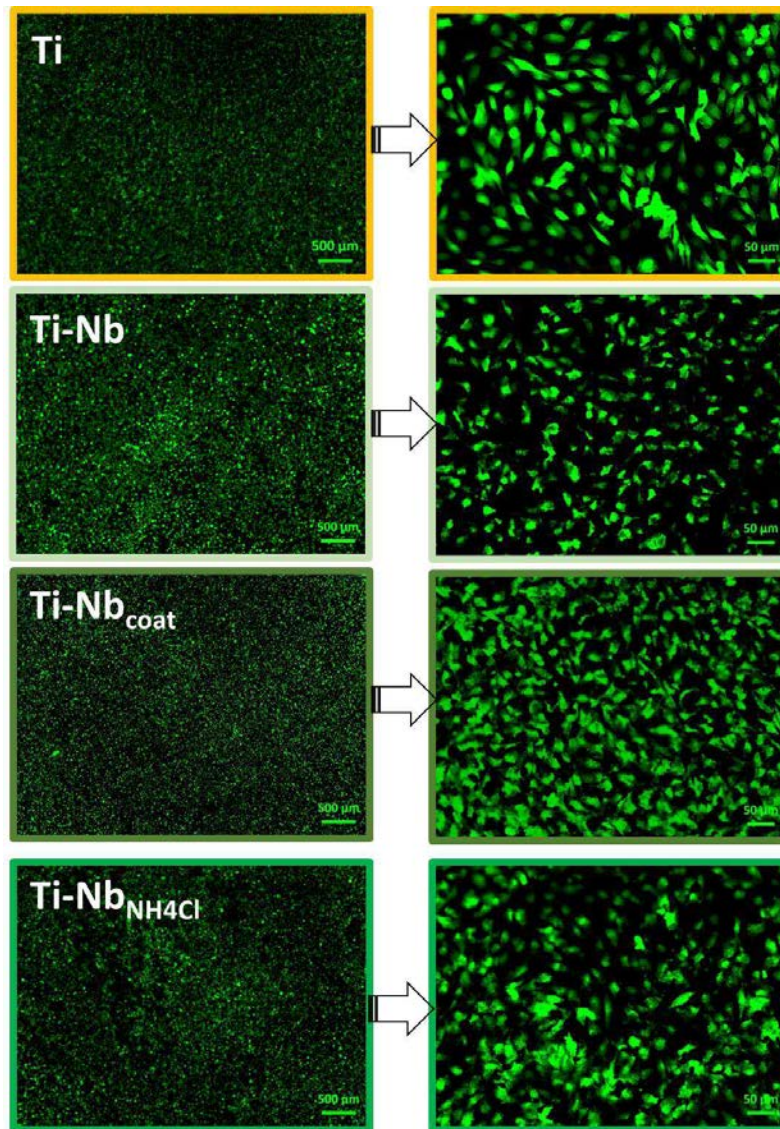


**Figure 4.18** Living human osteoblast-like MG-63 cells after culturing for 2 days on modified Ti surfaces.

Cell viability of MG-63 cells was determined through a reduction reaction of the indicator WST-8 by dehydrogenases from cells. This led to the yellow-orange color pointing out the formation of formazan compound (directly proportional to the number of living cells). The absorbance was measured at 450 nm, and the cell viability for each material was expressed as the 100% of cell viability for the Ti sample; obtaining values higher than 40 % for Ti-Nb, 70 % for Ti-Nb<sub>NH<sub>4</sub>Cl</sub> and 120 % for Ti-Nb<sub>coat</sub> composition. Therefore, the high number of cells adhered to all surfaces demonstrated the non-cytotoxic effect of Nb confirming a positive cell-material interaction of the modified Ti surfaces. The three Ti-Nb surfaces designed with different surface conditions exhibited good cell behaviour. It could be seen that the combination of a rough (2.2 μm) and Nb-rich surface (Ti-Nb<sub>coat</sub>) led to the most cell colonized surface. Moreover, the presence of a porous nitride titanium-niobium

surface (Ti-Nb<sub>NH4Cl</sub>) with a surface roughness value of 1.8  $\mu\text{m}$  also showed positive cell-interaction. There is still a not well defined consensus about wettability in biocompatibility, since some authors report surfaces hydrophilic as beneficial whereas other researches establish the hydrophobicity as more suitable for protein absorption. However in these surfaces, it seems that contact angles of 90 ° and 104 ° are suitable for the biological response of the human osteoblast-like cells.

Figure 4.19 presents a FE-SEM micrograph at high magnification showing the well spread of the cells and the connection and linking between each other promoting the cell-cell communication on the Ti-Nb<sub>coat</sub>. All the surfaces established connection with the neighboring cells; noticing that cells could anchor on these surfaces as well as into the internal pores due to the porosity created in them.

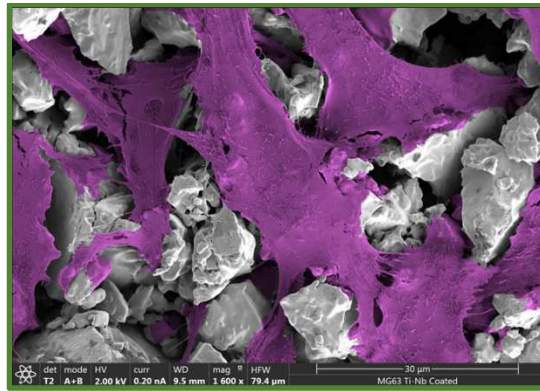


**Figure 4.19** FE-SEM image of MG-63 human osteoblast-like cells cultured on Ti-Nbcoat after 2 days.

Thereby, at this point is worth to mention that the improvement in the mechanical performance of these modified Ti surfaces (**Paper 2**) has a positive effect on their biological behaviour. The increase in hardness and decrease in elastic modulus result in an improved cell-material response.

**Paper 8** [5] shows the *osteogenic differentiation* results of the bone marrow stromal cells on Ti-Nb and Ti-Nb<sub>NH4Cl</sub>, considering aspects such as cell viability, cell proliferation, cell differentiation and bone mineralization after 21 days of cell culture.

The cellular viability and lactate dehydrogenase activity (LDH) of mice bone marrow stromal cells (ST-2) in contact with the different surface materials after 21 days of culture were assessed and compared to that of control reference material, Ti, set as 100 %. Both modified Ti surfaces exhibited high cell viability, from 75 % (Ti-Nb<sub>NH4Cl</sub>) to 110 % (Ti-Nb) referred to Ti control. Regarding LDH activity values, around 90-100 % were obtained for three surfaces, indicating similar amount of cells



in both Ti-Nb and Ti surfaces. Regarding the cell differentiation, alkaline phosphatase (ALP) activity is an indication of cells expression in their early differentiation stage and an important quantitative marker of osteogenesis. Therefore, the osteogenic differentiation of the ST-2 cells in the Ti surfaces was monitored by the activity of alkaline phosphatase enzyme (ALP). The specific ALP activity was expressed in all samples, significantly higher in Ti-Nb. Hence, ALP was positively affected by the low elastic modulus of Ti-Nb as well as by the surface porosity of Ti-Nb<sub>NH4Cl</sub>; promoting the ALP induction.

The mineralization process of newly formed bone matrix is represented by expression of calcium which is considered as bone marker for osteogenic differentiation. The calcium phosphate deposits were identified by fluorescence osteolmage staining after culture for 21 days as shown in Figure 4.20. These green stained deposits revealed the main mineral content of bone which is mostly hydroxyapatite [ $\text{Ca}_{10}(\text{PO}_4)_6(\text{OH})_2$ ]. Qualitatively, the amount of CaP nodules seemed to cover most of the area on the three surfaces. Although Ti-Nb sample exhibited slightly less green color, no significant difference were found by image analysis. These results are also in agreement with the in vitro hydroxyapatite formation on these surfaces after 21 days of immersion in simulated body fluid. In both cases hydroxyapatite is shown after 21 days, by immersion in SBF or due to the osteogenic differentiation of cells indicating the new bone matrix formation.

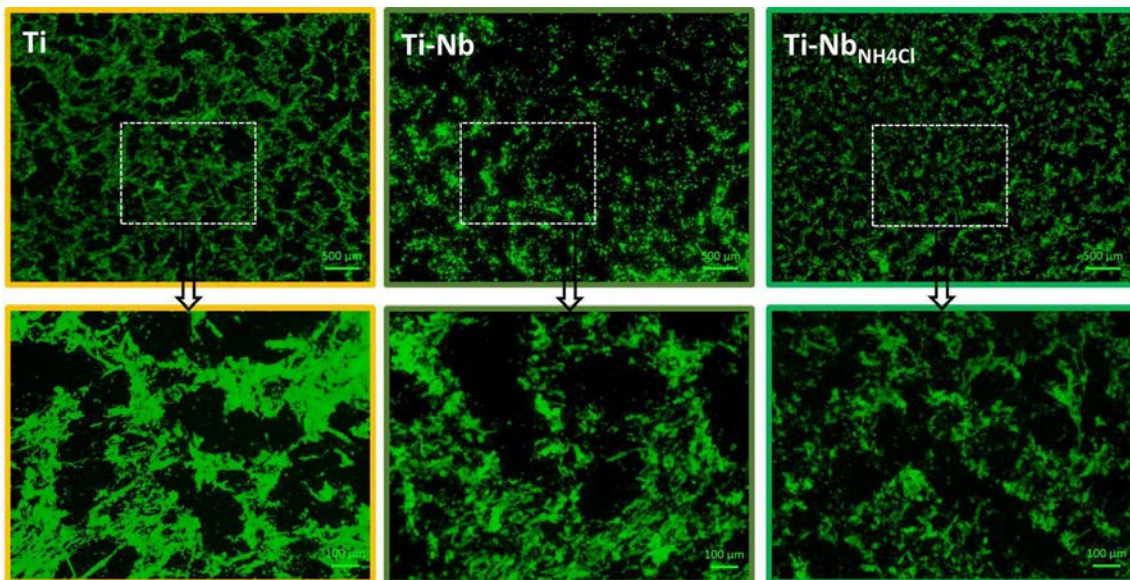


**Figure 4.20** Bone-like nodules created by bone marrow stromal ST-2 cells after culturing for 21 days, showing the in vitro bone mineralization.

The merged fluorescence micrographs representing the mineralized area (green) and distribution of DAPI-stained cell nuclei (blue) of mice bone marrow stromal cells are shown in Figure 4.21. A uniform cell distribution on the three surfaces is observed, including mineralized part (green) and rest of the surface. A High density of cell nuclei and thus, the good cell adhesion and positive cell-material interaction on the three materials are evidenced.

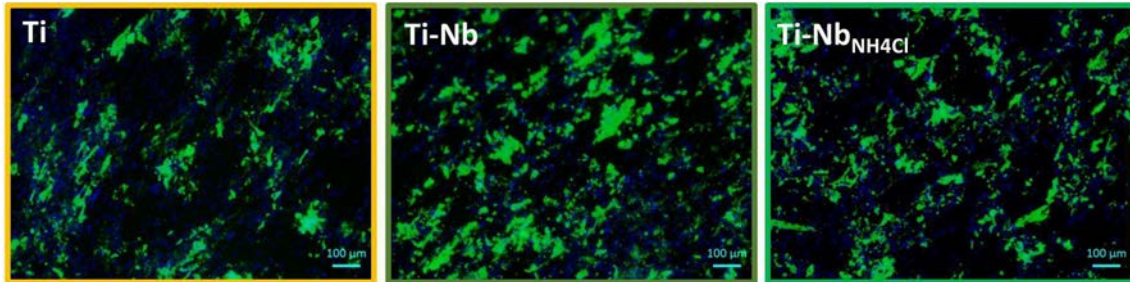


**Figure 4.21** Merged images of bone nodules area and DAPI stained ST-2 cells cultured for 21 days. Mineralized area (green) and cell nuclei (blue).

Figure 4.22 shows an example of cell morphology on Ti-Nb surface, displaying a fibroblastic phenotype shape with cytoplasmic extensions. Ti-Nb surface showed extensions over the surface looking forward to link with neighboring cells through the niobium particles and pores, and a greater amount of extracellular matrix (ECM) deposited.

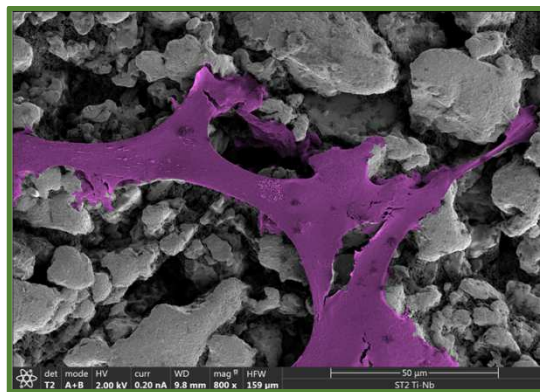


**Figure 4.22** FE-SEM image of bone marrow stromal ST-2 cells cultured on Ti-Nb after 21 days.

**The complete results and detailed discussion is published in: [Paper 7 to 8]**

## 4.5 References

- [1] L. Zhu *et al.*, “Measurement of interdiffusion and impurity diffusion coefficients in the bcc phase of the Ti–X (X = Cr, Hf, Mo, Nb, V, Zr) binary systems using diffusion multiples,” *J. Mater. Sci.*, vol. 52, no. 6, pp. 3255–3268, 2017.
- [2] “DICTRA Version 27 Examples, Thermo-Calc Software AB, Stockholm, 2013.”
- [3] S. A. Tsipas and E. Gordo, “Molybdeno-Aluminizing of Powder Metallurgy and Wrought Ti and Ti-6Al-4V alloys by Pack Cementation process,” *Mater. Charact.*, vol. 118, pp. 494–504, 2016.
- [4] J. Ureña *et al.*, “Surface Modification of Powder Metallurgy Titanium by Colloidal Techniques and Diffusion Processes for Biomedical Applications,” *Adv. Eng. Mater.*, vol. 19, no. 6, p. 1600207, 2016.
- [5] J. Ureña, S. Tsipas, A. Jiménez-morales, E. Gordo, R. Detsch, and A. R. Boccaccini, “Cellular behaviour of bone marrow stromal cells on modified Ti-Nb surfaces,” *Mater. Des.*, vol. 140, pp. 452–459, 2018.
- [6] J. Ureña *et al.*, “Role of beta-stabilizer elements in microstructure and mechanical properties evolution of PM modified Ti surfaces designed for biomedical applications,” *Powder Metall.*, p. doi: 10.1080/00325899.2018.1426185, 2018.
- [7] M. Niinomi, “Mechanical biocompatibilities of titanium alloys for biomedical applications,” *J. Mech. Behav. Biomed. Mater.*, vol. 1, no. 1, pp. 30–42, 2008.
- [8] J. Gong, J. Wu, and Z. Guan, “Examination of the Indentation Size Effect in Low-load Vickers Hardness Testing of Ceramics,” *J. Eur. Ceram. Soc.*, vol. 19, pp. 2625–2631, 1999.
- [9] P. Neacsu, D. Gordin, V. Mitran, T. Gloriant, M. Costache, and A. Cimpean, “In vitro performance assessment of new beta Ti–Mo–Nb alloy compositions,” *Mater. Sci. Eng. C*, vol. 47, pp. 105–113, 2015.
- [10] M. W. D. Mendes, C. G. Ágrede, A. H. A. Bressiani, and J. C. Bressiani, “A new titanium based alloy Ti–27Nb–13Zr produced by powder metallurgy with biomimetic coating for use as a biomaterial,” *Mater. Sci. Eng. C*, vol. 63, pp. 671–677, 2016.
- [11] J. Ureña, E. Tabares, S. Tsipas, A. Jiménez-Morales, and E. Gordo, “Dry sliding wear behaviour of  $\beta$ -type Ti-Nb and Ti-Mo surfaces designed by diffusion treatments for biomedical applications,” *J. Mech. Behav. Biomed. Mater.*, p. accepted, 2018.
- [12] M. Geetha, a. K. Singh, R. Asokamani, and a. K. Gogia, “Ti based biomaterials, the ultimate choice for orthopaedic implants - A review,” *Prog. Mater. Sci.*, vol. 54, no. 3, pp. 397–425, 2009.
- [13] L. Kunčická, R. Kocich, and T. C. Lowe, “Advances in Metals and Alloys for Joint Replacement,” *Prog. Mater. Sci.*, no. April, 2017.
- [14] J. Ureña, E. Gordo, E. M. Ruiz-Navas, N. Vilaboa, L. Saldaña, and A. Jiménez-

- Morales, “Electrochemical comparative study on corrosion behavior of conventional and powder metallurgy titanium alloys in physiological conditions,” *Met. Powder Rep.*, vol. 72, no. 2, pp. 118–123, 2017.
- [15] C. Sittig, M. Textor, N. D. Spencer, M. Wieland, and P. H. Vallotton, “Surface characterization of implant materials c.p. Ti, Ti-6Al-7Nb and Ti-6Al-4V with different pretreatments,” *J. Mater. Sci. Mater. Med.*, vol. 10, no. 1, pp. 35–46, 1999.
- [16] T. M. Manhabosco, S. M. Tamborim, C. B. dos Santos, and I. L. Müller, “Tribological, electrochemical and tribo-electrochemical characterization of bare and nitrided Ti6Al4V in simulated body fluid solution,” *Corros. Sci.*, vol. 53, no. 5, pp. 1786–1793, 2011.
- [17] E. Gordo, J. Ureña, F. Toptan, A. M. Pinto, B. Ferrari, and S. Tsipas, “Design and Evaluation of PM Ti Surfaces Modified by Colloidal Techniques and Diffusion Processes for Biomedical Applications,” *Proc. World PM16 Conf.*, pp. 1–6, 2016.
- [18] J. Ureña, S. Tsipas, A. M. Pinto, F. Toptan, and E. Gordo, “Corrosion and tribocorrosion behaviour of  $\beta$  -type Ti-Nb and Ti-Mo surfaces designed by diffusion treatments for biomedical applications,” *Corros. Sci.*, p. submitted, 2018.
- [19] R. Chelariu *et al.*, “Metastable beta Ti-Nb-Mo alloys with improved corrosion resistance in saline solution,” *Electrochim. Acta*, vol. 137, pp. 280–289, 2014.
- [20] Z. Doni *et al.*, “Dry sliding and tribocorrosion behaviour of hot pressed CoCrMo biomedical alloy as compared with the cast CoCrMo and Ti6Al4V alloys,” *Mater. Des.*, vol. 52, pp. 47–57, 2013.
- [21] D. R. N. Correa, P. A. B. Kuroda, C. R. Grandini, L. A. Rocha, and F. G. M. Oliveira, “Tribocorrosion behavior of  $\beta$ -type Ti-15Zr-based alloys,” *Mater. Lett.*, vol. 179, pp. 118–121, 2016.
- [22] D. Landolt and S. Mischler, *Tribocorrosion of passive metals and coatings*, ISBN: 978-1-84569-966-6. 2011.
- [23] J. Ureña, S. Tsipas, A. Jiménez-Morales, E. Gordo, R. Detsch, and A. R. Boccaccini, “In-vitro study of the bioactivity and cytotoxicity response of Ti surfaces modified by Nb and Mo diffusion treatments,” *Surf. Coat. Technol.*, vol. 335, pp. 148–158, 2018.

# **Concluding Remarks**

5

## **5.1 Concluding Remarks**

## 5.1 Concluding Remarks

In this PhD Thesis, the surface modification of titanium processed by powder metallurgy has been proposed to obtain modified Ti surfaces by niobium and molybdenum diffusion treatments with improved properties for biomedical applications.

The main conclusion of this work is that the global objective of designing a new family of functionally modified Ti surfaces with improved properties for biomaterials has been achieved reaching a compromise between their mechanical performance, wear, corrosion, tribocorrosion and biological behaviour.

This general conclusion can be divided in more specific ones regarding the different topics studied in this research:

### Conclusions related to the surface modification process by diffusion treatments

- DICTRA software allowed the selection of the experimental diffusion conditions with the simulation of the diffusion process.
- Aqueous suspensions of  $\beta$ -stabilizing elements have been achieved through colloidal techniques and sprayed onto the Ti substrates.
- The first route of surface modification: co-sintering + diffusion was successfully performed in the green Ti substrates, obtaining the modified Ti-Nb or Ti-Mo surfaces in one step. The surface modification was also achieved through the second route: diffusion treatment in sintered Ti substrates. The third route: thermo-reactive diffusion in sintered Ti substrates allowed depositing the  $\beta$ -stabilizing elements and also nitride the surfaces.
- Microstructure studies confirmed the phase-transformation and the microstructure evolution due to the Nb or Mo introduction into the Ti. The diffusion treatments originated diffusion layers with functionally gradients in microstructure ( $\beta / \alpha + \beta / \alpha$ ) and composition (Ti-Nb or Ti-Mo) from surface inwards. The deepness of these gradients reached 100-140  $\mu\text{m}$  with  $\beta$  lamellas very close near the surface and more separated as getting deeper.
- The thermo-reactive diffusion treatment led to a modified Ti surface of 20-30 microns depth with a TiN layer on surface, some nitrogen diffusion and surface porosity, remaining practically all the Nb or Mo on surface.

### Conclusions related to the mechanical properties

- The modified Ti surfaces achieved an improvement in hardness with values between 4-5 GPa, twice the hardness of CP-Ti.
- The microstructure gradient resulted in a gradient of elastic modulus where the lowest values corresponded to the  $\beta$ -region between 54-65 GPa, achieving a decrease up to 40-50 % with respect to the elastic modulus of CP-Ti (102-105 GPa) and Ti6Al4V (110-114 GPa).
- Relative lower elastic modulus values were reached by Nb diffusion while slightly harder values by Mo diffusion. The co-sintered samples presented slightly smaller elastic modulus with respect to the modified sintered samples.

### Conclusions related to the wear, corrosion and tribocorrosion behaviour

- The surface modification of titanium by Nb or Mo diffusion treatments allowed enhancing the dry sliding wear behaviour of Ti. Metal-on-metal (stainless steel on Ti surfaces) produced more signs of abrasion and adhesion wear, leading to higher wear rate than ceramic-on-metal (alumina on Ti surfaces).
- The modified Ti surfaces showed wear rate values between 53-96 % lower compared to Ti under 2 N load against ceramic. They also exhibited reduced values up to 79 % lower than bare Ti surface under 5 N. Ti-Mo<sub>NH<sub>4</sub>Cl</sub> surface presented the best wear behaviour.
- Ti-Nb and Ti-Mo surfaces exhibited better protective properties toward corrosion than either CP-Ti or the surfaces obtained through co-sintering and diffusion.
- All the modified Ti surfaces presented high impedance modulus, around  $10^5$ - $10^6 \Omega$ , at low frequencies. This was attributed to a high corrosion resistance performance, indicating no deterioration of Ti corrosion resistance.
- Under tribological action the modified Ti surfaces showed similar coefficient of friction and lower tendency to corrosion compared to CP-Ti. Ti-Nb surfaces presented the highest repassivation rate while the Ti-Mo<sub>NH<sub>4</sub>Cl</sub>, the least signs of abrasive wear.

## Conclusions related to the final surface conditions and their biocompatibility character

- The surface chemical composition together with the roughness and wettability parameters selected led to positive results in terms of bioactivity in each Ti-Nb and Ti-Mo surfaces designed. Hydroxyapatite formation on the modified Ti surfaces was shown, indicating their in vitro bone bonding ability after 21 days of immersion in simulated body fluid.
- Ti-Nb surfaces designed through the different diffusion treatments with suitable surface parameters exhibited a positive cell-material interaction and non-cytotoxic response. Specially, the Ti-Nb surface labelled as-coated without post surface treatment (Ti-Nb<sub>coat</sub>) showed the highest cell viability and proliferation after its cytotoxicity evaluation for two days.
- The osteogenic differentiation study of bone marrow stromal cells indicated cell differentiation and bone mineralization after culturing for 21 days on both surfaces Ti-Nb and Ti-Nb<sub>NH<sub>4</sub>Cl</sub>, being comparable to the biocompatible CP-Ti biomaterial. The maximum expression of the osteogenic marker (specific ALP activity) was exhibited for the Ti-Nb surface. This suggests the promising biological behaviour of these modified Ti surfaces.



# **Future Lines**

6

## **6.1 Future lines**

## 6.1 Future lines

Based on the results obtained during this PhD Thesis and keeping in mind this line of researching about the surface modification of titanium alloys with improved mechanical and biological performance for biomedical applications, many interesting ideas for further works could be suggested:

- ✓ To study the surface modification process employing a longer diffusion time, trying to get deeper diffusion layers and thus, deeper  $\beta$ -regions. This deeper diffusion gradient would allow an easier surface finishing since grinding the surfaces without removing the  $\beta$ -region of the surface is one of the most challenging parts of this work.
- ✓ To study these surface modification treatments on the Ti6Al4V or Ti6Al7Nb alloy since they have been developed in a previous thesis work in this research group through powder metallurgy processing. It would be interesting to study the microstructure evolution with the aim to compare to the surface modification of titanium and to study the final properties for biomedical applications.
- ✓ Some preliminary surface modification studies were carried out on the Ti6Al4V alloy since is the most employed Ti alloy for biomaterials. Mo and Nb diffusion treatments were conducted under same diffusion conditions, obtaining Mo or Nb-rich Ti6Al4V surfaces with diffusion layers between 40-60  $\mu\text{m}$  and hardened surfaces: GreenTi6Al4V-Mo ( $380 \pm 19$  HV), GreenTi6Al4V-Nb ( $347 \pm 15$  HV), Ti6Al4V-Mo ( $392 \pm 14$  HV), and Ti6Al4V-Nb ( $362 \pm 13$  HV) with respect to Ti6Al4V ( $300 \pm 10$  HV).
- ✓ To study the corrosion behaviour of these materials in simulated body fluid at temperature of human body ( $37$  °C) during different immersion times, since for long immersion times these properties could be affected by the surface properties.
- ✓ To explore another surface finishing conditions with the idea of evaluating their influence on corrosion, wear or tribocorrosion behaviour.



J. Ureña, C. Mendoza, B. Ferrari, Y. Castro, S. Tsipas, A. Jiménez-Morales and E. Gordo

## **Surface modification of powder metallurgy titanium by colloidal techniques and diffusion processes for biomedical applications**

This work was orally presented at AMPT 2015 Conference celebrated in Madrid and included in the book of abstract of this congress.

Later, it was published in the journal Advanced Engineering Materials, Vol. 19, no. 6, 1600207, 2016 by courtesy of AMPT.

URI: <http://hdl.handle.net/10016/27395>

J. Ureña, E. Tejado, J.Y. Pastor, F. Velasco, S. Tsipas, A. Jiménez-Morales and E. Gordo

### **Role of beta-stabilizer elements in microstructure and mechanical properties evolution of powder metallurgy modified Ti surfaces designed for biomedical applications**

This work was distinguished as keynote oral presentation at EURO PM17 Conference celebrated in Milan and included in the proceedings of this congress. The manuscript was refereed by Dr. Thomas Ebel, Helmholtz-Zentrum Geesthacht.

Then, it was published in Powder Metallurgy Journal, DOI: 10.1080/00325899.2018.1426185, 2018

URI: <http://hdl.handle.net/10016/27501>

J. Ureña, E. Tabares, F. Toptan, A. M. Pinto, S. Tsipas, A. Jiménez-Morales and E. Gordo

## **Dry sliding wear behaviour of $\beta$ -type Ti-Nb and Ti-Mo surfaces designed by diffusion treatments for biomedical applications**

Results from this work were orally presented at IBERTRIB 2017 Conference celebrated in Guimarães and included in the book of abstract of this congress, ISBN: 978-972-99596-2-2

It is accepted in Journal of Mechanical behaviour of biomedical materials, 2018

URI: <http://hdl.handle.net/10016/28285>

J. Ureña, E. Gordo, E. Ruiz-Navas, N. Vilaboa, L. Saldaña and A. Jiménez-Morales

### **Electrochemical comparative study on corrosion behavior of conventional and powder metallurgy titanium alloys in physiological conditions**

This work was presented at EURO PM15 Conference celebrated in Reims and included in the CD of proceedings of this congress, ISBN 978-1-899072-47-7.

Later, it was published in the journal Metal Powder Report, Vol. 72, no. 2, pp. 118-123, 2017

URI: <http://hdl.handle.net/10016/27378>

E. Gordo, J. Ureña, F. Toptan, A. M. Pinto, B. Ferrari, S. Tsipas and A. Jiménez-Morales

### **Design and evaluation of powder metallurgy titanium surfaces modified by colloidal techniques and diffusion processes for biomedical applications**

This work was orally presented at World PM16 Conference celebrated in Hamburg and included in the CD of proceedings of this congress. The manuscript was refereed by Dr. José Manuel Martín (CEIT, Spain).

URI: <http://hdl.handle.net/10016/28050>



J. Ureña, S. Tsipas, F. Toptan, A. M. Pinto, E. Gordo and A. Jiménez-Morales

## **Corrosion and tribocorrosion behaviour of $\beta$ -type Ti-Nb and Ti-Mo surfaces designed by diffusion treatments for biomedical applications**

Results from this work were orally presented at CNMAT 2016 Conference celebrated in Gijón (Spain).

It is submitted to Corrosion Science, 2018

URI: <http://hdl.handle.net/10016/27386>

J. Ureña, S. Tsipas, A. Jiménez-Morales, E. Gordo, R. Detsch and A. R. Boccaccini

**In-vitro study of the bioactivity and cytotoxicity response of titanium surfaces modified by niobium and molybdenum diffusion treatments**

This work was orally presented at EUROMAT 2017 Conference celebrated in Thessaloniki.

It was published in the journal Surface & Coatings Technology, vol. 335, pp. 148-158, 2018

URI: <http://hdl.handle.net/10016/27442>

J. Ureña, S. Tsipas, A. Jiménez-Morales, E. Gordo, R. Detsch and A. R. Boccaccini

### **Cellular behaviour of bone marrow stromal cells on modified Ti-Nb surfaces**

This work was orally presented at EUROMAT 2017 Conference celebrated in Thessaloniki.

It was published in the journal Materials & Design, vol. 140, pp. 452-459, 2018

URI: <http://hdl.handle.net/10016/27417>